# Temperature dependent dynamical nuclear polarization bistabilities in double quantum dots in the spin-blockade regime

Anders Mathias Lunde,[1] Carlos López-Monís,[1,2] Ioanna A. Vasiliadou,[3,4] Luis L. Bonilla,[3,5] and Gloria Platero[1]
[1] *Instituto de Ciencia de Materiales de Madrid, CSIC, 28049 Cantoblanco, Madrid, Spain*
[2] *Institute for Theoretical Physics, University of Regensburg, D-93040 Regensburg, Germany*
[3] *G. Millan Institute, Fluid Dynamics, Nanoscience and Industrial Mathematics, Universidad Carlos III de Madrid, 28911 Leganés, Spain*
[4] *Materials Science and Engineering and Chemical Engineering Department, Universidad Carlos III de Madrid, 28911 Leganés, Spain*
[5] *Unidad Asociada al Instituto de Ciencia de Materiales de Madrid, CSIC, 28049 Cantoblanco, Madrid, Spain*
(Dated: November 30, 2012)

The interplay of dynamical nuclear spin polarization and leakage current through a double quantum dot in the spin-blockade regime is analyzed. A finite nuclear polarization is build up due to a competition between hyperfine-induced spin-flip transitions and another inelastic escape mechanism from the triplets, which block transport. We focus on the temperature dependence of the dynamical nuclear polarization in the zero energy-detuning configuration (i.e. zero electrostatic energy difference between having one electron in each dot and having a singlet in the right dot). We show that for temperatures $T$ below a certain *transition temperature*, the nuclear polarization becomes *bistable*, which produces *hysteresis* in the leakage current versus external magnetic field. The bistability and its consequences are studied in detail in two different cases. (i) Close to the (energetically isolated) crossing of the three triplet energy levels near zero magnetic field. In this case, the spin-blockade of the triplet with zero angular momentum projection is lifted by the inhomogeneity of the effective magnetic field from the nuclei. (ii) At higher external magnetic fields, where the two spin-polarized triplets simultaneously cross two different singlet energy levels. We develop simplified models for these two situations, which both lead to implicit equations for the polarization. These, in turn, give *different* transition temperatures $T_{c,\mathrm{TT}}$ and $T_{c,\mathrm{ST}}$ for the crossing of the triplet levels and the singlet-triplet crossings, respectively. We find $T_{c,\mathrm{TT}}$ analytically to be given *solely* by the hyperfine coupling constants, whereas $T_{c,\mathrm{ST}}$ depends on various external parameters. Moreover, $T_{c,\mathrm{ST}}$ is *enhanced* compared to $T_{c,\mathrm{TT}}$ for experimentally relevant parameters, such that in the regime $T_{c,\mathrm{TT}} < T < T_{c,\mathrm{ST}}$ current hysteresis appears for finite magnetic fields, but *not* close to zero magnetic field. For both kinds of level crossings, the transition temperatures are shown to stem from the fact that the hyperfine transitions are *phonon mediated*. Specifically, we point out that the exponential suppression of phonon absorption compared to phonon emission in a hyperfine transition is the key reason for the existence of transition temperatures at zero energy-detuning. Finally, by comparing the rate equation approach with Monte Carlo simulations, we discuss the importance of having a competition between hyperfine interactions and at least one more escape mechanism from the triplets in order to induce a finite nuclear spin polarization.

PACS numbers: 73.63.Kv, 73.23.Hk, 05.70.Ln, 72.25.Rb

arXiv:1211.7042v1 [cond-mat.mes-hall] 29 Nov 2012

## I. INTRODUCTION

Quantum dots provide highly tunable systems allowing for detailed manipulation of electrons in confined quantum states.[2–5] The high degree of experimental control and advantages in fabrication technics allow to investigate various geometries and materials, where different mechanisms dominate the essential physics of these nanoscale devices.

In a series of experiments, Ono *et al.*[1,6] revealed that, not only the charge, but also the Pauli exclusion principle for spin states can play a crucial role in the electronic transport through quantum dot systems. More specifically for two quantum dots in series, it is possible to tune the gate-voltages asymmetrically such that a single electron with a definite spin is trapped in the right dot, see Fig. 1. This means that for a non-linear forward bias, $\mu_{\mathrm{L}} > \mu_{\mathrm{R}}$, an electron with the same spin as in the right dot will sooner or later tunnel into the left dot from the left lead. (Here $\mu_{\mathrm{L(R)}}$ is the chemical potential of the left (right) lead.) This in turn blocks the current through the double quantum dot (DQD), because (i) the state with two electrons of equal spins in the right dot is tuned to be very high in energy and (ii) the chemical potential of the left lead is too high for the electron to tunnel back into the contact. On the contrary, if an electron with opposite spin to the one in the right dot tunnels into the left dot, then there is no blocking, since having two electrons with opposite spins in the right dot is energetically allowed. In other words, the two electron states with equal spins block transport through the system, while the singlet states containing two electrons of opposite spins do not. This is the so-called spin-blockade (SB) phenomenon[1,7–9] — a clear consequence of the Pauli exclusion principle. For the opposite (reversed) bias, $\mu_{\mathrm{L}} < \mu_{\mathrm{R}}$, the transport is not blocked. The reason is that an electron with opposite spin (to the trapped one in the right dot) can always enter from the right lead and

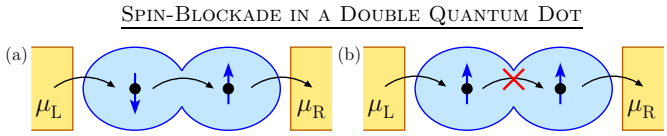


FIG. 1. (color online) A double quantum dot (DQD) coupled to two leads at chemical potential $\mu_L$ and $\mu_R$, respectively. In the spin-blockade (SB) regime, the gate-voltages are tuned asymmetrically for the two dots such that an electron with a definite spin (spin-up in the figure) is trapped in the right dot. This means that an electron with the opposite spin (spin-down in the figure) can pass through the DQD from the left to right lead as seen in Fig. (a). However, once an electron with spin up enters the left dot [Fig. (b)], then transport through the DQD is blocked for non-linear forward bias ($\mu_L - \mu_R \gg k_B T$). In contrast, for opposite bias ($\mu_L - \mu_R < 0$) the system is not blocked and a current flows.[1] Hyperfine interactions, co-tunneling processes and spin-orbit coupling are able to lift the SB and cause a small – yet measurable – leakage current. This in turn can polarize the nuclei and can cause observable phenomena like current hysteresis.

pass through the system. In contrast, an electron with equal spin (to the trapped one in the right dot) cannot enter the DQD, such that the system never enters the blocking states. This current rectification is one of the key experimental observations of SB in DQDs.[1]

### A. Leakage current as a measure of the spin relaxation mechanisms in a DQD

An electron can escape from the states blocking transport by a spin relaxation process. This in turn leads to a small leakage current in the SB regime. Therefore analyzing the leakage current is an excellent tool to obtain information about the spin relaxation processes in the DQD from a transport experiment.[6,10,11] There are several ways to escape from the blocking states in the DQD. For instance, via co-tunneling processes,[1,12–16] spin-orbit meditated spin relaxation[17–25] and/or by hyperfine (HF) interaction[26] between the electronic spins and the nuclear spin environment of the host material.[6,10,11,27–47] The relative importance of these mechanisms depends on the material and the external parameters. For instance, a specific co-tunneling process can become important by tuning the gate-voltages such that the virtual energy exchange in the co-tunneling process becomes low.[12,48]

Ever since the experiments by Ono *et al.*[1,6] in vertical GaAs heterostructured DQDs, several experimental geometries and materials have been used to further investigate the leakage current in the SB regime due to different relaxation mechanisms.[10,11,19,49–53] For instance, a well-designed experiment by Churchill *et al.*[52] on carbon nanotube DQDs analyzed the leakage current in the SB regime in different samples with a variable amount of the nuclear isotope $^{13}$C present. Since $^{13}$C is the only stable carbon isotope with a non-zero nuclear spin, this amounts to varying the importance of the spin relaxation due to HF interaction in the experiment from very important (high $^{13}$C concentration) to not important (close to zero $^{13}$C concentration). This shows experimentally[52] how different the leakage current can be versus external parameters like the magnetic field with and without nuclear spins present. Note that in recent years spin-orbit coupling is also thought to play a role in carbon nanotubes.[54–56] In passing, we remark that the phenomenon of so-called valley-spin blockade have also been investigated theoretically[57,58] and experimentally[59] in carbon nanotube DQDs.

SB in Silicon DQDs has also been investigated.[51,53,60–63] Along the same lines as Churchill *et al.*[52], a recent study by Lai *et al.*[53] of SB in Silicon DQDs also eliminated the HF interaction by isotopic purification. In this case, co-tunneling processes caused the leakage current in the SB regime (in good agreement with recent theories[15,16]), since the spin-orbit coupling is expected to be weak in Silicon.[53] In contrast, spin-orbit interaction is generally believed to be strong in InAs, which enabled Pfund *et al.*[19] to investigate its importance on the leakage current in the SB regime of InAs nanowire DQDs. In this case, the leakage current were found to be due to a competition between spin-orbit and HF induced spin relaxation.

### B. Dynamical nuclear polarization and the leakage current

A spin relaxation process from one of the blocking states due to HF interaction will flip the electronic spin from say spin-up to spin-down, while the nuclear spin will flip in the opposite direction, Fig. 2(b). The electronic spin relaxation in the SB regime can change the average occupations of the nuclear spin states, since the nuclear spin relaxation time is very long compared to the electronic tunneling timescales.[10,52,64] In other words, the repeated electronic spin-flip due to the leakage current through the DQD can produce a dynamical nuclear polarization (DNP) in the nuclear environment of the DQD. The DNP acts back on the electronic states of the DQD as an effective magnetic field, the so-called Overhauser field.[65] The Overhauser field is generally *inhomogeneous* and therefore often different in the two quantum dots. Effects of DNP are also investigated in optical[66–75] and quantum Hall[76–86] systems.

It is important to emphasize that even though the HF induced spin-relaxation do flip a nuclear spin, it will not *always* change the *average* nuclear polarization in the steady state of the SB regime. For instance, if HF interaction is the *only* spin relaxation mechanism causing the leakage current, then the nuclear spins remain unpolarized.[30,33] Essentially, this is because tunneling into one of the two blocking states consisting of two spin-up electrons, $|\uparrow,\uparrow\rangle$, or two spin-down electrons, $|\downarrow,\downarrow\rangle$, are equal. Escape from these two states will polarize

the nuclei in opposite directions and therefore on average the polarization does not change. This is so, even though the escape rates from the blocking states might be very different.[19,33] In this case of HF interaction being the *only* cause of the leakage current, the nuclear spins can be modeled as an effective magnetic field with *zero* mean value and non-zero statistical deviation[30,87–90] as has also been used to fit experimental data.[11] Nevertheless, if *more than one* spin relaxation mechanism contribute to the leakage current in the SB regime, then the nuclei can indeed obtain a *non-zero* polarization.[33,34,37]

The finite DNP – created by the multiple escape paths from the blocking states – leads to experimentally measurable signatures in the leakage current.[6,10,19,31,32,44–46,52] Perhaps the most fascinating of these signatures is that of a *hysteretic* leakage current versus external parameters like the magnetic field or a gate-voltage as has been observed[6,10,19,45,52,91]. For instance, Pfund *et al.*[19] found hysteresis due to a competition between HF and spin-orbit induced escape from the blocking states. The hysteresis signals a *bistability* in the nuclear polarization: For a certain range of parameters, there exists two stable values of the polarization leading to two values of the current. For other parameters the nuclear spins might be polarized, but the polarization is single-valued and hence also the current.[92]

In DQDs polarization as high as about *half* of the nuclear spins have been estimated from the experiments,[31] and even higher polarizations were not excluded. Spin-diffusion from the DQD to the surrounding material and dipole-dipole interactions are very weak, but nevertheless expected to be able to reduce the highest polarizations somewhat experimentally.[10,52,64]

Other experimental findings like long-lived current oscillations in time[6,10] and transient phenomena in the leakage current[44] have also been attributed to the nuclear spin environment.[93–95] Furthermore, it has been shown that DNP can be build up in DQDs by cycles in gate-voltage space, but without transport through the DQD.[96,97]

The Zeeman splitting of the nuclear spins states are negligible compared to the one of the electronic states.[98] Therefore, the HF interaction is most effective to break SB close to the crossing of the energy levels between e.g. a triplet and the singlet state such that energy is conserved in the spin-flip process. In order to get close to a level crossing, the local gate voltages on the dots, the inter-dot tunneling or the external magnetic field can be varied experimentally. The local gate voltages change the energy levels of the individual dots and thereby the so-called *energy detuning*, which is the electrostatic energy difference between having one electron in each dot and having a singlet in the right dot. The barrier between the dots controls the wavefunction overlap and therefore the quantum mechanical *exchange energy* between the singlet and triplet states. Furthermore, the external magnetic field splits up the three triplet levels.

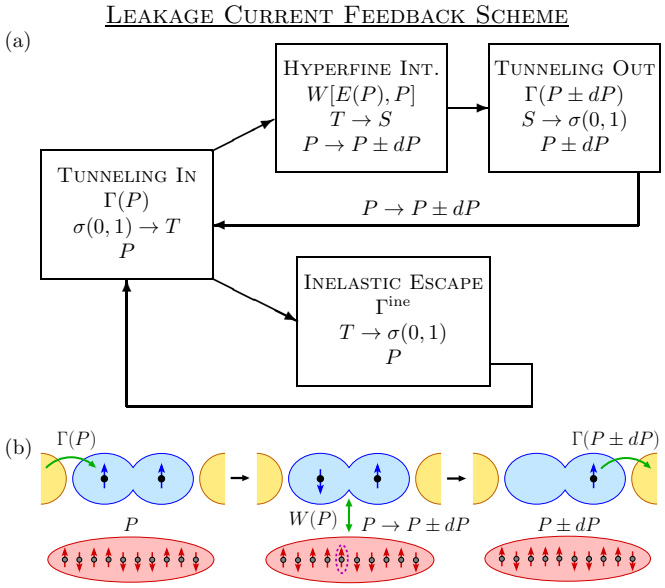


FIG. 2. (Color online) (a) Illustration of the two escape paths from the blocking triplet states $T$, which compete to create a non-zero dynamical nuclear polarization in the spin-blockade regime. The cycle of transporting an electron through a blocking triplet state $T$ begins and ends with a single electron trapped in the right dot $\sigma(0,1)$. During a single transport cycle, the polarization $P$ is changed by a small amount $\pm dP$ (depending on the specific transition), if the escape from the state $T$ is hyperfine mediated (upper branch). The polarization acts back on the energy levels $E(P)$ via the Overhauser magnetic fields and, in turn, on both the HF spin-flip rates $W$ and the tunneling rates $\Gamma$. In contrast, the weaker inelastic escape mechanism[33–36] (lower branch) leaves the polarization unchanged. In this work, we describe this feedback and the competition between the escape paths by a set of non-linear rate equations and by Monte Carlo simulations. (b) An example of a hyperfine-induced escape process from a triplet states, which changes the polarization [i.e. an example of a process contributing to the upper branch in (a)].

### C. Main ideas of this work and comparison to previous works

In this work, the leakage current and the DNP due to transport through a DQD in the SB regime is analyzed. We study the case of DNP occurring due to a competition between (i) the HF-induced escape from the blocking states and (ii) another weaker inelastic escape mechanism such as co-tunneling or spin-orbit interaction — following previous works by Rudner *et al.*[33–36] The induced DNP acts back on the electronic energy levels of the DQD, which in turn change the transition rates until the steady state is reached. Therefore we are dealing with a non-linear system with feedback present. The competition between various escape paths and the feedback are illustrated in Fig. 2.

We consider the configuration with *zero energy detuning*, i.e. the *electrostatic* energy of having one electron

in each dot and having a singlet in the right dot is the same. Therefore, the external magnetic field is varied in order to get close to level crossings. The effective Overhauser magnetic field from the nuclear polarization is different in each dot, which mix the triplet and singlet states with zero total angular momentum projection on the $z$-axis.[36,45] Thus, it makes sense to study two kinds of level crossings in detail: The crossing of the triplet (like) states and the crossing between singlets and triplets. What we name the crossing of triplet states is in fact the crossing of the pure triplets with angular momentum projection $\pm 1$ and the triplet, which has a small – but finite – mixing with the singlet subspace due to the Overhauser field gradient.[10] Hence, escape from this state is possible for non-zero Overhauser field difference between the dots.

The main focus of this work is the presence and description of a *transition temperature* $T_c$ for the nuclear spin environment. For temperatures $T$ below $T_c$ the leakage current shows hysteresis versus the external magnetic field $B$, while for $T > T_c$ the hysteresis disappears even though the system can still have a non-zero DNP. The transition temperature is related to a bistability of the DNP for $T < T_c$, which is the reason for the current hysteresis. Interestingly, we find that the transition temperatures corresponding to the crossing of the triplet states near $B = 0$, $T_{c,\mathrm{TT}}$, and the singlet-triplet crossing at finite $B$-field, $T_{c,\mathrm{ST}}$, respectively, are in general *different*. Moreover, the later is *larger*, $T_{c,\mathrm{TT}} < T_{c,\mathrm{ST}}$, for typical parameters. Thus, for a temperature $T$ between $T_{c,\mathrm{TT}}$ and $T_{c,\mathrm{ST}}$ current hysteresis is expected near the singlet-triplet level crossing at finite magnetic field, but *not* near the crossing of the triplet levels.

The nuclei spin polarization in the SB regime is current induced and, hence, a result of a *non-equilibrium* situation. It is remarkable to note that spontaneous order of the nuclear spins in *equilibrium* generally happens at orders of magnitude lower temperatures than $T_{c,\mathrm{TT}}$ and $T_{c,\mathrm{ST}}$ due to the weakness of dipole-dipole interaction among the nuclear spins.[26,33,99]

Here, we find the transition temperature $T_{c,\mathrm{TT}}$ for the crossing of the triplet levels analytically. It is *solely* given by the strength of the HF coupling in the DQD. This is derived from a simplified model valid in the limit of the singlets being far away in energy from the triplets, i.e. at large exchange energy. To describe the singlet-triplet crossing, we also derive a simplified model, which leads to an implicit equation for the DNP. The transition temperature $T_{c,\mathrm{ST}}$ for the singlet-triplet crossing is found to depend on various system parameters – in contrast to $T_{c,\mathrm{TT}}$. Interestingly, the enhancement of $T_{c,\mathrm{ST}}$ compared to $T_{c,\mathrm{TT}}$ is found to be due to an interplay between the triplet-triplet and singlet-triplet HF transition rates, even though the latter often dominate by at least an order of magnitude.

The possibility of not conserving energy in the HF-induced spin-flip transitions is present both in the present study and in the works by Rudner *et al.*[33–36] Refs.[33–36] include this effect as level broadening, whereas we allow for energy emission and absorption by phonons in the HF-induced spin-flip transitions. This means that the energy absorption and emission in the spin-flip process is *equally likely* in the works [33–36]. In contrast, here the probability for energy absorption via phonons is exponentially suppressed compared to energy emission.[100–102] In this paper, we show that this is indeed an *essential difference* between this study and the previous ones[33–36], because the presence of a transition temperature for both the crossing of the triplet levels and for the singlet-triplet level crossing exactly stems from the probability difference between absorption and emission of energy.

In previous works by some of us,[37–39] DNP in the SB regime was also analyzed. In these works, a non-zero DNP arise due to the competition between HF-induced spin-relaxation processes and escape from the blocking states by tunneling through excited states in the right dot. In contrast, such excited states are assumed to be far away in energy in the present work and therefore do not play a role. Moreover, we do not use incoherently coupled dots, i.e. here the inter-dot tunneling is not treated as a perturbation as in the previous works.[37–39] Instead we work with coherently coupled dots. This approach, for instance, includes the expected triplet with zero angular momentum projection on the $z$-axis, which is a superposition of spin up and down in the two dots. Moreover, previously[37–39] phonon absorption processes were neglected, so the physics treated here regarding the transition temperature were therefore missed.

Some of us have investigated numerically a similar approach recently.[42] However, in this case, the rate equation for the DNP turned out not to be appropriate, because HF interactions was taken to be the *only* escape mechanism from the blocking states. In contrast, here we find DNP to appear due to a competition between HF induced escape and another inelastic escape mechanism, which is essential as pointed out by Rudner and Levitov.[33,34] Here we put our results from the rate equation approach on a firm basis by comparing to Monte Carlo simulations. Furthermore, we point out in detail how the rate equation approach becomes sensitive to some initial occupations in the case without an inelastic escape path, and therefore become unable to describe the physical setup. Moreover, we emphasize that this work contains many new insights and results compared to Ref.[42]. For instance, the simple analytical models describing the crossing of the triplet levels and the crossing of the singlet and triplet levels, respectively, which lead to the transition temperatures described above.

The paper is organized as follows. We begin by describing the electronic states of the DQD and how these are coupled to each other and to the DNP in Sec. II. Then we present the simplified rate equations modeling the crossing of the triplet levels in Sec. III, which is followed by the model and calculations on the singlet-triplet level crossing in Sec. IV. Finally, in Sec. V the Monte Carlo simulations are discussed.

## II. THE MODEL

Next, we describe the model used in this work. It aims at describing the basic physics of a DQD coupled to a nuclear environment in the SB regime – instead of focusing on a specific material.

### A. The DQD states, the Hamiltonian and the Overhauser field

The DQD states blocking the transport in the SB regime are the three triplet states

$$|T_+\rangle = d^\dagger_{\mathrm{L}\uparrow} d^\dagger_{\mathrm{R}\uparrow}|0\rangle, \tag{1a}$$

$$|T_0\rangle = \frac{1}{\sqrt{2}}\left(d^\dagger_{\mathrm{L}\uparrow} d^\dagger_{\mathrm{R}\downarrow} + d^\dagger_{\mathrm{L}\downarrow} d^\dagger_{\mathrm{R}\uparrow}\right)|0\rangle, \tag{1b}$$

$$|T_-\rangle = d^\dagger_{\mathrm{L}\downarrow} d^\dagger_{\mathrm{R}\downarrow}|0\rangle, \tag{1c}$$

where the indices 0 and $\pm$ represent the total angular momentum projection on the $z$ axis, $m_z = 0, \pm 1$. The singlet states with one electron in each dot, $|S(1,1)\rangle$, and two electrons in the right dot, $|S(0,2)\rangle$, respectively, are

$$|S(1,1)\rangle = \frac{1}{\sqrt{2}}\left(d^\dagger_{\mathrm{L}\uparrow} d^\dagger_{\mathrm{R}\downarrow} - d^\dagger_{\mathrm{L}\downarrow} d^\dagger_{\mathrm{R}\uparrow}\right)|0\rangle, \tag{2a}$$

$$|S(0,2)\rangle = d^\dagger_{\mathrm{R}\downarrow} d^\dagger_{\mathrm{R}\uparrow}|0\rangle. \tag{2b}$$

Furthermore, a single electron with spin $\sigma$ trapped in the right dot is described by the one-electron state

$$|\sigma(0,1)\rangle = d^\dagger_{\mathrm{R}\sigma}|0\rangle \quad \text{for} \quad \sigma = \uparrow, \downarrow . \tag{3}$$

Here we only include a single spin-degenerate state created (annihilated) by $d^\dagger_{\alpha\sigma}$ ($d_{\alpha\sigma}$) in the right ($\alpha = \mathrm{R}$) and left ($\alpha = \mathrm{L}$) dot with spin $\sigma$. The empty state is $|0\rangle$.

The entire system is described by the Hamiltonian

$$H = H_{\mathrm{DQD}} + H_{\mathrm{leads}} + H_{\mathrm{T}} + H_{\mathrm{HF}}, \tag{4}$$

where $H_{\mathrm{DQD}}$, $H_{\mathrm{leads}}$ and $H_{\mathrm{T}}$ describe the two quantum dots in series, the electronic leads and the tunneling coupling between them, respectively (see Fig. 1). The HF interaction, $H_{\mathrm{HF}}$, is between the localized electrons in the DQD and the nuclei in the host material. The DQD is described by an Anderson-type Hamiltonian

$$H_{\mathrm{DQD}} = \sum_{\alpha=\mathrm{L,R}} \left(\varepsilon_\alpha n_\alpha + U_\alpha n_{\alpha\uparrow} n_{\alpha\downarrow} + g\mu_B B S_{z,\alpha}\right) + U_{\mathrm{RL}} n_{\mathrm{R}} n_{\mathrm{L}} + t\sum_\sigma \left(d^\dagger_{\mathrm{L}\sigma} d_{\mathrm{R}\sigma} + d^\dagger_{\mathrm{R}\sigma} d_{\mathrm{L}\sigma}\right), \tag{5}$$

where $n_\alpha = n_{\alpha\uparrow} + n_{\alpha\downarrow}$ (for $\alpha = \mathrm{R}, \mathrm{L}$) is the number operator on each dot, $n_{\alpha\sigma} = d^\dagger_{\alpha\sigma} d_{\alpha\sigma}$, and the $z$-component of the spin operator on dot $\alpha$ is $S_{z,\alpha} = \frac{1}{2}(n_{\alpha\uparrow} - n_{\alpha\downarrow})$. Both inter-dot Coulomb interaction $U_{\mathrm{RL}}$ and intra-dot Coulomb interaction $U_\alpha$ are included. The onsite energies $\varepsilon_\alpha$ and the inter-dot tunneling $t$ can be tuned experimentally by gates. Furthermore, an external magnetic field $B$ causes a Zeeman splitting in each dot, $g\mu_B B$, where $g$ is the $g$-factor and $\mu_B$ is the Bohr magneton. (The magnetic field is taken to be in-plane, such that orbital effects can be safely neglected.[6,16]) For zero inter-dot tunneling, $t = 0$, the triplets Eq.(1) and singlets Eq.(2) are eigenstates of $H_{\mathrm{DQD}}$. A finite inter-dot tunneling, $t \neq 0$, mixes the singlet states in Eq.(2).

The leads and the coupling of the leads to the DQD are described by

$$H_{\mathrm{leads}} = \sum_{\alpha\mathbf{k}\sigma} \varepsilon_{k\sigma\alpha} c^\dagger_{\mathbf{k}\sigma\alpha} c_{\mathbf{k}\sigma\alpha}, \tag{6a}$$

$$H_{\mathrm{T}} = \sum_{\alpha\mathbf{k}\sigma} \left(t_{\alpha\mathbf{k}} c^\dagger_{\mathbf{k}\sigma\alpha} d_{\alpha\sigma} + t^*_{\alpha\mathbf{k}} d^\dagger_{\alpha\sigma} c_{\mathbf{k}\sigma\alpha}\right), \tag{6b}$$

where $c^\dagger_{\mathbf{k}\sigma\alpha}$ ($c_{\mathbf{k}\sigma\alpha}$) creates (annihilates) the orbital state $\mathbf{k}$ with spin $\sigma$ in lead $\alpha$ of energy $\varepsilon_{k\sigma\alpha}$. The tunneling couplings between the leads and the dots are $t_{\alpha\mathbf{k}}$.

Using the Fermi contact interaction[103], the HF interaction becomes[26,104] $H_{\mathrm{HF}} = \sum_{\alpha,n} A_\alpha(\mathbf{R}_n)\mathbf{S}_\alpha \cdot \mathbf{I}_n$, which connects the electronic spin $\mathbf{S}_\alpha = (S_{x,\alpha}, S_{y,\alpha}, S_{z,\alpha})$ on dot $\alpha = \mathrm{L}, \mathrm{R}$ with the nuclear spin $\mathbf{I}_n = (\mathbf{I}_{x,n}, \mathbf{I}_{y,n}, \mathbf{I}_{z,n})$ at position $\mathbf{R}_n$. The coupling between the spins depends on the value of the electronic envelope wave function $\Psi_\alpha(\mathbf{r})$ of the quantum dot[26] $\alpha = \mathrm{L}, \mathrm{R}$ at the position of the nuclear spin $\mathbf{R}_n$, i.e. $A_\alpha(\mathbf{R}_n) = \nu A |\Psi_\alpha(\mathbf{R}_n)|^2$. Here $\nu$ is the unit cell volume and $A$ is the atomic HF coupling constant[26,104] related the atomic wave function at the nuclear spin. For simplicity, the nuclear spins are taken to be spin–1/2. The details of the inhomogeneities of the nuclear coupling constants $A_\alpha(\mathbf{R}_n)$ are not essential for the description of the DNP, so therefore we replace them by homogeneous HF couplings[105,106], $A_\alpha/N$, i.e.

$$H_{\mathrm{HF}} = \sum_\alpha \frac{A_\alpha}{N} \sum_n \mathbf{S}_\alpha \cdot \mathbf{I}_n, \tag{7}$$

where $N$ is the total number of nuclear spins in the DQD. The HF constants $A_\alpha$ for the two dots $\alpha = \mathrm{L}, \mathrm{R}$ are of the same order of magnitude, but are not necessarily the same[42,90,106] for realistic dots due to e.g. differences in the confinement potentials. As we shall see, this plays an important role in the leakage current dynamics.

The polarization of the nuclei acts back on the electronic states as an effective Overhauser[65] magnetic field. In order to include this physical effect into the description, we divide the HF Hamiltonian into a mean-field part $H^{\mathrm{MF}}_{\mathrm{HF}}$, the Overhauser field, and a spin-flip part $H^{\mathrm{sf}}_{\mathrm{HF}}$, which leads to the HF-induced spin flips necessary for *dynamically* polarizing the nuclear spins. The external magnetic field provides a direction along which the nuclei can polarize[26,44], such that the rotational symmetry is broken as in the experimental situation.[44] This is a customary approach for mean-field theories describing phenomena such as magnetization of a ferromagnet.[107]

Therefore, the mean field from the nuclei is taken to be along the $z$ direction as the external $B$-field and given in terms of the average number of spin up and down $N_\sigma$ ($\sigma =\uparrow,\downarrow$) in the nuclear environment[31,36,42], i.e. $\sum_n \langle \mathbf{I}_n\rangle = \sum_n \langle I_{z,n}\rangle = (N_\uparrow - N_\downarrow)/2$. Thus,

$$H_{\rm HF}^{\rm MF} = \sum_{\alpha={\rm L,R}} \frac{1}{2} A_\alpha P S_{z,\alpha}, \tag{8}$$

where the nuclear spin polarization

$$P \equiv \frac{N_\uparrow - N_\downarrow}{N} \tag{9}$$

was introduced and $N = N_\uparrow + N_\downarrow$ is the total number of nuclear spins. The number of nuclear spin species $N_\sigma$ – and thus $P$ – change dynamically according to the external conditions of the leakage current. The spin-flip part of the HF interaction is given by

$$H_{\rm HF}^{\rm sf} = \sum_{\alpha,n} \frac{A_\alpha}{2N} \left( S_{-,\alpha} I_{+,n} + S_{+,\alpha} I_{-,n} \right), \tag{10}$$

where $S_{\pm,\alpha} = S_{x,\alpha} \pm i S_{y,\alpha}$ and $I_{\pm,n} = I_{x,n} \pm i I_{y,n}$ are the raising and lowering operators of the electronic and nuclear spins, respectively. This interaction induces electronic spin-flip processes, which are included perturbatively in the rate equations below (see Sec. II B).

From $H_{\rm HF}^{\rm MF}$, we can explicitly read off the effective Overhauser magnetic field in each dot[37]

$$B_{\rm nuc}^{\alpha} = \frac{A_\alpha P}{2 g \mu_B}. \tag{11}$$

Importantly, the effective Overhauser fields in the two dots are different, $B_{\rm nuc}^{\rm R} \neq B_{\rm nuc}^{\rm L}$, which is crucial for lifting the SB[10,45] (as will be clear in the following sections). Here we introduce this difference by having $A_{\rm L} \neq A_{\rm R}$, but keep the nuclear polarization $P$ as a common quantity for both dots.[33–35,42] This is consistent with our approach of using coherently coupled dots. However, it is also possible to adopt an alternative approach by using different nuclear polarizations in the two dots[36,37] and $A_{\rm L} = A_{\rm R}$. This approach can also produce different Overhauser fields in the two dots, and it is more relevant for well-separated dots.[108]

Next, we find our basis states of the DQD including the effective Overhauser fields and the finite inter-dot tunneling. To this end, we diagonalize the Hamiltonian $H_{\rm DQD} + H_{\rm HF}^{\rm MF}$ within the space of triplets $|T_{m_z}\rangle$ Eq.(1), singlets Eq.(2) and one-electron states $|\sigma(0,1)\rangle$ Eq.(3), since all other states are not energetically relevant in the SB regime.[109] In this work, we specialize to the limit of *zero detuning* such that the electrostatic energy of having one electron in each dot, $\varepsilon_{\rm L} + \varepsilon_{\rm R} + U_{\rm RL}$, and having a singlet in the right dot, $2\varepsilon_{\rm R} + U_{\rm R}$, are the same. We choose the zero of energy such that $\varepsilon_{\rm L} + \varepsilon_{\rm R} + U_{\rm RL} = 2\varepsilon_{\rm R} + U_{\rm R} = 0$. The diagonalization for zero detuning gives the following particularly simple molecular basis

Energy levels for zero detuning and $P = 0$

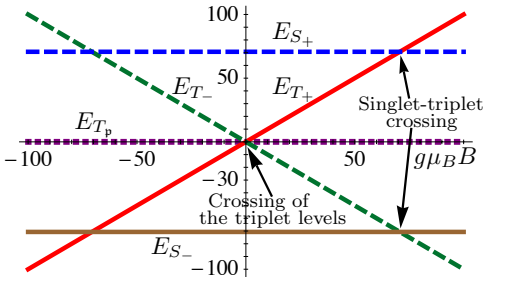


FIG. 3. (Color online) The energy levels Eq.(14) versus magnetic field (in energy units) $g\mu_B B$ for the five two-electron states $T_+$ (red full line), $T_-$ (green dashed line), $T_\mathfrak{p}$ (purple dotted line), $S_+$ (blue dashed line) and $S_-$ (brown full line) in the case of zero detuning and zero nuclear polarization, $P = 0$. The crossings of the three triplets and the triplet-singlet crossing points (for $g\mu_B B > 0$) are indicated. An inter-dot tunneling of $t = 50\mu$eV is used.

states for describing SB in a DQD ($\hbar = 1$):

$$|T_+\rangle = d_{\rm L\uparrow}^\dagger d_{\rm R\uparrow}^\dagger |0\rangle, \tag{12a}$$

$$|T_-\rangle = d_{\rm L\downarrow}^\dagger d_{\rm R\downarrow}^\dagger |0\rangle, \tag{12b}$$

$$|T_\mathfrak{p}\rangle = \frac{1}{\mathcal{N}} \Big[ |T_0\rangle - \mathfrak{p} |S(0,2)\rangle \Big], \tag{12c}$$

$$|S_\pm\rangle = \frac{1}{\sqrt{2}} \left[ |S(1,1)\rangle \pm \frac{1}{\mathcal{N}} \Big( |S(0,2)\rangle + \mathfrak{p} |T_0\rangle \Big) \right], \tag{12d}$$

and the one-electron states remain the same, $|\sigma(0,1)\rangle = d_{\rm R\sigma}^\dagger |0\rangle$. Here we introduced

$$\mathfrak{p} \equiv \frac{A_-}{2\sqrt{2}t} P, \quad \mathcal{N} \equiv \sqrt{1+\mathfrak{p}^2}, \quad A_\pm \equiv \frac{A_{\rm L} \pm A_{\rm R}}{2} \tag{13}$$

and the energies are found to be (see Fig. 3)

$$E_{T_\mathfrak{p}} = 0, \tag{14a}$$

$$E_{T_\pm} = \pm \left( g\mu_B B + \frac{1}{2} A_+ P \right), \tag{14b}$$

$$E_{S_\pm} = \pm \sqrt{2} t \mathcal{N}. \tag{14c}$$

Here the inter-dot tunneling mixes the two singlet states $|S(0,2)\rangle$ and $|S(1,1)\rangle$. Furthermore, these two singlets mix with the triplet $T_0$ due to the *difference* of the effective Overhauser fields in the two dots[36,42,45], $g\mu_B(B_{\rm nuc}^{\rm L} - B_{\rm nuc}^{\rm R}) = A_- P/2$. The triplet-singlet mixing is controlled by the dimensionless parameter $\mathfrak{p}$ given in Eq.(13). The *sum* of the effective Overhauser fields in the dots, $g\mu_B(B_{\rm nuc}^{\rm L} + B_{\rm nuc}^{\rm R}) = A_+ P$, splits the spin-polarized triplets $T_\pm$ as the magnetic field does. Therefore $E_{T_\pm}$ depend stronger on the polarization than the exchange energy splitting $|E_{S_\pm} - E_{T_\mathfrak{p}}| = \sqrt{2} t \mathcal{N}$ for small singlet-triplet mixing $\mathfrak{p} \ll 1$. Here, $\mathfrak{p}$ is indeed small, since we are interested in the limit of $A_-$ smaller than the inter-dot tunneling $t$. This also means that we can keep calling the

state $T_\mathfrak{p}$ a *triplet* state and the two states $S_\pm$ for *singlet* states (as indicated by the notation), even though that *strictly speaking* they are *not*.

In the SB regime, the triplets $T_\pm$ and $T_0$ block the transport through the DQD. Due to the singlet-triplet mixing, the state $T_\mathfrak{p}$ is not a blocking state anymore, whereas $T_\pm$ still block transport. Therefore, if the polarization is zero, $P = 0$, or the HF constants are equal, $A_- = 0$, then the triplet-singlet mixing is zero, $\mathfrak{p} = 0$, which in turn leads to transport blocking by all three triplets ($T_\mathfrak{p} \to T_0$).

From the form of the energy levels Eq.(14), it is clear that the crossing of the singlet and triplet energies always happens in pairs, e.g. $T_+$ and $S_+$ cross if and only if $T_-$ and $S_-$ cross. This is in contrast to the case of *finite* detuning, where a single singlet-triplet crossing can occur.[10,31–33,45] Moreover, within this model, the energy levels relative differences have certain symmetries around $E_{T_\mathfrak{p}}$: $E_{T_+} - E_{T_\mathfrak{p}} = E_{T_\mathfrak{p}} - E_{T_-}$ and $E_{S_+} - E_{T_+} = E_{T_-} - E_{S_-}$.

### B. The dynamical coupling of the nuclear spins to the DQD and the leakage current

We determine the dynamics of the electronic flow through the DQD in the SB regime by a rate equation approach.[15,16,34,35,37,42] To this end, we use the two-electron states (12) and the one-electron states $|\sigma\rangle$ (written with the short-hand notation $|\sigma\rangle = |\sigma(0,1)\rangle$ for $\sigma = \uparrow, \downarrow$). The rate equations for the average occupations $n_\nu$ of the seven electronic states $\nu = T_\pm, T_\mathfrak{p}, S_\pm, \uparrow, \downarrow$ are given by

$$\dot{n}_{T_+} = W_{T_+,S_+} n_{S_+} + W_{T_+,S_-} n_{S_-} + W_{T_+,T_\mathfrak{p}} n_{T_\mathfrak{p}} + \Gamma_{T_+,\uparrow} n_\uparrow - \big[W_{S_+,T_+} + W_{S_-,T_+} + W_{T_\mathfrak{p},T_+} + \Gamma^{\text{ine}}_{\uparrow,T_+} + \Gamma^{\text{ine}}_{\downarrow,T_+}\big] n_{T_+}, \quad (15a)$$

$$\dot{n}_{T_-} = W_{T_-,S_+} n_{S_+} + W_{T_-,S_-} n_{S_-} + W_{T_-,T_\mathfrak{p}} n_{T_\mathfrak{p}} + \Gamma_{T_-,\downarrow} n_\downarrow - \big[W_{S_+,T_-} + W_{S_-,T_-} + W_{T_\mathfrak{p},T_-} + \Gamma^{\text{ine}}_{\downarrow,T_-} + \Gamma^{\text{ine}}_{\uparrow,T_-}\big] n_{T_-}, \quad (15b)$$

$$\dot{n}_{T_\mathfrak{p}} = W_{T_\mathfrak{p},T_+} n_{T_+} + W_{T_\mathfrak{p},T_-} n_{T_-} + \Gamma_{T_\mathfrak{p},\uparrow} n_\uparrow + \Gamma_{T_\mathfrak{p},\downarrow} n_\downarrow - \big[W_{T_+,T_\mathfrak{p}} + W_{T_-,T_\mathfrak{p}} + \Gamma_{\uparrow,T_\mathfrak{p}} + \Gamma_{\downarrow,T_\mathfrak{p}} + \Gamma^{\text{ine}}_{\uparrow,T_\mathfrak{p}} + \Gamma^{\text{ine}}_{\downarrow,T_\mathfrak{p}}\big] n_{T_\mathfrak{p}}, \quad (15c)$$

$$\dot{n}_{S_+} = W_{S_+,T_+} n_{T_+} + W_{S_+,T_-} n_{T_-} + \Gamma_{S_+,\uparrow} n_\uparrow + \Gamma_{S_+,\downarrow} n_\downarrow - \big[W_{T_+,S_+} + W_{T_-,S_+} + \Gamma_{\uparrow,S_+} + \Gamma_{\downarrow,S_+}\big] n_{S_+}, \quad (15d)$$

$$\dot{n}_{S_-} = W_{S_-,T_+} n_{T_+} + W_{S_-,T_-} n_{T_-} + \Gamma_{S_-,\uparrow} n_\uparrow + \Gamma_{S_-,\downarrow} n_\downarrow - \big[W_{T_+,S_-} + W_{T_-,S_-} + \Gamma_{\uparrow,S_-} + \Gamma_{\downarrow,S_-}\big] n_{S_-}, \quad (15e)$$

$$\dot{n}_\uparrow = \Gamma_{\uparrow,S_+} n_{S_+} + \Gamma_{\uparrow,S_-} n_{S_-} + (\Gamma_{\uparrow,T_\mathfrak{p}} + \Gamma^{\text{ine}}_{\uparrow,T_\mathfrak{p}}) n_{T_\mathfrak{p}} + \Gamma^{\text{ine}}_{\uparrow,T_+} n_{T_+} + \Gamma^{\text{ine}}_{\uparrow,T_-} n_{T_-} - \big[\Gamma_{S_+,\uparrow} + \Gamma_{S_-,\uparrow} + \Gamma_{T_\mathfrak{p},\uparrow} + \Gamma_{T_+,\uparrow}\big] n_\uparrow, \quad (15f)$$

$$\dot{n}_\downarrow = \Gamma_{\downarrow,S_+} n_{S_+} + \Gamma_{\downarrow,S_-} n_{S_-} + (\Gamma_{\downarrow,T_\mathfrak{p}} + \Gamma^{\text{ine}}_{\downarrow,T_\mathfrak{p}}) n_{T_\mathfrak{p}} + \Gamma^{\text{ine}}_{\downarrow,T_-} n_{T_-} + \Gamma^{\text{ine}}_{\downarrow,T_+} n_{T_+} - \big[\Gamma_{S_+,\downarrow} + \Gamma_{S_-,\downarrow} + \Gamma_{T_\mathfrak{p},\downarrow} + \Gamma_{T_-,\downarrow}\big] n_\downarrow, \quad (15g)$$

where $\dot{n}_\nu$ denotes the time derivative of the average occupation $n_\nu$. Moreover, the normalization condition is $\sum_\nu n_\nu = 1$. Figure 4 provides an illustration of the rates connecting the different states and thereby of the above system of rate equations. Here we include three kinds of transitions: (i) The HF-induced spin-flip transitions $W_{f,i}$ within the DQD from the initial state $|i\rangle$ to the final state $|f\rangle$ (both two-electron states). (ii) The tunneling rates $\Gamma_{f,i}$ from $|i\rangle$ to $|f\rangle$, which connect the leads to the DQD. (iii) Finally, we include another inelastic escape rate $\Gamma^{\text{ine}}_{f,i}$ from the triplet states $T_\pm$ and $T_\mathfrak{p}$. The caption of Fig. 4 provides a more detailed description of these three kinds of rates, and they are explicitly given below in Sec. II C.

DNP occurs as a result of angular momentum transfer from the electrons to the nuclei. Therefore, in order to obtain non-zero DNP the system needs to have a preferred direction of angular momentum transfer. *If* HF interaction is the *only* source of SB lifting, then no such preferred direction exist. The reason is that HF-induced escape from the two spin-polarized triplets $T_\pm$ changes the polarization in opposite directions and since the probabilities of loading $T_+$ and $T_-$ are equal ($\Gamma_{T_+,\uparrow} = \Gamma_{T_-,\downarrow}$), no net nuclear polarization builds up.[19,30,33,34] This is so, even though the HF-induced escape rates from $T_\pm$ might be very different, but since only a single way to escape the blocking state exist, it does not matter if escaping from $T_+$ or $T_-$ is the fastest.

Here we allow *two* ways to escape from the triplet states in the DQD, both lifting SB. Either by the HF-induced spin-flip transitions $W_{f,i}$ or by the inelastic escape rates $\Gamma^{\text{ine}}_{f,i}$. The additional inelastic rates can for instance be provided by co-tunneling[12–16] or spin-orbit mediated[19–23] spin relaxation processes. The important point is that the inelastic processes contained in $\Gamma^{\text{ine}}_{f,i}$ give an additional escape path from the triplets *without* a nuclear spin flip in contrast to the HF-induced escape paths. Therefore, the two escape paths from the blocking states now compete, such that it becomes important which of the HF-induced escape paths from $T_+$ or $T_-$ is the fastest. This competition is therefore crucial to obtain non-zero DNP.[19,33,34] Here we follow Rudner *et al.*[33–36] and do not specify the inelastic escape rate further.

Every time the nuclear spins mediate an electronic spin-flip, a nuclear spin also flips. This changes the polarization by an amount $dP = \pm 2/N$ depending on the transition, see Fig. 4 and Eq.(9). Therefore in the case of competing escape rates in the DQD, we describe the

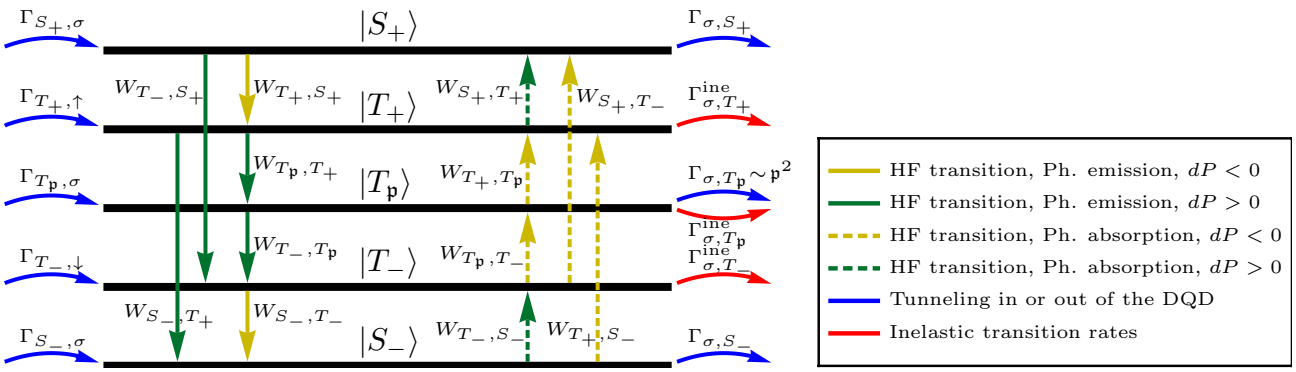


FIG. 4. (Color online) Illustration of the transition rates connecting the various states. Each hyperfine-induced transition $W_{f,i}$ between two two-electron states flips the electronic spin in one direction, while flipping a nuclear spin in the opposite direction and thereby conserves angular momentum. From the definition of the nuclear polarization $P$ in Eq.(9), it follows that a single nuclear spin flip will change $P$ by $dP=+2/N$ or $dP=-2/N$ depending on the transition – as specified in the label of the figure. Furthermore, we allow for the emission or absorption of energy in the form of e.g. a phonon (ph.) in the hyperfine-induced spin-flip processes. Thus, transitions between misaligned energy levels can also happen. Hyperfine-induced transitions become less probable the larger the energy difference between the electronic levels. Moreover, as discussed in the main text, absorption of a phonon is suppressed by a factor of $e^{-\Delta E/k_{\text{B}}T}$ compared to emission, where $\Delta E>0$ is the energy difference between the electronic levels. In the figure, additional inelastic escape rates $\Gamma^{\text{ine}}_{f,i}$ from the triplets are also included (red arrows). These rates do not flip a nuclear spin and therefore the competition between these and the hyperfine-induced rates creates the possibility of non-zero DNP.[19,33,34] Here we work in the high bias limit, such that electrons can only tunnel into the system from the left lead and only leave the system to the right lead (blue arrows). This means that transitions from one-electron states to two-electron states is *always* associated with tunneling into the DQD from the left lead. Vice versa tunneling out of the DQD to the right lead is always related to a transition from a two-electron to a one-electron state, as illustrated in the figure. Note that in this figure, we have chosen a particular order in energy of the electronic levels. This order depends on the exchange energy $\sqrt{2}t\mathcal{N}$, the magnetic field and the DNP as evident from Eq.(14).

DNP, $P$, by the rate equation

$$\begin{aligned}\dot{P}=\frac{2}{N}\Big[&\left(W_{T_-,S_+}-W_{T_+,S_+}\right)n_{S_+}\\&+\left(W_{T_-,S_-}-W_{T_+,S_-}\right)n_{S_-}+\left(W_{T_-,T_\mathfrak{p}}-W_{T_+,T_\mathfrak{p}}\right)n_{T_\mathfrak{p}}\\&+\left(W_{S_+,T_+}+W_{S_-,T_+}+W_{T_\mathfrak{p},T_+}\right)n_{T_+}\\&-\left(W_{S_+,T_-}+W_{S_-,T_-}+W_{T_\mathfrak{p},T_-}\right)n_{T_-}\Big].\end{aligned}\tag{16}$$

Similar rate equations for the DNP have been used in several other studies.[31,33–37,96] The idea behind the rate equation (16) is to describe a competition between various rates that polarize the nuclear spins in opposite directions, which is different from the aforementioned competition between various escape paths. However, in order to *have* a competition between various rates that polarize the nuclei in the first place, it is strictly necessary to have competing escape paths, i.e. to have both $W_{f,i}$ and $\Gamma^{\text{ine}}_{f,i}$ non-zero. In section V, we show that the rate equation approach (15-16) fails without the inelastic escape rate, $\Gamma^{\text{ine}}_{f,i}=0$. Moreover, we validate the rate equation description in the limit of $\Gamma^{\text{ine}}_{f,i}\neq 0$, by showing that it leads to the same results as a Monte Carlo simulation.

Furthermore, we neglect processes leading to depolarization of the nuclear bath in equilibrium,[110] since these are much slower than the HF spin-flip processes during transport through the DQD.[10,52,64]

Here we consider the *high bias limit*, where electrons only can enter the DQD from the left lead and leave it to the right lead. Therefore, we can easily find the particle leakage current $I$ through the DQD by all the transition processes from the two-electron states to the one-electron states, i.e.

$$\begin{aligned}I=\sum_{\sigma=\uparrow,\downarrow}\Big[&\Gamma^{\text{ine}}_{\sigma,T_+}n_{T_+}+\Gamma^{\text{ine}}_{\sigma,T_-}n_{T_-}+(\Gamma^{\text{ine}}_{\sigma,T_\mathfrak{p}}+\Gamma_{\sigma,T_\mathfrak{p}})n_{T_\mathfrak{p}}\\&+\Gamma_{\sigma,S_+}n_{S_+}+\Gamma_{\sigma,S_-}n_{S_-}\Big].\end{aligned}\tag{17}$$

Therefore, in order to find the stationary leakage current $I$, we need to solve the non-linear system of rate equations (15-16), which is done below both by analytical and numerical means.

### C. The transition rates

Now we give the transition rates used in the explicit calculations.

### 1. The inelastic escape rates

We are interested in the limit where the largest of the HF-induced spin-flip rates dominates over the inelastic escape rates close to the level crossings. Experimentally, the magnitude of the co-tunneling rates can be decreased by tuning the level positions compared to the Fermi levels of the leads[12], while the spin-orbit strength for instance can be decreased by material choice.[19] For simplicity, we take the inelastic escape rates to be equal and constant following Refs. [33–36], i.e.

$$\Gamma^{\rm ine}_{\sigma,T_+} = \Gamma^{\rm ine}_{\sigma,T_-} = \Gamma^{\rm ine}_{\sigma,T_{\mathfrak{p}}} \equiv \Gamma^{\rm ine} \quad \text{for} \quad \sigma = \uparrow,\downarrow . \tag{18}$$

Since the HF rates dominate close to the energy level crossings, leaving out the energy dependence of the inelastic rate plays less of a role.[33–36] In Appendix A some discussion on non-equal inelastic rates is given.

### 2. The tunneling rates

The tunneling rates between the leads and the DQD are found by the Fermi golden rule using $H_{\rm T}$ (6b). In general, the rates for tunneling into (out of) the DQD are proportional to (one minus) the Fermi distribution of the corresponding lead.[107] Since we work in the *high bias limit*, only tunneling from the left lead to the DQD and from the DQD to the right lead is present, and we can leave out the Fermi functions from the explicit expressions of the tunneling rates.

The non-zero transition rates for tunneling into the DQD from the left lead are found to be[42]

$$\Gamma_{T_+,\uparrow} = \Gamma_{T_-,\downarrow} = \Gamma_{\rm L}, \tag{19a}$$

$$\Gamma_{T_{\mathfrak{p}},\uparrow} = \Gamma_{T_{\mathfrak{p}},\downarrow} = \frac{\Gamma_{\rm L}}{2}\frac{1}{\mathcal{N}^2}, \tag{19b}$$

$$\Gamma_{S_+,\uparrow} = \Gamma_{S_-,\downarrow} = \frac{\Gamma_{\rm L}}{4}\left(1-\frac{\mathfrak{p}}{\mathcal{N}}\right)^2, \tag{19c}$$

$$\Gamma_{S_-,\uparrow} = \Gamma_{S_+,\downarrow} = \frac{\Gamma_{\rm L}}{4}\left(1+\frac{\mathfrak{p}}{\mathcal{N}}\right)^2, \tag{19d}$$

and the non-zero transition rates for tunneling out of the DQD to the right lead are (for $\sigma = \uparrow,\downarrow$)

$$\Gamma_{\sigma,T_{\mathfrak{p}}} = \Gamma_{\rm R}\frac{\mathfrak{p}^2}{\mathcal{N}^2}, \tag{20a}$$

$$\Gamma_{\sigma,S_+} = \Gamma_{\sigma,S_-} = \frac{\Gamma_{\rm R}}{2}\frac{1}{\mathcal{N}^2}, \tag{20b}$$

i.e. the probability of leaving behind a single electron in the right dot with spin up or down are equal. It is seen that the rate of leaving $T_{\mathfrak{p}}$ goes to zero for $\mathfrak{p} \to 0$ (i.e. $P \to 0$ or $A_{\rm L} \to A_{\rm R}$), since the triplet-singlet mixing vanish such that $T_{\mathfrak{p}}$ becomes a blocking state. Here we introduced the energy-independent $\Gamma_\alpha = 2\pi|t_{\alpha k}|^2 D_\alpha$ for $\alpha = {\rm L},{\rm R}$ in the standard wide-band approximation,[107,111,112] where $D_\alpha$ is the density of states of lead $\alpha$.

To get an overview of the tunneling matrix elements and for the calculations below, it is helpful to note that they are invariant under the simultaneous interchange of

$$\uparrow \leftrightarrow \downarrow, \quad T_+ \leftrightarrow T_- \quad \text{and} \quad S_+ \leftrightarrow S_-. \tag{21}$$

### 3. The hyperfine-induced spin-flip rates

The HF-induced spin-flip rates are calculated perturbatively in $H^{\rm sf}_{\rm HF}$ Eq.(10) using the Fermi golden rule.[33,34,37,42,107] The transition from, say, $T_+$ to $S_+$ decreases the electronic angular momentum by one and therefore a nuclear spin has to flip from down to up. Thus, the transition $T_+ \to S_+$ requires the presence of a spin down among the nuclei, and the transition rate $W_{S_+,T_+}$ is therefore proportional to the probability of finding a random nuclear spin to be spin down: i.e. $W_{S_+,T_+} \propto N_\downarrow/N$, where $N_\sigma$ is the number of nuclei with spin $\sigma = \downarrow,\uparrow$ and $N = N_\uparrow + N_\downarrow$ is the total number of nuclei.[33,34,37,42,113] Likewise the other HF-induced spin-flip rates $W_{f,i}$ are proportional to either

$$\frac{N_\downarrow}{N} = \frac{1-P}{2} \quad \text{or} \quad \frac{N_\uparrow}{N} = \frac{1+P}{2} \tag{22}$$

depending on the direction of the nuclear spin-flip in the process, see Fig. 4. Here the definition (9) was used.

Furthermore, we allow the HF-induced spin-flip transitions to exchange energy with the environment in the form of e.g. phonons.[27,37,61,78,88,114–116] Experimentally, phonon emission has been shown to be significant even at low temperatures in transport through quantum dots.[100,115] In the transition between the electronic states, it is much easier to give away energy in the form of phonon emission compared to absorbing energy by phonon absorption.[100,101] The reason is that the rate for *absorbing* an energy of $\hbar\omega$ is proportional to the phonon occupation factor $n_B(\hbar\omega)$, while the rate for *emitting* an energy of $\hbar\omega$ is proportional to $n_B(\hbar\omega)+1$ (due to the bosonic nature of phonons). Here $n_B(E) = [e^{E/k_{\rm B}T}-1]^{-1}$ is the Bose function at temperature $T$.[88,100,101,114] Thus, the absorption rate is suppressed by $n_B(\hbar\omega)/[n_B(\hbar\omega)+1] = e^{-\hbar\omega/k_{\rm B}T}$ compared to the emission rate, which we show below to be crucial for the DNP bistability at zero detuning.

Now we have discussed the two main physical ingredients of the HF rates $W_{f,i}$ given below: (i) They include the asymmetry between absorption and emission of phonons and, (ii) they are proportional to the number of the relevant nuclei spin species needed for the transition (22). A detailed derivation of the rates used here is given in Ref. 42. The non-zero HF-induced spin-flip

rates between the triplets are found to be

$$W_{T_\mathfrak{p},T_+} = W_{T_-,T_\mathfrak{p}} \tag{23a}$$
$$= \frac{1}{2N}\left[\frac{1-P}{2}\right]\left[\frac{\sqrt{2}A_+}{\mathcal{N}}\right]^2 \mathcal{F}_{ph}(E_{T_+} - E_{T_\mathfrak{p}}),$$
$$W_{T_+,T_\mathfrak{p}} = W_{T_\mathfrak{p},T_-} \tag{23b}$$
$$= \frac{1}{2N}\left[\frac{1+P}{2}\right]\left[\frac{\sqrt{2}A_+}{\mathcal{N}}\right]^2 \mathcal{F}_{ph}(E_{T_\mathfrak{p}} - E_{T_+}),$$

where $\mathcal{F}_{ph}(E_i - E_f)$ is the phonon part of the rate – depending only on the energy difference between the initial and final state.[117] Note that $E_{T_\mathfrak{p}} - E_{T_-} = E_{T_+} - E_{T_\mathfrak{p}}$ follows from Eq.(14). The non-zero HF-induced spin-flip rates between the singlets and triplets are

$$W_{S_+,T_+} = W_{T_-,S_-} \tag{24a}$$
$$= \frac{1}{2N}\left[\frac{1-P}{2}\right]\left[A_- - \frac{\mathfrak{p}A_+}{\mathcal{N}}\right]^2 \mathcal{F}_{ph}(E_{T_+} - E_{S_+}),$$
$$W_{T_+,S_+} = W_{S_-,T_-} \tag{24b}$$
$$= \frac{1}{2N}\left[\frac{1+P}{2}\right]\left[A_- - \frac{\mathfrak{p}A_+}{\mathcal{N}}\right]^2 \mathcal{F}_{ph}(E_{S_+} - E_{T_+}),$$
$$W_{S_-,T_+} = W_{T_-,S_+} \tag{24c}$$
$$= \frac{1}{2N}\left[\frac{1-P}{2}\right]\left[A_- + \frac{\mathfrak{p}A_+}{\mathcal{N}}\right]^2 \mathcal{F}_{ph}(E_{T_+} - E_{S_-}),$$
$$W_{T_+,S_-} = W_{S_+,T_-} \tag{24d}$$
$$= \frac{1}{2N}\left[\frac{1+P}{2}\right]\left[A_- + \frac{\mathfrak{p}A_+}{\mathcal{N}}\right]^2 \mathcal{F}_{ph}(E_{S_-} - E_{T_+}),$$

remembering that $E_{T_+} - E_{S_-} = E_{S_+} - E_{T_-}$ from Eq.(14) such that the difference between initial and final states are the same for e.g. $W_{S_-,T_+}$ and $W_{T_-,S_+}$. In the explicit calculations, we use the function

$$\mathcal{F}_{ph}(E_i - E_f) = \frac{\gamma_{ph}}{\gamma_{ph}^2 + (E_i - E_f)^2} c(E_i - E_f) \tag{25}$$

to account for the phonon emission/absorption. Here $\gamma_{ph}$ is a characteristic phonon energy scale (e.g.[100] $\gamma_{ph} \sim \mu$eV) and $c(E_i - E_f) = \theta(E_i - E_f) + \theta(E_f - E_i)e^{-(E_f - E_i)/k_\text{B}T}$ is the crucial factor that exponentially suppresses the absorption of energy compared to emission. Here $\theta(E)$ is the unit step function. Therefore, we disregard many details of the phonon description for simplicity. We only include two important aspects: (i) the asymmetry between absorption and emission of energy (as discussed above) and (ii) that the further apart the energy levels are, the less probable a transition becomes – included phenomenologically in the Lorentzian.[37,38,42] In order to do a more detailed description of the phonon part of the rates, both $H_\text{HF}^\text{sf}$ and the electron-phonon interaction could be included as perturbations in a $T$-matrix approach[107], which gives a description with more parameters depending on e.g. the material.[61,88,114]

An important difference between the triplet-triplet and singlet-triplet rates, is that the triplet-triplet rates Eq.(23) are proportional to $A_+^2$, whereas the singlet-triplet rates Eq.(24) have a common prefactor of $A_-^2$ (remembering that $\mathfrak{p} \propto A_-$). Therefore, the strength of the two kinds of rates near the respective crossings are very different, and the singlet-triplet rates are sensitive to the difference in the Overhauser field between the dots in contrast to the triplet-triplet rates. Nevertheless, it is worth to note that if $A_\text{R} = A_\text{L}$, then all three triplets are blocking states, since the triplet-singlet mixing is zero ($\mathfrak{p} = 0$) such that $\Gamma_{\sigma,T_\mathfrak{p}} = 0$, see Eq.(20a).

Finally, we observe that the HF-induced rates Eqs.(23-24) are invariant under the interchange of

$$\uparrow \leftrightarrow \downarrow,\ T_+ \leftrightarrow T_-,\ S_+ \leftrightarrow S_- \text{ and initial} \leftrightarrow \text{final}. \tag{26}$$

This is not the same as the invariances for the tunneling rates in Eq.(21), since we also have to interchange the final and initial state for $W_{f,i}$.

## III. THE CROSSING OF THE TRIPLETS

In this section, we analyze the DNP and leakage current close to the crossing of the three triplets $T_-$, $T_\mathfrak{p}$ and $T_+$, i.e. close to zero magnetic field. Since $T_\mathfrak{p}$ is not a pure triplet state (due to its small singlet component, see Eq.(12c)), it is not a blocking state, and therefore allows for leakage current. As we shall see below, analytical insights – such as the *transition temperature* – can be achieved from the rate equations (15-16) in this case.

### A. The implicit equation for the nuclear polarization and the simplified rate equations

Now we derive an implicit equation for the DNP $P$ from a simplified system of rate equations - valid close to the crossing of the triplet levels. We use the limit of large energy separation between the triplet and singlet levels compared to $\gamma_{ph}$. This can be obtained by having the inter-dot tunneling $t$ much larger than $\gamma_{ph}$ and sweeping the magnetic field close to zero. In this limit, the HF-induced spin-flip rates between the singlets and triplets in Eq.(24) are negligible compared to the HF-induced triplet-triplet rates Eq.(23). Thus, neglecting all singlet-triplet rates and using equal inelastic escape rates $\Gamma^\text{ine}$ Eq.(18), the system of rate equations (15) for the average occupations simplifies to

$$\dot{n}_{T_+} = W_{T_+,T_\mathfrak{p}} n_{T_\mathfrak{p}} + \Gamma_{T_+,\uparrow} n_\uparrow - [W_{T_\mathfrak{p},T_+} + 2\Gamma^{\text{ine}}] n_{T_+}, \tag{27a}$$

$$\dot{n}_{T_-} = W_{T_-,T_\mathfrak{p}} n_{T_\mathfrak{p}} + \Gamma_{T_-,\downarrow} n_\downarrow - [W_{T_\mathfrak{p},T_-} + 2\Gamma^{\text{ine}}] n_{T_-}, \tag{27b}$$

$$\dot{n}_{T_\mathfrak{p}} = W_{T_\mathfrak{p},T_+} n_{T_+} + W_{T_\mathfrak{p},T_-} n_{T_-} + \Gamma_{T_\mathfrak{p},\uparrow} n_\uparrow + \Gamma_{T_\mathfrak{p},\downarrow} n_\downarrow - \left[W_{T_+,T_\mathfrak{p}} + W_{T_-,T_\mathfrak{p}} + \Gamma_{\uparrow,T_\mathfrak{p}} + \Gamma_{\downarrow,T_\mathfrak{p}} + 2\Gamma^{\text{ine}}\right] n_{T_\mathfrak{p}}, \tag{27c}$$

$$\dot{n}_{S_+} = \Gamma_{S_+,\uparrow} n_\uparrow + \Gamma_{S_+,\downarrow} n_\downarrow - \left[\Gamma_{\uparrow,S_+} + \Gamma_{\downarrow,S_+}\right] n_{S_+}, \tag{27d}$$

$$\dot{n}_{S_-} = \Gamma_{S_-,\uparrow} n_\uparrow + \Gamma_{S_-,\downarrow} n_\downarrow - \left[\Gamma_{\uparrow,S_-} + \Gamma_{\downarrow,S_-}\right] n_{S_-}, \tag{27e}$$

$$\dot{n}_\uparrow = \Gamma_{\uparrow,S_+} n_{S_+} + \Gamma_{\uparrow,S_-} n_{S_-} + (\Gamma_{\uparrow,T_\mathfrak{p}} + \Gamma^{\text{ine}}) n_{T_\mathfrak{p}} + \Gamma^{\text{ine}}(n_{T_+} + n_{T_-}) - \left[\Gamma_{S_+,\uparrow} + \Gamma_{S_-,\uparrow} + \Gamma_{T_\mathfrak{p},\uparrow} + \Gamma_{T_+,\uparrow}\right] n_\uparrow, \tag{27f}$$

$$\dot{n}_\downarrow = \Gamma_{\downarrow,S_+} n_{S_+} + \Gamma_{\downarrow,S_-} n_{S_-} + (\Gamma_{\downarrow,T_\mathfrak{p}} + \Gamma^{\text{ine}}) n_{T_\mathfrak{p}} + \Gamma^{\text{ine}}(n_{T_-} + n_{T_+}) - \left[\Gamma_{S_+,\downarrow} + \Gamma_{S_-,\downarrow} + \Gamma_{T_\mathfrak{p},\downarrow} + \Gamma_{T_-,\downarrow}\right] n_\downarrow, \tag{27g}$$

as illustrated in Fig. 5. Similarly, Eq.(16) for the time evolution of $P$ simplifies to

$$\dot{P} = \frac{2}{N}\Big[(W_{T_-,T_\mathfrak{p}} - W_{T_+,T_\mathfrak{p}}) n_{T_\mathfrak{p}} + W_{T_\mathfrak{p},T_+} n_{T_+} - W_{T_\mathfrak{p},T_-} n_{T_-}\Big]. \tag{28}$$

In this approximation, the rate equations for the triplet and singlet occupations *only* couple indirectly through the occupations for the one-electron states $n_\sigma$. Moreover, we avoid to use very low temperatures, where the approximation could fail.[118]

We wish to find the stationary DNP, i.e. solve the system of rate equations (27) and (28) for $\dot{P} = 0$ and $\dot{n}_\nu = 0$ for all $\nu$. To this end, we subtract $\dot{n}_\downarrow$ Eq.(27g) from $\dot{n}_\uparrow$ Eq.(27f) and use the symmetries under interchange of indices for the tunneling rates (see Eqs.(19-21)), i.e.

$$\dot{n}_\uparrow - \dot{n}_\downarrow = (\Gamma_{T_+,\uparrow} + \Gamma_{S_+,\downarrow} + \Gamma_{S+,\uparrow} + \Gamma_{T_\mathfrak{p},\sigma})(n_\downarrow - n_\uparrow) \quad \text{such that} \quad n_\downarrow = n_\uparrow \tag{29}$$

in the stationary limit. Using the symmetries for the tunneling rates and the HF rates, the relation (29) leads to

$$\dot{n}_{T_+} - \dot{n}_{T_-} + \frac{N}{2}\dot{P} = 2\Gamma^{\text{ine}}(n_{T_-} - n_{T_+}) = 0 \quad \text{i.e.} \quad n_{T_+} = n_{T_-} \tag{30}$$

in the stationary limit. Therefore Eq.(28) for $\dot{P} = 0$ becomes

$$\dot{P} = \frac{2}{N}\left(W_{T_\mathfrak{p},T_+} - W_{T_+,T_\mathfrak{p}}\right)\left(n_{T_\mathfrak{p}} + n_{T_+}\right) = 0 \tag{31}$$

using that $W_{T_\mathfrak{p},T_-} = W_{T_+,T_\mathfrak{p}}$ and $W_{T_-,T_\mathfrak{p}} = W_{T_\mathfrak{p},T_+}$, see Eq.(23). Thus, since the occupations are positive, we arrive at

$$W_{T_\mathfrak{p},T_+} = W_{T_+,T_\mathfrak{p}}, \tag{32}$$

which is *the implicit equation for the steady state DNP* $P$ – remembering that both rates depend on $P$ explicitly and through the Overhauser split energy levels $E_{T_\pm}$ [see Eq.(23)]. Equivalently, this can be written as $W_{T_\mathfrak{p},T_-} = W_{T_-,T_\mathfrak{p}}$ using Eq.(23). Physically, the relation (32) means that the polarization stabilizes at a value such that the phonon emission and absorption transitions between the two levels $T_\mathfrak{p}$ and $T_+$ ($T_-$) become equally probable. Inserting Eq.(23), the relation (32) can be rewritten as

$$\frac{1+P}{1-P} = \frac{\mathcal{F}_{ph}(E_{T_+} - E_{T_\mathfrak{p}})}{\mathcal{F}_{ph}(E_{T_\mathfrak{p}} - E_{T_+})}. \tag{33}$$

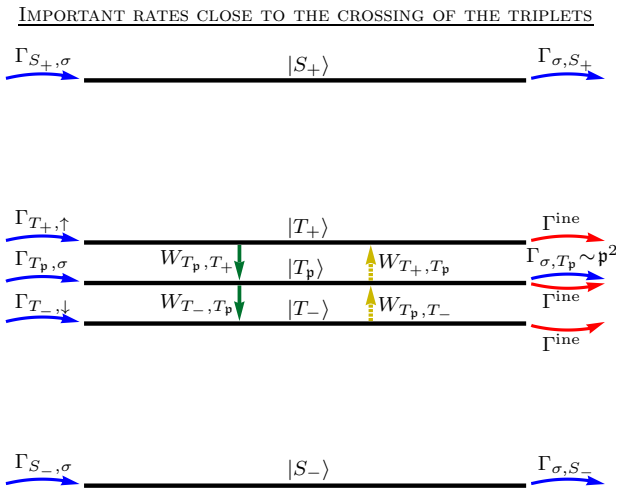


FIG. 5. (Color online) The relevant transition rates in the limit of large energy separation between the singlets and triplets and close to the crossing of the three triplets, i.e. the limit used in the rate equations (27). In this case, only hyperfine-induced spin-flip rates between the triplets are effective: $W_{T_+,T_\mathfrak{p}} = W_{T_\mathfrak{p},T_-}$ Eq.(23b) (vertical yellow dashed arrows) polarizing the nuclei negatively ($dP < 0$) and $W_{T_\mathfrak{p},T_+} = W_{T_-,T_\mathfrak{p}}$ Eq.(23a) (vertical green full arrows) polarizing the nuclei positively ($dP > 0$). The tunneling in and out of the DQD $\Gamma_{f,i}$ (blue arrows) and the inelastic escape rates $\Gamma^{\text{ine}}$ (red arrows) are the same as shown in Fig. 4. In the present case, we show in Sec. III A that the stationary polarization is determined by the condition that all triplet-triplet rates are equal: $W_{T_+,T_\mathfrak{p}} = W_{T_\mathfrak{p},T_+} = W_{T_\mathfrak{p},T_-} = W_{T_-,T_\mathfrak{p}}$.

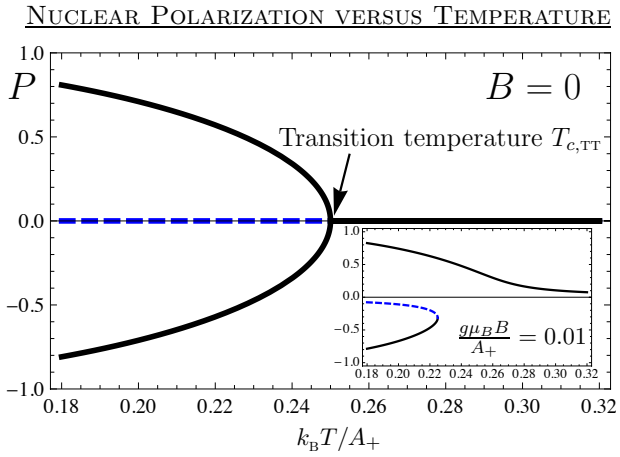


FIG. 6. (Color online) The dynamical nuclear polarization $P$ versus temperature in units of the average hyperfine coupling, $k_\mathrm{B}T/A_+$, at zero external magnetic field $B = 0$ (main figure) and at finite magnetic field $g\mu_B B/A_+ = 0.01$ (inset). Both figures are obtained by solving numerically the implicit equation (34) for the polarization. For zero magnetic field and below the transition temperature $T_{c,\mathrm{TT}} = \frac{1}{4k_\mathrm{B}}A_+$, the polarization have two stable solutions (full black lines) and one unstable solution (dashed blue line). Above $T_{c,\mathrm{TT}}$, only a single stable polarization exist. Similar behavior is found in the case of a finite external magnetic field in the inset, but here the multiple polarization solutions appear at a lower temperature.

This shows that the polarization $P$ is insensitive to the part of $\mathcal{F}_{ph}$, which is even in energy, and therefore *only* depends on the difference between emission and absorption of energy. In other words, the even-energy part of the phonon function $\mathcal{F}_{ph}$ cancels out on the right-hand side of Eq.(33) and we are left with the ratio between absorbing and emitting energy in the transition. This means that the DNP is largely independent of the way the phonons are modeled in the HF-induced rates, as long as the important asymmetry between emission and absorption of energy is included.[119] Furthermore, here we observe a crucial difference to the works of Rudner *et al.*[33–36], where non-zero DNP is only found at non-zero detuning, since emission and absorption of energy is modeled as being equally likely in these works (see also Sec. I C). Finally, by inserting the energies in Eq.(14) into Eq.(33), we end up with the following implicit equation for the DNP

$$P = \tanh\left(\frac{g\mu_B B + \frac{1}{2}A_+ P}{2k_\mathrm{B}T}\right). \tag{34}$$

From this equation, it is not possible to obtain a closed analytical expression for $P$. Remarkably, it shows that the polarization $P$ near the crossing of the triplet levels *only* depends on the Zeeman splitting $g\mu_B B/A_+$ and the temperature $k_\mathrm{B}T/A_+$ — both measured in units of the average HF constant of the two dots $A_+ = (A_\mathrm{L} + A_\mathrm{R})/2$.

The form of the implicit equation (34) resembles the one found by using mean-field theory to a Heisenberg spin model, which describes the equilibrium ferromagnetic phase transition driven by temperature.[107] In contrast, here the nuclear polarization is dynamically driven by the current passing through the DQD, i.e. a *non-equilibrium* situation.

The DNP can now easily be found by solving Eq.(34) numerically, which leads to the polarization versus temperature for $B = 0$ and $B \neq 0$ seen in Fig. 6. For $B = 0$, the polarization has a bifurcation at a certain transition temperature $T_{c,\mathrm{TT}}$, where the system goes from having one stable polarization for $T > T_{c,\mathrm{TT}}$ to having two stable polarizations and an unstable one for $T < T_{c,\mathrm{TT}}$. The stability of the polarization solutions are found by numerical iteration of the set of differential equations.[120] The *transition temperature* for $B = 0$ is readily found from Eq.(34) to be[121]

$$k_\mathrm{B}T_{c,\mathrm{TT}} = \frac{1}{4}A_+. \tag{35}$$

This is a remarkably simple and insightful result. It shows that the transition temperature $T_{c,\mathrm{TT}}$ is given *only* by the average HF coupling $A_+ = (A_\mathrm{L} + A_\mathrm{R})/2$. For $T < T_{c,\mathrm{TT}}$ the DNP can have two stable values and therefore so can the leakage current. In other words, the leakage current can show a *hysteretic behavior* for $T < T_{c,\mathrm{TT}}$, while the hysteresis disappears for $T \geq T_{c,\mathrm{TT}}$.

For $B \neq 0$, the DNP also has multiple solutions below a certain temperature, which is generally lower than the transition temperature $T_{c,\mathrm{TT}}$ Eq.(35) for $B = 0$ (see the inset of Fig. 6 for an example). Figure 7 shows the number of DNP solutions for a specific value of $g\mu_B B$ and $k_\mathrm{B}T$. From Fig. 7 it is evident that by sweeping the external magnetic field $B$, the region of multiple solutions of DNP – and therefore also current hysteresis – becomes broader the lower the temperature. Especially, multiple solutions appears only for $T < T_{c,\mathrm{TT}}$, which underlines the importance of the transition temperature $T_{c,\mathrm{TT}} = A_+/(4k_\mathrm{B})$ in connection to the leakage current hysteresis. The leakage current and its hysteresis will be treated in greater detail in Sec. III B.

For $B = 0$ and close to the transition temperature, it is possible to expand the right-hand side of Eq.(34) in $|P| \ll 1$. This gives that the polarization vanishes close to $T_{c,\mathrm{TT}}$ as $P \propto \pm[(T_{c,\mathrm{TT}} - T)/T_{c,\mathrm{TT}}]^{1/2}$ for $0 \leq (T_{c,\mathrm{TT}} - T)/T_{c,\mathrm{TT}} \ll 1$. This is typical behavior for mean-field theories[107] as the one used here [see Eq.(8)].

Above equal inelastic escape rates are used. If we instead use non-equal inelastic rates following the symmetries (21) under interchange of indices, then the implicit equation (32) for the DNP and the transition temperature (35) remain *unchanged*, see Appendix A. However, in other cases the polarization condition (32) and transition temperature might change.

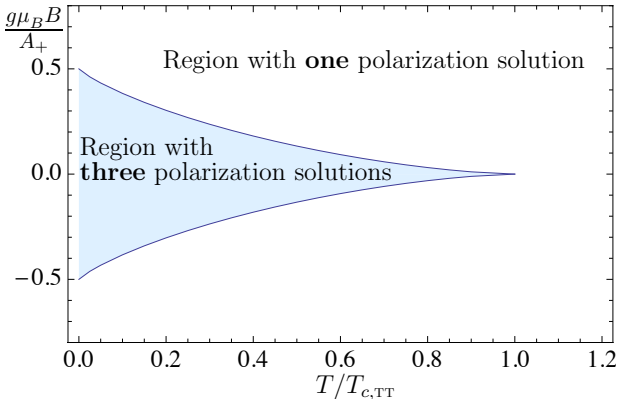


FIG. 7. (Color online) The regions in parameter space with one (white region) or three (blue region) solutions of the dynamical nuclear polarization, respectively. These regions are found by solving numerically the implicit equation (34) for the polarization $P$, valid close to the crossing of the triplets. Out of the three polarization solutions in the blue region, only two are stable against small fluctuations. From Eq.(34), it is evident that the polarization *only* depend on $g\mu_B B/A_+$ (vertical axis) and $T/T_{c,\mathrm{TT}}$ (horizontal axis), where $T_{c,\mathrm{TT}} = A_+/(4k_\mathrm{B})$. The polarization versus magnetic field for fixed temperature seen in Fig. 8, corresponds to vertical sweeps in this figure.

### B. The leakage current and the occupations close to the crossing of the triplets

#### 1. *Analytical stationary occupation and current expressions in terms of the rates*

Next, we find the leakage current close to the crossing of the three triplets. As before, we analyze the limit of the singlet-triplet rates being negligible compared to the triplet-triplet spin-flip rates and equal inelastic escape rates, i.e. the stationary limit of the rate equations (27) and (28).

In order to find the leakage current, we first find the stationary average occupations. Previously in Eq.(29) and (30), we found that $n_\downarrow = n_\uparrow$ and $n_{T_+} = n_{T_-}$, which lead to the implicit equation for the polarization (32), i.e.

$$W_{T_\mathfrak{p},T_+} = W_{T_+,T_\mathfrak{p}} = W_{T_\mathfrak{p},T_-} = W_{T_-,T_\mathfrak{p}} \tag{36}$$

in steady state. Furthermore, subtracting $\dot{n}_{S_+}$(27d) and $\dot{n}_{S_-}$ (27e) [and using $n_\uparrow = n_\downarrow$ and the index invariances of the tunneling rates Eqs.(19-21)], we find

$$\begin{aligned} &\dot{n}_{S_+} - \dot{n}_{S_-} = 2\Gamma_{\uparrow,S_+}(n_{S_-} - n_{S_+}) = 0 \\ &\text{such that} \quad n_{S_-} = n_{S_+} \end{aligned} \tag{37}$$

in the stationary limit. This in turn simplifies the sum of $\dot{n}_{S_+}$ (27d) and $\dot{n}_{S_-}$ (27e), $\dot{n}_{S_+} + \dot{n}_{S_-} = 0$, and therefore leads to

$$n_{S_+} = \frac{\Gamma_{S_+,\downarrow} + \Gamma_{S_+,\uparrow}}{2\Gamma_{\uparrow,S_+}}\, n_\uparrow \tag{38}$$

by again using $n_\uparrow = n_\downarrow$ and the symmetries under exchange of indices of the tunneling rates Eqs.(19-21). Inserting the above relations between the occupations into the normalization condition $\sum_\nu n_\nu = 1$, we get

$$n_\uparrow = \frac{\Gamma_{\uparrow,S_+}}{\Upsilon}[1 - n_{T_\mathfrak{p}} - 2n_{T_+}], \tag{39a}$$

where

$$\Upsilon \equiv 2\Gamma_{\uparrow,S_+} + \Gamma_{S_+,\downarrow} + \Gamma_{S_+,\uparrow}. \tag{39b}$$

By inserting Eqs.(29), (30), (32), (37), (38) and (39) into $\dot{n}_{T_\mathfrak{p}} = 0$ (27c) and $\dot{n}_{T_+} + \dot{n}_{T_-} = 0$ (27a-27b), we obtain two coupled equations for the occupations $n_{T_\mathfrak{p}}$ and $n_{T_+}$ with the solution

$$n_{T_\mathfrak{p}} = \frac{\Gamma_{\uparrow,S_+}\big[2\Gamma^{\mathrm{ine}}\Gamma_{T_\mathfrak{p},\uparrow} + W_{T_+,T_\mathfrak{p}}(\Gamma_{T_+,\uparrow}+\Gamma_{T_\mathfrak{p},\uparrow})\big]}{\Lambda}, \tag{40a}$$

$$n_{T_+} = \frac{\Gamma_{\uparrow,S_+}}{\Lambda}\Big[\Gamma_{T_+,\uparrow}(\Gamma^{\mathrm{ine}}+\Gamma_{\uparrow,T_\mathfrak{p}}) + W_{T_+,T_\mathfrak{p}}(\Gamma_{T_+,\uparrow}+\Gamma_{T_\mathfrak{p},\uparrow})\Big], \tag{40b}$$

where

$$\begin{aligned} \Lambda \equiv &\Gamma_{\uparrow,S_+}\Big[2\Gamma_{T_+,\uparrow}\Gamma_{\uparrow,T_\mathfrak{p}} + (2\Gamma^{\mathrm{ine}}+3W_{T_+,T_\mathfrak{p}})(\Gamma_{T_+,\uparrow}+\Gamma_{T_\mathfrak{p},\uparrow})\Big] \\ &+\Upsilon\Big[2\Gamma^{\mathrm{ine}}(\Gamma^{\mathrm{ine}}+\Gamma_{\uparrow,T_\mathfrak{p}}) + (3\Gamma^{\mathrm{ine}}+\Gamma_{\uparrow,T_\mathfrak{p}})W_{T_+,T_\mathfrak{p}}\Big]. \end{aligned} \tag{40c}$$

The explicit expressions for $n_\uparrow = n_\downarrow$ can easily be found by inserting Eq.(40) into Eq.(39). This in turn lead to the expression for $n_{S_+} = n_{S_-}$ via Eq.(38). Thus, we have now found *all the stationary occupations* close to the crossing of the triplets in terms of the rates.

The leakage current in the high bias limit can now be obtained by inserting the occupations into Eq.(17), i.e.

$$\begin{aligned} I = &\frac{2\Gamma_{\uparrow,S_+}}{\zeta}(\Gamma_{T_+,\uparrow} + \Gamma_{S_+,\downarrow} + \Gamma_{S_+,\uparrow} + \Gamma_{T_\mathfrak{p},\uparrow}) \\ &\times \Big[2\Gamma^{\mathrm{ine}}(\Gamma^{\mathrm{ine}} + \Gamma_{\uparrow,T_\mathfrak{p}}) + W_{T_+,T_\mathfrak{p}}(3\Gamma^{\mathrm{ine}} + \Gamma_{\uparrow,T_\mathfrak{p}})\Big] \end{aligned} \tag{41a}$$

where we introduced

$$\begin{aligned} \zeta \equiv &(\Gamma^{\mathrm{ine}} + \Gamma_{\uparrow,T_\mathfrak{p}})(2\Gamma_{T_+,\uparrow}\Gamma_{\uparrow,S_+} + 2\Gamma^{\mathrm{ine}}\Upsilon) \\ &+ 2\Gamma^{\mathrm{ine}}\Gamma_{\uparrow,S_+}\Gamma_{T_\mathfrak{p},\uparrow} \\ &+W_{T_+,T_\mathfrak{p}}\Big[3\Gamma_{T_+,\uparrow}\Gamma_{\uparrow,S_+}+3\Gamma_{\uparrow,S_+}\Gamma_{T_\mathfrak{p},\uparrow}+\Upsilon(3\Gamma^{\mathrm{ine}}+\Gamma_{\uparrow,T_\mathfrak{p}})\Big]. \end{aligned} \tag{41b}$$

We emphasize that in the derivation of the occupations and the leakage current, we have only used the invariance of the rates under exchange of indices (see Secs. II C 2 and II C 3) and *not* the explicit expressions for the rates. Thus, the above expressions are indeed rather general.

Furthermore, equal inelastic escape rates $\Gamma^{\mathrm{ine}}$ from the three triplets were used here. However, in Appendix A we show that if the inelastic rates are not equal, but instead are invariant under interchange of indices in the same way as the tunneling rates, then the above expressions

for the current only change slightly.

Next, we specialize to the case of the explicit tunneling rates in Eqs.(19-20). Inserting these into the current formula (41) leads to a leakage current overall proportional to $\Gamma_{\rm L}$, i.e.

$$\frac{I}{\Gamma_{\rm L}} = \frac{8\gamma_{\rm RL}}{\xi}\Big\{\gamma_{\rm ine}(2\gamma_{\rm ine}+3w) + \big[2\gamma_{\rm ine}(\gamma_{\rm ine}+\gamma_{\rm RL})+(3\gamma_{\rm ine}+\gamma_{\rm RL})w\big]\mathfrak{p}^2\Big\} \tag{42a}$$

where we introduced

$$\gamma_{\rm RL}\equiv\frac{\Gamma_{\rm R}}{\Gamma_{\rm L}},\quad \gamma_{\rm ine}\equiv\frac{\Gamma^{\rm ine}}{\Gamma_{\rm L}},\quad w\equiv\frac{W_{T_+,T_{\mathfrak{p}}}}{\Gamma_{\rm L}}, \tag{42b}$$

and

$$\begin{aligned}\xi \equiv&(2\gamma_{\rm ine}+3w)\big[3\gamma_{\rm RL}+2\gamma_{\rm ine}(1+2\gamma_{\rm RL})\big]\\ &+2\Big[4\gamma_{\rm ine}\gamma_{\rm RL}(1+\gamma_{\rm RL})+\gamma_{\rm ine}^2(6+4\gamma_{\rm RL})\\ &+3\gamma_{\rm ine}(3+2\gamma_{\rm RL})w+2\gamma_{\rm RL}(\gamma_{\rm RL}w+\gamma_{\rm RL}+2w)\Big]\mathfrak{p}^2\\ &+4\Big[2\gamma_{\rm ine}(\gamma_{\rm ine}+\gamma_{\rm RL})+(3\gamma_{\rm ine}+\gamma_{\rm RL})w\Big]\mathfrak{p}^4.\end{aligned} \tag{42c}$$

Thus, we have here expressed the current in terms of the dimensionless triplet-singlet mixing parameter $\mathfrak{p}$ in Eq.(13) and the three rates, $\gamma_{\rm RL}$, $\gamma_{\rm ine}$ and $w$ — all measured in units of the basic tunneling rate of the left lead $\Gamma_{\rm L}$. Here $\gamma_{\rm RL}=\Gamma_{\rm R}/\Gamma_{\rm L}$ describes the asymmetry between the coupling of the DQD to the left and right contact, such that $\gamma_{\rm RL}=1$ describes the symmetric case. Therefore, $\gamma_{\rm RL}$ is on the order of unity. In contrast, both the dimensionless HF triplet-triplet rate[122] $w$ and the dimensionless inelastic escape rate $\gamma_{\rm ine}$ are much smaller than unity, i.e. $\gamma_{\rm ine},\ w\ll\gamma_{\rm RL}\sim 1$. Furthermore, here we are interested in the limit of the inelastic escape rate being much smaller than the HF rate close to the crossing of the triplet levels.

From the current (42), we note that *without* singlet-triplet mixing, $\mathfrak{p}=0$ (i.e. $P=0$ or $A_{\rm L}=A_{\rm R}$), the current reduces to

$$\frac{I(\mathfrak{p}=0)}{\Gamma_{\rm L}}=\frac{8\gamma_{\rm RL}\gamma_{\rm ine}}{3\gamma_{\rm RL}+2\gamma_{\rm ine}(1+2\gamma_{\rm RL})}, \tag{43}$$

which is independent of the HF rate $w$. Physically, this can be understood in the following way. For $\mathfrak{p}=0$, the escape channel from $T_{\mathfrak{p}}$ due to singlet-triplet mixing disappears. Thus, for $\mathfrak{p}=0$ only the inelastic escape channel $\Gamma^{\rm ine}$ contributes to the current through the three triplet states (remembering that the $S_\pm$ singlet levels are far away in energy). Since equal inelastic escape rates $\Gamma^{\rm ine}$ from the three triplet states are used here, the current does not depend on from which triplet state the electron tunnels out. Thus, the current has to be independent of the HF-induced transitions between the three triplet states for $\mathfrak{p}=0$ as found above in Eq.(43). In contrast, if the inelastic escape rates from the three triplets are *not* equal, then the current can indeed depend on the HF rate even for $\mathfrak{p}=0$. An example of this can be found in Eq.(A4) in Appendix A.

It is important to make clear that the rates still depend on the DNP, $P$, which in general is *not* analytically known in terms of the external parameters. Thus, the above occupations (40) and current expressions (41) and (42) are also not solely explicit functions of the external parameters. In order to obtain explicit expression versus external parameters, the DNP needs to be found from the implicit polarization equation (34). This will be done below.

### *2. The leakage current versus magnetic field: Emergence of hysteresis below the transition temperature*

Next, we analyze the leakage current versus external magnetic field $B$ as shown in Fig. 8 for temperatures $T<T_{c,\rm TT}$, $T=T_{c,\rm TT}$ and $T>T_{c,\rm TT}$. To this end, the stationary DNP $P$ is found numerically from the implicit polarization equation (34) [Fig. 8(a,d,g)] and then inserted into the current Eq.(42) [Fig. 8(b,e,h)]. Therefore, if there are multiple stable polarization solutions present, then there will also be multiple possible stable values of the leakage current. The actually stationary leakage current and DNP in a concrete situation therefore depend on the initial value in time of the polarization as in other non-linear dynamical systems.[120]

The hysteresis in the current comes about in the following way: Consider $T<T_{c,\rm TT}$ and the magnetic field tuned so high that there is only a single polarization solution, e.g. $g\mu_B B=7\mu$eV in Fig. 8(a). By decreasing the magnetic field one will enter the region of multiple possible polarizations [at $g\mu_B B\sim 2.34\mu$eV in Fig. 8(a)]. Since the polarization is a stable solution against small fluctuations, the system will remain on the upper stable branch ($P>0$) until the critical magnetic field, where the upper branch cease to exist [about $g\mu_B B\sim -2.34\mu$eV in Fig. 8(a)]. At this critical field, the system has to go to the lower stable polarization branch (with $P<0$). Thus, the stationary polarization change discontinuous as a function of $B$. This in turn leads to a *jump* in the leakage current (as seen in Fig. 8(b) for the blue full curve representing sweeping the field backwards from a high value of $g\mu_B B$). For magnetic fields lower than the critical one, the polarization is single valued again and so is the current. Now, if at this point the field is increased beyond the critical field [of $g\mu_B B\sim -2.34\mu$eV in Fig. 8(a)] one will follow the *lower* stable polarization branch with $P<0$, leading to the dashed red curve in Fig. 8(b). This sweep direction also leads to a sharp jump once the lower stable polarization branch cease to exist [at $g\mu_B B\sim +2.34\mu$eV in Fig. 8(a)]. Thus, the hysteretic behavior of the leakage current for $T<T_{c,\rm TT}$ is now evident. The discontinuity versus magnetic field for $T<T_{c,\rm TT}$ is also seen in the energy levels Fig. 8(c), where only one sweeping direction is shown for clarity.

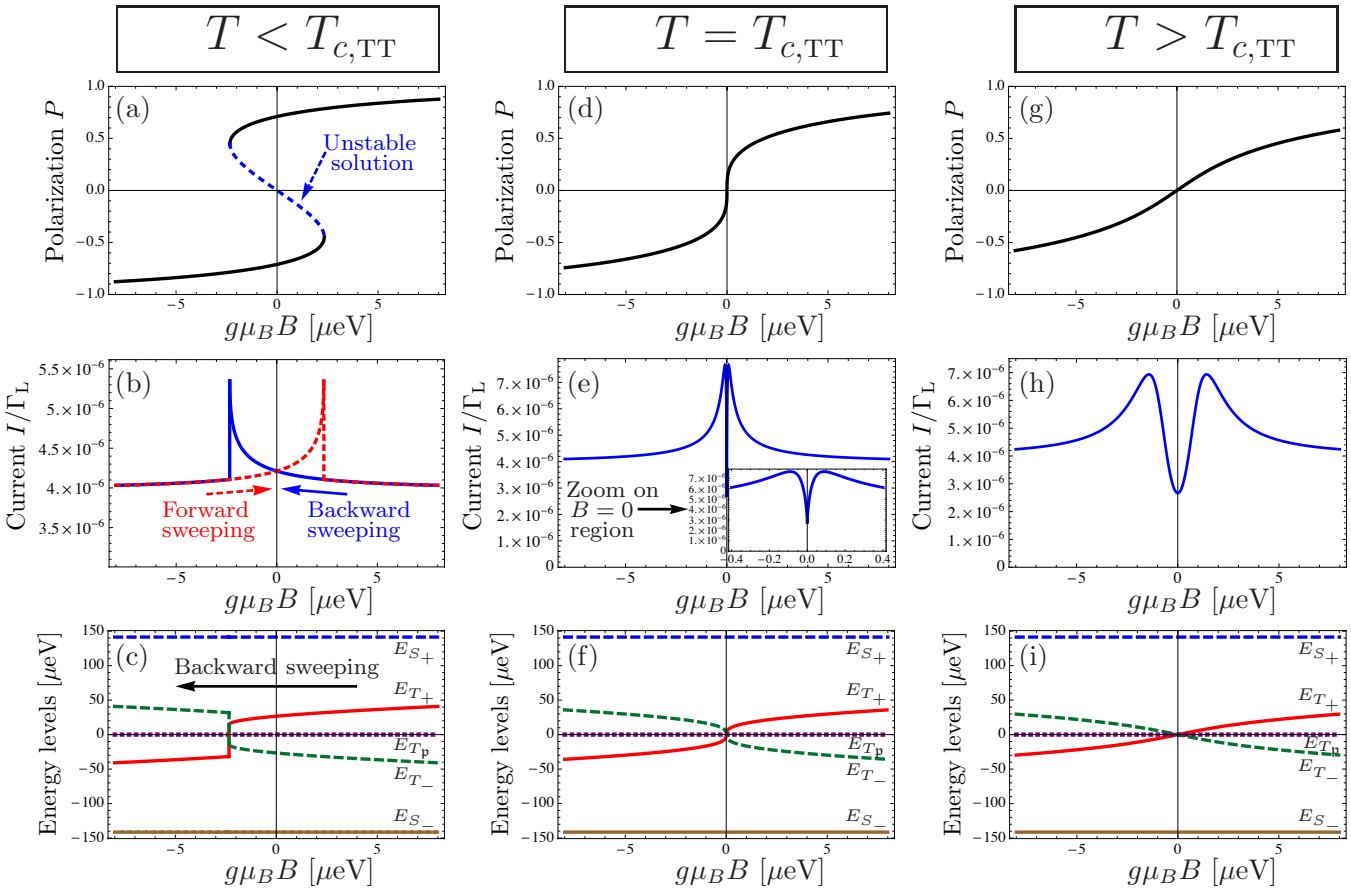


FIG. 8. (Color online) The dynamical nuclear polarization $P$, the leakage current $I/\Gamma_\mathrm{L}$ Eq.(42) and the energy levels versus external magnetic field $g\mu_B B$ (in energy units) close to the crossing of the triplet states $T_+$, $T_-$ and $T_\mathrm{p}$ for temperatures $T = 0.8T_{c,\mathrm{TT}} < T_{c,\mathrm{TT}}$ (a-c), $T = T_{c,\mathrm{TT}}$ (d-f) and $T = 1.2T_{c,\mathrm{TT}} > T_{c,\mathrm{TT}}$ (g-i). It is clearly seen that a hysteretic current appears only below the transition temperature $T < T_{c,\mathrm{TT}}$. The reason is that for $T < T_{c,\mathrm{TT}}$ a magnetic field region with two stable polarizations (black full lines) exists as seen in Fig. (a). In this region, an unstable solution to the polarization (blue dashed line) also shows up. In contrast, for $T \geq T_{c,\mathrm{TT}}$ only a single stable polarization is found in Figs. (d) and (g) [see also Fig. 7]. For clarity, only the backward sweeping of the magnetic field (from a $g\mu_B B$ higher than $2.34\mu$eV) is seen for the energy levels on Fig. (c). Furthermore, note that the vertical scale in (b) does not include zero, in contrast to (e) and (h). Fig. (e) for $T = T_{c,\mathrm{TT}}$ includes an inset, where the sharp current dip at very low magnetic fields can be clearly seen. The parameters used here are: $A_\mathrm{L} = 80\mu$eV, $A_\mathrm{R} = 70\mu$eV, $t = 100\mu$eV, $\gamma_{ph} = 1\mu$eV, $\Gamma_\mathrm{L} = \Gamma_\mathrm{R}$ (i.e. $\gamma_\mathrm{RL} = 1$) and[123] $\hbar\Gamma_\mathrm{L} N = 10^7\mu$eV. Moreover, we choose the dimensionless inelastic escape rate to be $\gamma_\mathrm{ine} = \Gamma^\mathrm{ine}/\Gamma_\mathrm{L} = 10^{-6}$, such that it is much smaller than the HF rate $w$ Eq.(42b) in the regions close to the crossing of the triplets (see Fig. 9).

We observe that the width of the hysteresis loop increases with decreasing temperature. This is evident from Fig. 7, where the width is given by the vertical distance between the two (full blue) lines.

Identifying that the transition temperature $T_{c,\mathrm{TT}}$ as simply given by the average HF coupling Eq.(35), is an important result of this paper. Experimentally, the HF couplings are of order[19,52] $100\mu$eV such that $T_{c,\mathrm{TT}}$ is on the order of 300mK, which is within the range of modern solid state experiments.

The results presented in Fig. 8 have been found by neglecting all HF-induced triplet-singlet transitions (Sec. III). In order to test the validity of this simplification, we have also numerically iterated the full set of rate equations (15-16) including *all* the rates. For the chosen parameters of figure 8 – where the $S_\pm$ energy levels are far way from the triplet levels – the two calculations are found to produce the same results (not shown in the figure), i.e. the presented simplified model works well.

Now we give a better understanding of the form of the current versus magnetic field. In this work, we focus on the limit where the HF-induced spin-flip rates dominate the constant inelastic escape rates close to the level crossings following Refs. [33–36]. Nevertheless, the inelastic escape rate plays an important role for the current in the following. First we analyze in detail current versus $g\mu_B B$ for $T \geq T_{c,\mathrm{TT}}$, where the DNP is single valued and therefore no current hysteresis is found [Fig. 8(e,h)]. The polarization goes continuously through $P = 0$ at $g\mu_B B = 0$. As discussed below Eq.(43), the singlet-

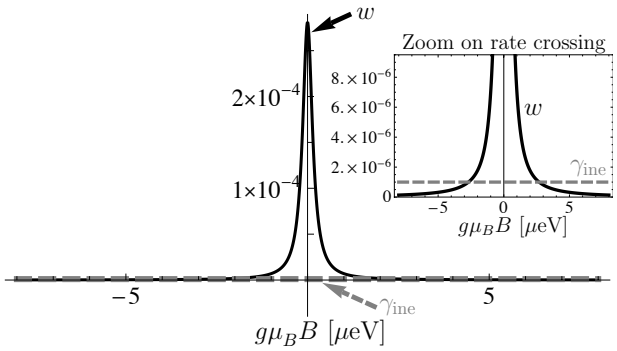


FIG. 9. (Color online) The dimensionless hyperfine rate $w$ (black full line) and inelastic escape rate $\gamma_{\mathrm{ine}} = \Gamma^{\mathrm{ine}}/\Gamma_{\mathrm{L}}$ (gray dashed line) versus magnetic field $g\mu_B B$ (in energy units) for $T = 1.2T_{c,\mathrm{TT}}$. The inset shows that $\gamma_{\mathrm{ine}} \gtrsim w$ for $|g\mu_B B| \gtrsim 2.7\mu$eV. In contrast, the hyperfine rate $w$ dominates by orders of magnitude over $\gamma_{\mathrm{ine}}$ around zero magnetic field. [Remember that due to the implicit polarization equation (32) all the hyperfine-induced triplet-triplet rates are equal in steady state, i.e. $w = W_{T_+,T_\mathfrak{p}}/\Gamma_{\mathrm{L}} = W_{T_\mathfrak{p},T_+}/\Gamma_{\mathrm{L}} = W_{T_-,T_\mathfrak{p}}/\Gamma_{\mathrm{L}} = W_{T_\mathfrak{p},T_-}/\Gamma_{\mathrm{L}}$.] The parameters are the same as in Fig. 8(g-i).

triplet mixing disappears at $P = 0$, which in turn closes the escape path from $T_\mathfrak{p}$ as $\Gamma_{\sigma,T_\mathfrak{p}} \sim P^2$ for $|P| \ll 1$, see Eq.(20a). This means that the current goes down for $B \to 0$ and $T \geq T_{c,\mathrm{TT}}$ to a value only given by the inelastic escape rate — even though it is weak. For $\gamma_{\mathrm{RL}} = 1$ Eq.(43) leads to

$$\frac{I(B=0, T \geq T_{c,\mathrm{TT}})}{\Gamma_{\mathrm{L}}} = \frac{8\gamma_{\mathrm{ine}}}{3 + 6\gamma_{\mathrm{ine}}}, \tag{44}$$

which agrees perfectly with the value of $\sim 2.7 \times 10^{-6}$ found in Fig. 8(e,h) for $B = 0$. The slope of $P$ at $g\mu_B B = 0$ increases rapidly when approaching $T = T_{c,\mathrm{TT}}$ from temperatures above $T_{c,\mathrm{TT}}$, see Fig. 8(d,g). Therefore, the dip in the current at $g\mu_B B = 0$ becomes increasingly sharper for $T$ approaching $T_{c,\mathrm{TT}}$, see Fig. 8(e,h) and the inset.

The HF-induced triplet-triplet transition rates decrease to zero as the triplet energy levels move apart. Thus, the HF rate $w$ decreases to zero by increasing the magnitude of the magnetic field as seen in Fig. 9. This means that the inelastic escape rate $\gamma_{\mathrm{ine}}$ will eventually become larger than $w$, since $\gamma_{\mathrm{ine}}$ is constant. For the values used in Fig. 8(g-i), the rate $\gamma_{\mathrm{ine}}$ is bigger than $w$ for $|g\mu_B B| \gtrsim 2.7\mu$eV as shown in the inset of Fig. 9. For the energy level splitting, this corresponds to $|E_{T_+} - E_{T_\mathfrak{p}}| \gtrsim 14\mu$eV. Thus, once the triplet levels move further apart, the triplet-triplet transition $w$ goes to zero and can be neglected in the current (42). That corresponds to $|g\mu_B B| \gtrsim 2.7\mu$eV for $T > T_{c,\mathrm{TT}}$ in the numerical example of Fig. 8(g-i). For $\gamma_{\mathrm{RL}} = 1$, we find[124]

$$\begin{aligned}\frac{I_{w\to 0}}{\Gamma_{\mathrm{L}}} &= \frac{8\gamma_{\mathrm{ine}}\left[\gamma_{\mathrm{ine}} + (1+\gamma_{\mathrm{ine}})\mathfrak{p}^2\right]}{2\mathfrak{p}^2 + \gamma_{\mathrm{ine}}(3+2\mathfrak{p}^2)\left[1 + 2\gamma_{\mathrm{ine}} + 2(1+\gamma_{\mathrm{ine}})\mathfrak{p}^2\right]} \\ &= 4\gamma_{\mathrm{ine}} + \mathcal{O}[(\gamma_{\mathrm{ine}})^2],\end{aligned} \tag{45}$$

where $\gamma_{\mathrm{ine}} \ll |\mathfrak{p}|$ for $|P| \gtrsim 0.1$ for $A_-$ and $t$ similar to those used in Fig. 8. In Figs. 8(b,e,h), we see that the current levels off to a constant value of about $4 \times 10^{-6}$ far away from the crossing of the levels, which is in perfect agreement with the prediction (45). Therefore, we have found that

$$\frac{I(B=0, T \geq T_{c,\mathrm{TT}})}{I_{w\to 0}} \simeq \frac{2}{3} \quad \text{for} \quad \gamma_{\mathrm{ine}} \ll 1 \tag{46}$$

such that the value at the crossing for $B = 0$ (for $T \geq T_{c,\mathrm{TT}}$) is generically smaller than the value that the current levels off to asymptotically [Fig. 8(e,h)].

Now we have shown that the current value both *at* the crossing of the triplet levels and *far away* form the crossing is determined by the constant inelastic escape rate. Albeit the HF interaction of course is essential in having a DNP in the first place. Next we discuss how the HF triplet-triplet transitions can increase the leakage current close to – but not exactly at – the crossing of the levels. At the crossing of the triplet levels ($B = 0$ for $T \geq T_{c,\mathrm{TT}}$), all three triplet states form the bottleneck for transport through the DQD. At finite $P$ the triplet-singlet mixing leads to the additional escape from $n_{T_\mathfrak{p}}$ such that the transport bottleneck (far away from the crossing) now only consist of the pure triplet states $T_\pm$. For $T \geq T_{c,\mathrm{TT}}$, we only get $P \neq 0$ for $B \neq 0$. Moreover, note that $n_{T_\mathfrak{p}}$ becomes negligible compared to $n_{T_\pm}$ far from the level crossing for $T \geq T_{c,\mathrm{TT}}$ (see Fig. 10). The point is that in the region close to the level crossing, the HF-induced triplet-triplet transitions leads to an escape path from the pure triplets $T_\pm$ via the state $T_\mathfrak{p}$. Since the HF rate $w$ is much larger than $\gamma_{\mathrm{ine}}$ close to the crossing, this escape route is so effective that it creates the side-peaks of the current at finite $g\mu_B B$ seen in Fig. 8(e,h). These current side-peaks are indeed sensitive to the value of the inelastic rate, e.g. if $\gamma_{\mathrm{ine}}$ is increased by a factor of 5 or more, then the side-peaks in Fig. 8(h) disappear. In contrast, if $\gamma_{\mathrm{ine}}$ is decreased the side-peaks remain. Figure 10 shows that near the current side-peaks [with maxima at $g\mu_B B \simeq \pm 1.4\mu$eV in Fig. 8(h)], the occupations $n_{T_\pm}$ are much larger than $n_{T_\mathfrak{p}}$.

Finally, we point out that the form of the leakage current for $T < T_{c,\mathrm{TT}}$ can be understood by using the above considerations, but taking into account that the polarization jumps between rather high values (e.g. $P \sim 0.45$ to $P \sim -0.8$ at $g\mu_B B \simeq 2.34\mu$eV in Fig. 8(a)). Therefore, the rich region around $P = 0$ is simply skipped. [Note also the change in vertical scale in Fig. 8(b) compared to (e) and (h).]

Therefore, we have now obtained an understanding of the leakage current versus magnetic field close to the

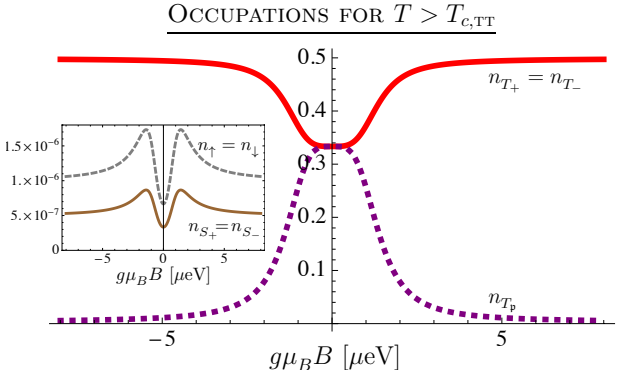


FIG. 10. (Color online) The occupations of the triplet states $n_{T_+} = n_{T_-}$ (red full line) and $n_{T_\mathfrak{p}}$ (purple dotted line) in Eq.(40) versus magnetic field $g\mu_B B$ in energy units for a temperature larger than the transition temperature, $T = 1.2T_{c,\mathrm{TT}} > T_{c,\mathrm{TT}}$. Inset: The occupations of the singlet states $n_{S_+} = n_{S_-}$ (brown full line) and the one-particle states $n_\uparrow = n_\downarrow$ (gray dashed line). In the spin blockade regime, the triplet states are the bottleneck of the transport such that the system spends a long time in these states, leading to high occupations. In contrast, the singlet and one-electron states have orders of magnitude lower occupations. Furthermore, note that at the leakage current side-peak positions $g\mu_B B \simeq \pm 1.4\mu$eV in Fig. 8(h), the occupations $n_{T_+} = n_{T_-}$ dominate $n_{T_\mathfrak{p}}$. The parameters are the same as in Fig. 8(g-i).

crossing of the triplet energy levels under the assumption that the singlet energy levels $E_{S_\pm}$ are far away.

### 3. *The current in the high temperature and low magnetic field limit*

Next, we briefly show that the leakage current can be given analytically in terms of the external parameters in the limit of low external magnetic fields and temperatures above the transition temperature $T_{c,\mathrm{TT}}$. Specifically, if

$$T > T_{c,\mathrm{TT}} \quad \text{and} \quad \left|\frac{2g\mu_B B}{A_+} + P\right| \ll \frac{T}{T_{c,\mathrm{TT}}}, \tag{47}$$

then the hyperbolic tangent in the implicit polarization equation (34) can be expanded, which leads to

$$P \simeq \frac{\frac{1}{2}g\mu_B B/k_\mathrm{B}}{T - T_{c,\mathrm{TT}}}. \tag{48}$$

This is similar to a Curie-Weiss law for a ferromagnet in the paramagnetic region and the fact that $P \propto (T - T_{c,\mathrm{TT}})^{-1}$ is typical for the mean-field approach used here.[125] Inserting the DNP Eq.(48) into the current (42), we obtain an explicit current expression versus magnetic field, albeit only for low fields:

$$\frac{I}{\Gamma_\mathrm{L}} \simeq \frac{8\gamma_\mathrm{RL}\gamma_\mathrm{ine}}{3\gamma_\mathrm{RL} + 2\gamma_\mathrm{ine}(1 + 2\gamma_\mathrm{RL})} + \frac{A_-^2}{4t^2}\frac{\gamma_\mathrm{RL}(\gamma_\mathrm{RL}^2 + \gamma_\mathrm{ine}\gamma_\mathrm{RL} - 4\gamma_\mathrm{ine}^2)}{\left[3\gamma_\mathrm{RL} + \gamma_\mathrm{ine}(2 + 4\gamma_\mathrm{RL})\right]^2}\left[\frac{g\mu_B B}{k_\mathrm{B}[T - T_{c,\mathrm{TT}}]}\right]^2. \tag{49}$$

This describes the current dip close to $B = 0$ seen in Fig. 8(h). It shows explicitly that the current increases by changing slightly $B$ away from $B = 0$, since $\gamma_\mathrm{ine} < (1 + \sqrt{17})\gamma_\mathrm{RL}/8$ for reasonable parameters. The expression (49) is obtained by expanding the current (42) in $P$. We observe that the HF rate $w$ only appears beyond the second order term, however, already the second order term contains explicitly the difference of the HF constants $A_- = (A_\mathrm{L} - A_\mathrm{R})/2$. The lowest order term for $B = 0$ coincides with the current Eq.(43) without the triplet-singlet mixing as expected.

## IV. THE SINGLET-TRIPLET CROSSING

In this section, we investigate the DNP and leakage current close to the energy level crossing of the singlet states $S_\pm$ and the pure triplet states $T_\pm$ at finite magnetic field. Since we consider the case of zero detuning, the crossing of the energy levels always happens in pairs, i.e. $E_{T_+}$ and $E_{S_+}$ cross at the same value of magnetic field as $E_{T_-}$ and $E_{S_-}$ do [see Eq.(14)]. Interestingly, here we show that the transition temperature $T_{c,\mathrm{ST}}$ for the singlet-triplet level crossing is enhanced compared to $T_{c,\mathrm{TT}}$ for the crossing of the triplet levels.

### A. A simplified model for the singlet-triplet crossing and its implicit polarization equation

Next, we develop a simplified set of rate equations valid close to the crossing of $E_{T_+}$ ($E_{T_-}$) and $E_{S_+}$ ($E_{S_-}$) for *positive* magnetic field splitting, $g\mu_B B > 0$. From these equations, we derive an implicit equation for the DNP. The level crossings at negative magnetic field follow along similar lines.[126]

As a first approach, one might intend to follow the same strategy as in Sec. III A for the crossing of the triplet levels: Keep only the HF-induced rates between the energy levels, which are close in energy. Hence, we keep only the HF terms in Eqs.(15-16) involving $W_{T_\pm,S_\pm}$ and $W_{S_\pm,T_\pm}$ in the present case. Such a simplification leads to $W_{S_+,T_+} = W_{T_+,S_+}$ as an implicit polarization equation for the DNP — much like in the case of the crossing of the triplet levels Eq.(32). This leads to approximately[127] the same transition temperature as $T_{c,\mathrm{TT}}$ in Eq.(35). *However, for the singlet-triplet level crossing, this approach is actually not a good approximation.* Explicitly, we find that this approach does *not* reproduce the DNP found by a numerical iteration of the

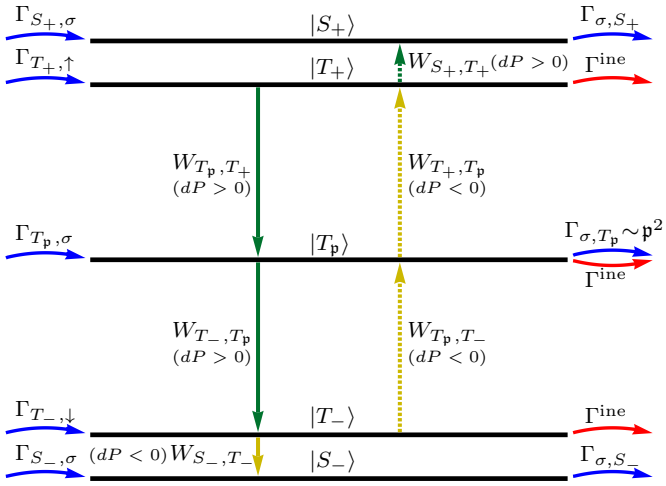


FIG. 11. (Color online) The transition processes included in the simplified rate equations (50-51) tailored to described the DNP and leakage current close to the singlet-triplet crossing for $g\mu_B B > 0$. The HF-induced transitions $S_\pm \to T_\pm$ are neglected, since they are much less probable than simply tunneling out of the singlet states. Furthermore, the triplet-triplet transitions are included, since these can play a role even though the levels have a large energy separation (see the main text for further discussion). The HF phonon emission (absorption) processes are shown as full (dotted) vertical arrows. The processes indicated by green (yellow) arrows change the nuclear polarization positively (negatively). The inelastic escape rates $\Gamma^{\rm ine}$ (red arrows) and the tunneling rates $\Gamma_{f,i}$ (blue arrows) are the same as in Fig. 4.

Important processes close to the singlet-triplet crossing

rate equations (15-16) including all transition processes (for an inter-dot coupling $t$ about two orders of magnitude larger than $\gamma_{ph}$).[128] The approach fails for the following reason. First of all, the occupations of the singlets $n_{S_\pm}$ are much smaller than the occupations of the triplets $n_{T_\pm}$ and $n_{T_\mathfrak{p}}$, since escape from the singlet states are much easier than from the triplets in the SB regime. Secondly, the triplet-triplet and the singlet-triplet HF rates have the overall prefactors of $A_+^2$ and $A_-^2$, respectively, such that the triplet-triplet rate is enhanced compared to the singlet-triplet rate (for comparable energy level splitting). Due to these two facts, the triplet-triplet HF terms can still be comparable in magnitude to the singlet-triplet terms in the rate equations (15-16) — even though the triplet-triplet energy splitting $|E_{T_\pm} - E_{T_\mathfrak{p}}|$ is much larger than $\gamma_{ph}$ close to the singlet-triplet energy crossing. In other words, we *cannot* neglect terms like $W_{T_\mathfrak{p},T_+} n_{T_+}$ compared to terms like $W_{S_+,T_+} n_{T_+}$.

Here, we have to adopt a different approach of simplifying the rate equations from the one used to describe the crossing of the triplets in Sec. III A. This is done in order to describe the regime of large singlet-triplet energy splitting $|E_{S_\pm} - E_{T_\mathfrak{p}}|$ compared to $\gamma_{ph}$, however, not so large that the triplet-triplet rates cannot still play a role. Our approach is to neglect two kinds of terms in the rate equations (15-16). (i) The HF singlet-triplet terms between $T_+$ ($T_-$) and $S_-$ ($S_+$) can safely be neglected, because of large energy separation (for $g\mu_B B > 0$) combined with an overall prefactor of $A_-^2$ in the rate. Thus, we neglect terms of the form $W_{T_\nu,S_\nu} n_{S_\nu}$ and $W_{S_{\bar\nu},T_\nu} n_{T_\nu}$, where $\nu = \pm$ and $\bar\nu = -\nu$. (ii) Due to the SB regime, the occupations of the singlets are much smaller than the occupations of the triplets. Therefore, we neglect the terms $W_{T_\pm,S_\pm} n_{S_\pm}$. We thereby neglect the possibility of going from $S_\pm$ into the pure triplet states via a HF-induced spin-flip transition, since tunneling out from the $S_\pm$ states are *much* more probable processes. These two simplifications lead to the following rate equations for positive magnetic fields

$$\dot n_{T_+} = W_{T_+,T_\mathfrak{p}} n_{T_\mathfrak{p}} + \Gamma_{T_+,\uparrow} n_\uparrow - \big[W_{S_+,T_+} + W_{T_\mathfrak{p},T_+} + 2\Gamma^{\rm ine}\big] n_{T_+}, \tag{50a}$$

$$\dot n_{T_-} = W_{T_-,T_\mathfrak{p}} n_{T_\mathfrak{p}} + \Gamma_{T_-,\downarrow} n_\downarrow - \big[W_{S_-,T_-} + W_{T_\mathfrak{p},T_-} + 2\Gamma^{\rm ine}\big] n_{T_-}, \tag{50b}$$

$$\dot n_{T_\mathfrak{p}} = W_{T_\mathfrak{p},T_+} n_{T_+} + W_{T_\mathfrak{p},T_-} n_{T_-} + \Gamma_{T_\mathfrak{p},\uparrow} n_\uparrow + \Gamma_{T_\mathfrak{p},\downarrow} n_\downarrow - \big[W_{T_+,T_\mathfrak{p}} + W_{T_-,T_\mathfrak{p}} + \Gamma_{\uparrow,T_\mathfrak{p}} + \Gamma_{\downarrow,T_\mathfrak{p}} + 2\Gamma^{\rm ine}\big] n_{T_\mathfrak{p}}, \tag{50c}$$

$$\dot n_{S_+} = W_{S_+,T_+} n_{T_+} + \Gamma_{S_+,\uparrow} n_\uparrow + \Gamma_{S_+,\downarrow} n_\downarrow - \big[\Gamma_{\uparrow,S_+} + \Gamma_{\downarrow,S_+}\big] n_{S_+}, \tag{50d}$$

$$\dot n_{S_-} = W_{S_-,T_-} n_{T_-} + \Gamma_{S_-,\uparrow} n_\uparrow + \Gamma_{S_-,\downarrow} n_\downarrow - \big[\Gamma_{\uparrow,S_-} + \Gamma_{\downarrow,S_-}\big] n_{S_-}, \tag{50e}$$

$$\dot n_\uparrow = \Gamma_{\uparrow,S_+} n_{S_+} + \Gamma_{\uparrow,S_-} n_{S_-} + (\Gamma_{\uparrow,T_\mathfrak{p}} + \Gamma^{\rm ine}) n_{T_\mathfrak{p}} + \Gamma^{\rm ine}(n_{T_+} + n_{T_-}) - \big[\Gamma_{S_+,\uparrow} + \Gamma_{S_-,\uparrow} + \Gamma_{T_\mathfrak{p},\uparrow} + \Gamma_{T_+,\uparrow}\big] n_\uparrow, \tag{50f}$$

$$\dot n_\downarrow = \Gamma_{\downarrow,S_+} n_{S_+} + \Gamma_{\downarrow,S_-} n_{S_-} + (\Gamma_{\downarrow,T_\mathfrak{p}} + \Gamma^{\rm ine}) n_{T_\mathfrak{p}} + \Gamma^{\rm ine}(n_{T_-} + n_{T_+}) - \big[\Gamma_{S_+,\downarrow} + \Gamma_{S_-,\downarrow} + \Gamma_{T_\mathfrak{p},\downarrow} + \Gamma_{T_-,\downarrow}\big] n_\downarrow, \tag{50g}$$

using equal inelastic escape rates (18). Likewise, Eq.(16) for the polarization simplifies to

$$\dot P = \frac{2}{N}\Big[(W_{T_-,T_\mathfrak{p}} - W_{T_+,T_\mathfrak{p}}) n_{T_\mathfrak{p}} + (W_{S_+,T_+} + W_{T_\mathfrak{p},T_+}) n_{T_+} - (W_{S_-,T_-} + W_{T_\mathfrak{p},T_-}) n_{T_-}\Big]. \tag{51}$$

The transition processes included in this description are illustrated on Fig. 11. By comparing to the rate equations (27-28) describing the situation close to the crossing of the triplets, we see that the only difference is the *direct* coupling of the singlet and triplet states via the terms $W_{S_\pm,T_\pm} n_{T_\pm}$.

Now we derive the implicit equation for the stationary DNP from these rate equations. To this end, we do not use the explicit form of the rates, but only that some rates are equal (e.g. $\Gamma_{T_+,\uparrow} = \Gamma_{T_-,\downarrow}$ etc.). We begin by noting that $\dot{n}_\uparrow - \dot{n}_\downarrow = 0$ leads to

$$n_\uparrow = n_\downarrow \tag{52}$$

in the stationary state. Inserting this into $\dot{n}_{T_+} - \dot{n}_{T_-} + (N/2)\dot{P} = 0$ gives

$$n_{T_+} = n_{T_-} \tag{53}$$

in the steady state. These two relations are the same as in the description of the triplet level crossing, see Eqs.(29-30). In fact, $n_\uparrow = n_\downarrow$ and $n_{T_+} = n_{T_-}$ can be derived form the rate equations (15-16) including all terms in the case of equal inelastic rates. However, at this point in the derivation the two descriptions separate, because the singlet occupations are no longer found to be equal in steady state [as in Eq.(37)]. Instead, we find

$$n_{S_+} = \frac{(\Gamma_{S_+,\downarrow} + \Gamma_{S_+,\uparrow}) n_\uparrow + W_{S_+,T_+} n_{T_+}}{2\Gamma_{\uparrow,S_+}}, \tag{54a}$$

$$n_{S_-} = \frac{(\Gamma_{S_+,\downarrow} + \Gamma_{S_+,\uparrow}) n_\uparrow + W_{S_-,T_-} n_{T_+}}{2\Gamma_{\uparrow,S_+}}, \tag{54b}$$

by solving $\dot{n}_{S_+} = 0$ and $\dot{n}_{S_-} = 0$, respectively, using the previous results $n_\uparrow = n_\downarrow$ and $n_{T_+} = n_{T_-}$ and that $\Gamma_{\uparrow,S_+} \neq 0$. Hence, $n_{S_+} \neq n_{S_-}$ if and only if $W_{S_-,T_-} \neq W_{S_+,T_+}$. These relations are used to derive the stationary triplet occupations to be

$$\begin{aligned} n_{T_+} =& n_\uparrow \frac{2}{\kappa}\Big[2\Gamma_{T_+,\uparrow}(\Gamma^{\mathrm{ine}} + \Gamma_{\uparrow,T_\mathfrak{p}}) \\ &+ (\Gamma_{T_\mathfrak{p},\uparrow} + \Gamma_{T_+,\uparrow})(W_{T_+,T_\mathfrak{p}} + W_{T_\mathfrak{p},T_+})\Big], \end{aligned} \tag{55a}$$

$$\begin{aligned} n_{T_\mathfrak{p}} =& n_\uparrow \frac{2}{\kappa}\Big[\Gamma_{T_\mathfrak{p},\uparrow}(4\Gamma^{\mathrm{ine}} + W_{S_+,T_+} + W_{S_-,T_-}) \\ &+ (\Gamma_{T_\mathfrak{p},\uparrow} + \Gamma_{T_+,\uparrow})(W_{T_+,T_\mathfrak{p}} + W_{T_\mathfrak{p},T_+})\Big] \end{aligned} \tag{55b}$$

from $\dot{n}_\uparrow + \dot{n}_\downarrow = 0$ and $\dot{n}_{T_\mathfrak{p}} = 0$. Here we introduced the non-zero quantity

$$\begin{aligned} \kappa \equiv& 8(\Gamma^{\mathrm{ine}})^2 + 2(\Gamma_{\uparrow,T_\mathfrak{p}} + 3\Gamma^{\mathrm{ine}})(W_{T_+,T_\mathfrak{p}} + W_{T_\mathfrak{p},T_+}) \\ &+ 8\Gamma^{\mathrm{ine}}\Gamma_{\uparrow,T_\mathfrak{p}} + (W_{S_+,T_+} + W_{S_-,T_-}) \\ &\times \big[2\Gamma^{\mathrm{ine}} + 2\Gamma_{\uparrow,T_\mathfrak{p}} + W_{T_+,T_\mathfrak{p}} + W_{T_\mathfrak{p},T_+}\big]. \end{aligned} \tag{55c}$$

Note that the triplet occupation expressions are proportional to the one-electron occupation. By inserting the occupation expressions into Eq.(51), we find that $\dot{P} = n_\uparrow \frac{2}{N}\frac{\chi}{\kappa}$, where $\chi$ is a combination of rates (given below). In order to satisfy $\dot{P} = 0$ in steady state, we have to require that $\chi = 0$, since the occupation is positive. Therefore, we finally arrive at the implicit equation for the stationary DNP, $\chi = 0$, which explicitly is given by

$$\begin{aligned} 0 =& (W_{T_+,T_\mathfrak{p}} - W_{T_\mathfrak{p},T_+})\Big\{\Gamma_{T_+,\uparrow}(\Gamma_{\uparrow,T_\mathfrak{p}} + \Gamma^{\mathrm{ine}}) + (W_{T_+,T_\mathfrak{p}} + W_{T_\mathfrak{p},T_+})(\Gamma_{T_+,\uparrow} + \Gamma_{T_\mathfrak{p},\uparrow}) + \Gamma_{T_\mathfrak{p},\uparrow}\Big[\frac{1}{2}(W_{S_+,T_+} + W_{S_-,T_-}) + 2\Gamma^{\mathrm{ine}}\Big]\Big\} \\ &+ (W_{S_-,T_-} - W_{S_+,T_+})\Big\{\Gamma_{T_+,\uparrow}(\Gamma_{\uparrow,T_\mathfrak{p}} + \Gamma^{\mathrm{ine}}) + \frac{1}{2}(W_{T_+,T_\mathfrak{p}} + W_{T_\mathfrak{p},T_+})(\Gamma_{T_+,\uparrow} + \Gamma_{T_\mathfrak{p},\uparrow})\Big\} = \chi. \end{aligned} \tag{56}$$

This implicit equation for $P$ is more involved than the one describing the DNP around the crossing of the triplet levels Eq.(32). Moreover, a simple formula for the transition temperature $T_{c,\mathrm{ST}}$ is not immediately apparent. Nevertheless, the implicit equation (56) does give some insights. For instance, it describes the crossing of the triplets as a special case: Close to the crossing of the triplets, $W_{S_\pm,T_\pm}$ is negligible such that Eq.(56) simplifies to $W_{T_+,T_\mathfrak{p}} - W_{T_\mathfrak{p},T_+} = 0$, which is exactly Eq.(32).

Furthermore, the implicit equation (56) shows that the transition temperature $T_{c,\mathrm{ST}}$ stems from the asymmetry between phonon emission and absorption in the HF spin-flip process. We show this by assuming the opposite, i.e. that absorbing or emitting an energy in the spin-flip process is equally likely.[129] This assumption leads to $(W_{S_-,T_-} - W_{S_+,T_+}) \propto P$ and $(W_{T_+,T_\mathfrak{p}} - W_{T_\mathfrak{p},T_+}) \propto P$ by using Eqs.(23,24), such that the implicit equation (56) can be written as $0 = PG(P)$, where $G(P)$ is a strictly positive function.[130] Thus, $P = 0$ is the only polarization solution without the asymmetry between emission and absorption of energy such that no DNP bistability occurs.

Here, we find the DNP from the implicit equation (56) numerically. This in turn gives the leakage current and transition temperature $T_{c,\mathrm{ST}}$ as we shall discuss next.

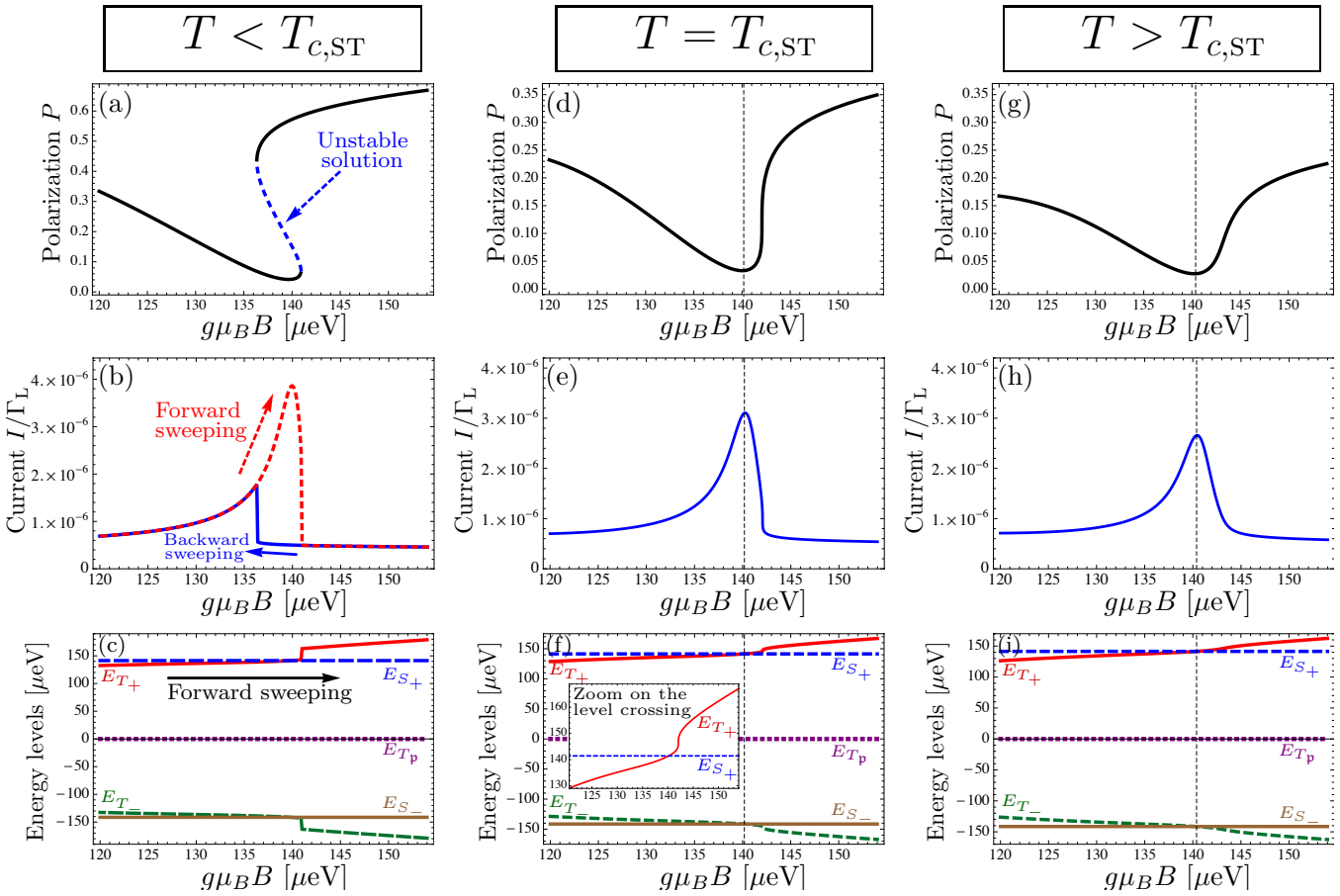


FIG. 12. (Color online) The nuclear polarization $P$, leakage current $I/\Gamma_\mathrm{L}$ and energy levels versus positive external magnetic field $g\mu_B B$ (in energy units) close to the singlet-triplet crossing for temperatures $T = 0.5T_{c,\mathrm{ST}} < T_{c,\mathrm{ST}}$ (a-c), $T = T_{c,\mathrm{ST}}$ (d-f) and $T = 1.5T_{c,\mathrm{ST}} > T_{c,\mathrm{ST}}$ (g-i). For $T < T_{c,\mathrm{ST}}$, we observe two stable DNP values (black full lines) and an unstable one (blue dashed line) in Fig. (a), which leads to the hysteretic leakage current as seen in Fig. (b). The corresponding energy levels are seen in Fig. (c), where only the case of sweeping the magnetic field forward is shown for clarity. For $T \geq T_{c,\mathrm{ST}}$, the DNP is single valued [Fig. (d,g)] such that no hysteresis appears in the leakage current, see Fig. (e,h). Note the difference in the vertical scales between the polarization in Fig. (a) and Fig. (d,g). The vertical dashed black line indicates the simultaneous crossing of (i) the triplet energy level $E_{T_+}$ (red full line) with the singlet energy level $E_{S_+}$ (blue dashed line) and (ii) $E_{T_-}$ (green dashed line) with $E_{S_-}$ (brown full line). The current is seen to peak at the level crossing – essentially due to the enhanced HF-induced singlet-triplet rate, which lifts the SB. The inset of Fig. (f) shows the non-monotonous energy level variation close to the crossing of $E_{T_+}$ and $E_{S_+}$. The transition temperature for the singlet-triplet crossing $T_{c,\mathrm{ST}}$ depends in general on several parameters of the system (see the main text). For the numerical example seen here, the transition temperature is found to be $k_\mathrm{B}T_{c,\mathrm{ST}} \simeq 2.80A_+$, which is about *one order of magnitude larger* than the transition temperature for the crossing of the triplet levels $k_\mathrm{B}T_{c,\mathrm{TT}} = A_+/4$. The parameters used here are: $A_\mathrm{L} = 80\mu$eV, $A_\mathrm{R} = 70\mu$eV, $t = 100\mu$eV, $\gamma_{ph} = 1\mu$eV, $\Gamma_\mathrm{L} = \Gamma_\mathrm{R}$ (i.e. $\gamma_\mathrm{RL} = 1$), $\hbar\Gamma_\mathrm{L}N = 10^6\mu$eV and the dimensionless inelastic escape rate is chosen to be $\gamma_\mathrm{ine} = \Gamma^\mathrm{ine}/\Gamma_\mathrm{L} = 10^{-7}$, such that the hyperfine-induced spin-flip rates dominates close to the singlet-triplet crossing (see Fig. 14).

### B. The dynamical nuclear polarization, leakage current and the singlet-triplet crossing transition temperature

We extract the DNP versus magnetic field for various temperatures numerically from the implicit equation (56), see Fig. 12(a,d,g). In this way, we can pinpoint the region of temperature and external magnetic field with one and three DNP solutions, respectively, as shown in Fig. 13. This in turn allows to determine the transition temperature $T_{c,\mathrm{ST}}$ for the triplet-singlet crossing, where the DNP becomes single-valued. In the specific case of parameters chosen in Fig. 12 and 13, we find $T_{c,\mathrm{ST}} \simeq 2.80A_+/k_\mathrm{B}$, which is about one order of magnitude larger than $T_{c,\mathrm{TT}} = A_+/(4k_\mathrm{B})$ Eq.(35).

We have repeated this procedure to find the transition temperatures for different parameters as seen in tables I and II. We find that *the transition temperature* $T_{c,\mathrm{ST}}$ *depends on various external parameters* — in contrast to the case of the model for the triplets crossing, where $T_{c,\mathrm{TT}}$ only depends on $A_+$. In table I, we find that $T_{c,\mathrm{ST}}$ seems largely insensitive to decreasing the inelastic rate

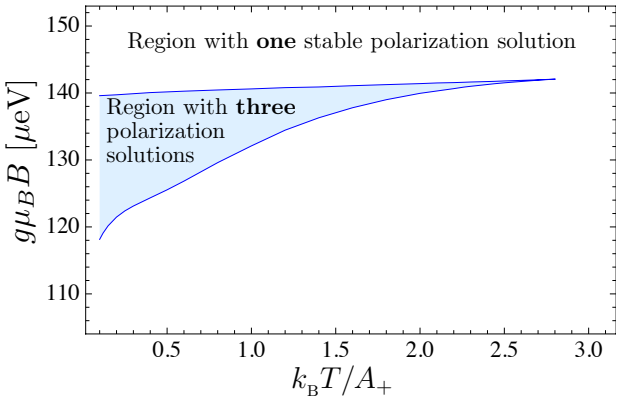


FIG. 13. (Color online) The regions in parameter space close to the singlet-triplet crossing with one (white region) or three (blue region) solutions of the polarization, respectively. Only two of the three solutions for $P$ in the blue region are stable against small fluctuations. A bistable nuclear polarization – and hence current hysteresis – is clearly solely found for $T$ below the transition temperature $T_{c,\mathrm{ST}} \simeq 2.80A_+/k_\mathrm{B}$. The parameters are the same as used in Fig. 12.

| | $\gamma_\mathrm{ine}=10^{-6}$ | $\gamma_\mathrm{ine}=10^{-7}$ | $\gamma_\mathrm{ine}=10^{-8}$ | $\gamma_\mathrm{ine}=10^{-9}$ |
|---|---|---|---|---|
| $t=50\mu$eV | $2.64A_+$ | $2.65A_+$ | $2.65A_+$ | $2.65A_+$ |
| $t=100\mu$eV | $2.72A_+$ | $2.80A_+$ | $2.81A_+$ | $2.82A_+$ |
| $t=150\mu$eV | $2.50A_+$ | $2.62A_+$ | $2.66A_+$ | $2.67A_+$ |

TABLE I. The transition temperatures $k_\mathrm{B}T_{c,\mathrm{ST}}$ for the singlet-triplet crossing for various inter-dot couplings $t$ and inelastic escape rates $\gamma_\mathrm{ine} = \Gamma^\mathrm{ine}/\Gamma_\mathrm{L}$. Here, $\gamma_\mathrm{ine}$ are chosen smaller than the dominant hyperfine rate close to the level crossing. The fixed parameters here are: $A_\mathrm{L} = 80\mu$eV, $A_\mathrm{R} = 70\mu$eV, $\gamma_{ph} = 1\mu$eV, $\Gamma_\mathrm{L} = \Gamma_\mathrm{R}$ and $\hbar\Gamma_\mathrm{L}N = 10^6\mu$eV.

$\gamma_\mathrm{ine} = \Gamma^\mathrm{ine}/\Gamma_\mathrm{L}$ as long as it is smaller than the dominant singlet-triplet rates close to the level crossing. This makes sense from the implicit equation (56), since a small $\Gamma^\mathrm{ine}$ is negligible compared to $W_{S_\pm,T_\pm}$ and $\Gamma_{\uparrow,T_\mathrm{p}}$. Table I also reveals a small non-monotonous dependence of $T_{c,\mathrm{ST}}$ on the inter-dot coupling $t$, which controls the level splitting $|E_{S_\pm} - E_{T_\mathrm{p}}|$ and, in turn, the size of the triplet-triplet HF rates close to the singlet-triplet crossing.

An effective way to change the relative magnitudes

| | $A_-=1\mu$eV ($A_\mathrm{L}=76\mu$eV) | $A_-=5\mu$eV ($A_\mathrm{L}=80\mu$eV) | $A_-=10\mu$eV ($A_\mathrm{L}=85\mu$eV) |
|---|---|---|---|
| $\hbar\Gamma_\mathrm{L}N=10^5\mu$eV | $6.65A_+$ | $2.38A_+$ | $1.32A_+$ |
| $\hbar\Gamma_\mathrm{L}N=10^6\mu$eV | $6.94A_+$ | $2.80A_+$ | $1.39A_+$ |

TABLE II. The transition temperatures $k_\mathrm{B}T_{c,\mathrm{ST}}$ for the singlet-triplet crossing varying the difference between the hyperfine coupling constants $A_- = (A_\mathrm{L} - A_\mathrm{R})/2$ and the number of nuclei $\hbar\Gamma_\mathrm{L}N$ (measured with the rate $\Gamma_\mathrm{L}$). By varying $A_-$, we change the overall strength of the singlet-triplet rates compared to the triplet-triplet rates. The fixed parameters here are: $A_+ = 75\mu$eV, $\gamma_\mathrm{ine} = 10^{-7}$, $t = 100\mu$eV, $\gamma_{ph} = 1\mu$eV and $\Gamma_\mathrm{L} = \Gamma_\mathrm{R}$.

of the singlet-triplet and the triplet-triplet rates, is to change $A_-$, since the singlet-triplet rate have an overall prefactor of $A_-^2$ (whereas $W_{T,T} \propto A_+^2$). Table II shows $T_{c,\mathrm{ST}}$ for varying the relative strength of the singlet-triplet and triplet-triplet rates. The largest transition temperature, $k_\mathrm{B}T_{c,\mathrm{ST}} \simeq 6.94A_+$, is found in the case, where the singlet-triplet, triplet-triplet and inelastic rates all are of the same order of magnitude. In contrast, the smallest value, $k_\mathrm{B}T_{c,\mathrm{ST}} \simeq 1.32A_+$, is found when the singlet-triplet rate dominates by more than two orders of magnitude over the triplet-triplet rate. Furthermore, the number of nuclei change $T_{c,\mathrm{ST}}$ slightly. Finally, we remark that the transition temperature $T_{c,\mathrm{ST}}$ is not simply proportional to $A_+$. Nevertheless, we give $k_\mathrm{B}T_{c,\mathrm{ST}}$ in units of $A_+$ in order to compare it with a typical energy scale of the problem. Altogether, we find that a common feature for all the parameters considered here, is that $T_{c,\mathrm{ST}}$ is found to be larger than $T_{c,\mathrm{TT}}$.

The leakage current is found from Eq.(17) by inserting the stable DNP found from the implicit equation (56). To this end, we use the normalization condition $\sum_\nu n_\nu = 1$ to specify all the occupations. In Fig. 12, we investigate the DNP, leakage current and energy levels in the regime, where the HF singlet-triplet rates dominate in magnitude over the triplet-triplet and inelastic rates close to the level crossing[131], see Fig. 14.

Current hysteresis is found as a natural consequence of two stable polarization solutions for $T < T_{c,\mathrm{ST}}$ — just as in the case of the crossing of the triplet levels. For instance, if one increases the magnetic field from, say, $g\mu_B B = 120\mu$eV for $T < T_{c,\mathrm{ST}}$ [Fig. 12(a)], then the polarization will remain on the lower DNP solution until the critical field of about $g\mu_B B \simeq 140.9\mu$eV, where the lower branch cease to exist. At this point, the polarization jumps discontinuously to the upper stable branch, such that the current also changes discontinuously as seen in Fig. 12(b). Likewise, when sweeping the field backwards from a high value of $g\mu_B B$, then a discontinues jump is found in the current at the point, where the upper stable DNP cease to exist.

The stability of the DNP solution does not follow directly from the solution of the implicit equation (56). In order to determine the stability of the DNP solution against small fluctuations, we numerically propagate the coupled rate equations (50-51) in time until a stationary solution is reached.[120]

Furthermore, the solution of the simplified rate equations (50-51) and the numerical solution of the full rate equations (15-16) with all transition processes included match extremely well. The results presented in Fig. 12-15 calculated in the two different ways fit perfectly.

Next, we consider the regime of $T \geq T_{c,\mathrm{ST}}$, Fig. 12(d-i). By increasing the magnetic field away from the crossing of the triplets at $B = 0$, the triplet-triplet rates decrease, while the singlet-triplet rates increase, since the triplet energy $E_{T_+}$ ($E_{T_-}$) approaches the singlet energy $E_{S_+}$ ($E_{S_-}$) from below (above) [Fig. 12(f,i)]. This means that two new processes come into play to lift the SB, namely

$T_+ \to S_+$ and $T_- \to S_-$, see Fig. 11. The closer the singlet and triplet levels are, the more effective are these two triplet-singlet processes, which in turn produce a leakage current peak at the singlet-triplet level crossing as seen in Fig12(e,h). Moreover, the pure triplet occupations $n_{T_\pm}$ decrease close to the singlet-triplet level crossing as a consequence of the enhanced triplet-singlet processes as seen in Fig. 15(a). Simultaneously, the occupation of the mixed triplet $T_\mathfrak{p}$ peaks at the level crossing. The reason is that the polarization decreases such that the escape rate $\Gamma_{\sigma,T_\mathfrak{p}} \sim \mathfrak{p}^2$ in Eq.(20a) becomes heavily suppressed as seen in Fig. 14(c).

The two dominant HF processes close to the singlet-triplet crossing, $T_+ \to S_+$ and $T_- \to S_-$, polarize the nuclei in opposite directions. When approaching the singlet-triplet crossing from below ($E_{T_+} < E_{S_+}$), the polarization decreases [Fig. 12(d,g)]. This is consistent with the fact that the negatively-polarizing phonon-emission process $T_- \to S_-$ is larger than the positively-polarizing phonon-absorption process $T_+ \to S_+$ as seen in Fig. 14(a).[132] The polarization is seen to increase again, once the magnetic field $g\mu_B B$ is tuned beyond the singlet-triplet crossing (indicated by the dashed vertical line in Fig. 12).

Interesting, a very sharp – yet continuous – increase in the polarization is seen for $T = T_{c,\mathrm{ST}}$ at a *higher* magnetic field than the one at which the singlet and triplet levels cross, see Fig. 12(d). This behavior is qualitatively different from the one observed for the crossing of the triplets. In that case, the sharp increase in polarization is found at the *same* magnetic field as the one where the triplet energy levels cross; compare Fig. 8(d) to Fig. 12(d). In both cases, the sharp polarization increase is a precursor of the DNP bistability. The sharp DNP increase at a $g\mu_B B$ beyond the singlet-triplet level crossing, is also reflected in the sudden increase of level splitting just *after* the level crossing as seen in the inset of Fig. 12(f). The mismatch between the level crossing and the sharp DNP increase indicates that triplet-singlet processes are not the only important ingredient close to the singlet-triplet crossing – although their rates dominate in magnitude. The triplet-triplet transitions also play a role. In fact, it is the inclusion of the triplet-triplet rates in the simplified rates (50-51) that leads to an enhancement of the transition temperature.

## V. MONTE CARLO SIMULATIONS AND THE BREAKDOWN OF THE RATE EQUATION APPROACH

In the following section, the rate equation approach is shown to be consistent with Monte Carlo simulation including an inelastic escape mechanism. We pay special attention to the case *without* the inelastic escape mechanism, where the rate equation description is shown to break down. In this case, the Monte Carlo simulations show that no nuclear polarization can be induced by the

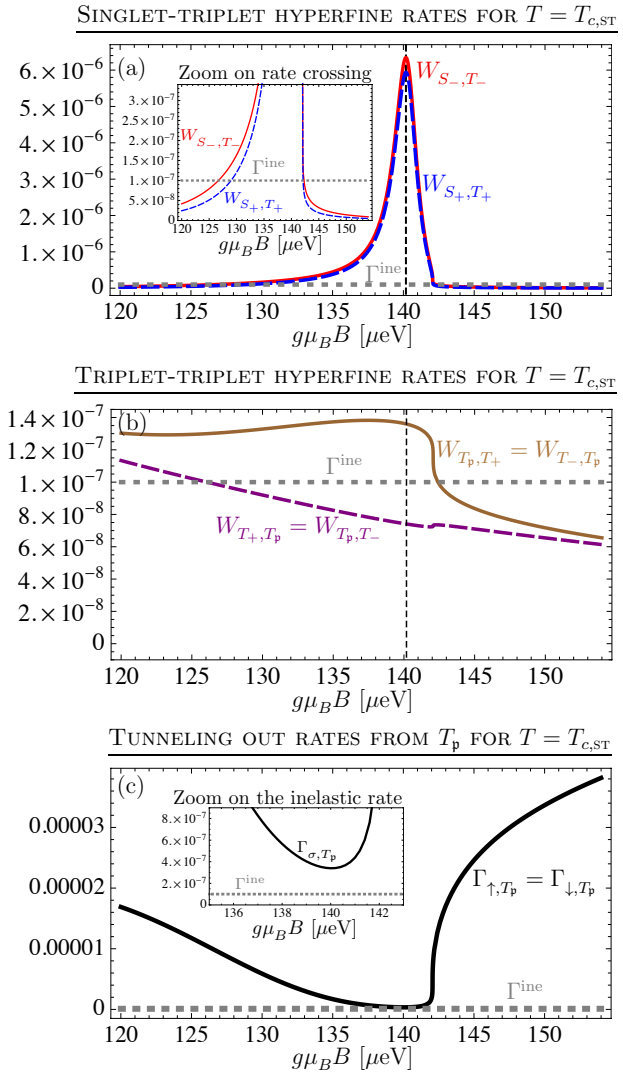


FIG. 14. (Color online) (a) The hyperfine-induced triplet-singlet rates $W_{S_-,T_-}$ (red full line) and $W_{S_+,T_+}$ (blue dashed line) become much larger than the inelastic escape rate $\gamma_{\mathrm{ine}} = \Gamma^{\mathrm{ine}}/\Gamma_{\mathrm{L}}$ (gray dotted line) close to the singlet-triplet energy level crossing (vertical dashed line). The inset shows that far away from the singlet-triplet crossing the hyperfine rates goes to zero such that the inelastic rate becomes larger. (b) The hyperfine-induced triplet-triplet rates $W_{T_\mathfrak{p},T_+} = W_{T_-,T_\mathfrak{p}}$ (brown full line) and $W_{T_+,T_\mathfrak{p}} = W_{T_\mathfrak{p},T_-}$ (violet dashed line) are seen to be on the same order of magnitude as the inelastic escape rate $\gamma_{\mathrm{ine}}$ (gray dotted line) close to the singlet-triplet crossing. (c) The rate $\Gamma_{\sigma,T_\mathfrak{p}}$ (black full line) for tunneling out of the DQD from $T_\mathfrak{p}$ is seen to be reduced close to the singlet-triplet crossing due to the fact that the polarization decreases [see Fig. 12(d)]. Therefore, $\Gamma_{\sigma,T_\mathfrak{p}}$ becomes on the order of the inelastic escape rate (dotted gray line) close to the level crossing (see inset). In (a), (b) and (c), all rates are in units of $\Gamma_{\mathrm{L}}$. The temperature is $T = T_{c,\mathrm{ST}}$ and the parameters are the same as in Fig. 12(d-e). For $T > T_{c,\mathrm{ST}}$ qualitatively similar curves are found.

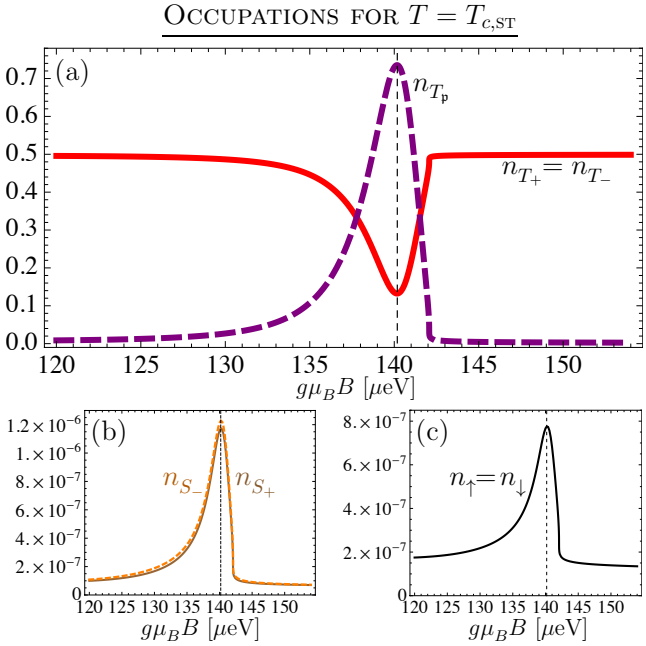


FIG. 15. (Color online) (a) Occupations of the triplet states $n_{T_-} = n_{T_+}$ (red full line) and $n_{T_\mathfrak{p}}$ (purple dashed line). (b) Occupations of the singlet states, $n_{S_-}$ (orange dotted line) and $n_{S_+}$ (brown full line), are seen to differ slightly as anticipated in Eq.(54). (c) Occupations of the one-electron states $n_\uparrow = n_\downarrow$ (black full line). The temperature is $T = T_{c,\mathrm{ST}}$ and the parameters are the same as in Fig. 12(d-e). However, the same qualitative behavior is found for $T > T_{c,\mathrm{ST}}$.The vertical dashed black line indicate the position of the singlet-triplet level crossing. We observe a decrease in the occupations of the pure triplets $T_\pm$ close to the level crossing due to the enhanced HF-induced singlet-triplet rates in this region, see Fig. 14(a). In contrast, the occupation of the triplet $T_\mathfrak{p}$ increases heavily due to the polarization decrease [Fig. 12(d)], which reduces the escape rate form $T_\mathfrak{p}$ [see Eq.(20a) and Fig. 14(c)].

leakage current as expected.[30,33]

### A. Breakdown of the rate equation description without the inelastic escape mechanism

In the SB setup, a non-zero average DNP comes about due to a competition between HF induced and (at least) one other escape mechanism from the blocking states[33] as discussed in Sec. I B. If HF interaction is the *only* mechanism to lift SB, then the nuclear polarization does not change on average.[30,33] We show now that this situation *cannot* be described by the rate equations (15-16). To see this, we use rate equations (15-16) to derive that

$$\dot{n}_{T_+} - \dot{n}_{T_-} + \frac{N}{2}\dot{P} + \frac{1}{2}[\dot{n}_\uparrow - \dot{n}_\downarrow] = \frac{1}{2}(\Gamma_{S_+,\downarrow} + \Gamma_{S_+,\uparrow} + \Gamma_{T_\mathfrak{p},\uparrow} - \Gamma_{T_+,\uparrow})[n_\downarrow - n_\uparrow] + 2\Gamma^{\mathrm{ine}}[n_{T_-} - n_{T_+}] \quad (57)$$

in the limit of equal inelastic escape rates (18) and by utilizing the index invariances Eqs.(21,26). Furthermore, the explicit expressions for the rates (19) lead to $(\Gamma_{S_+,\downarrow} + \Gamma_{S_+,\uparrow} + \Gamma_{T_\mathfrak{p},\uparrow} - \Gamma_{T_+,\uparrow}) = 0$ such that

$$\dot{n}_{T_+} - \dot{n}_{T_-} + \frac{N}{2}\dot{P} + \frac{1}{2}[\dot{n}_\uparrow - \dot{n}_\downarrow] = 2\Gamma^{\mathrm{ine}}[n_{T_-} - n_{T_+}]. \quad (58)$$

This shows that if $\Gamma^{\mathrm{ine}} = 0$, then the quantity $n_{T_+} - n_{T_-} + (N/2)P + (1/2)[n_\uparrow - n_\downarrow]$ is conserved in the time evolution of the rate equations. In other words, for $\Gamma^{\mathrm{ine}} = 0$ the stationary state of the rate equations *depends* on the *initial occupations* $n_{T_\pm}$ and $n_\sigma$, which is *unphysical*. Thus, the rate equation description in Eqs.(15-16) breaks down without the inelastic escape rate, i.e. for $\Gamma^{\mathrm{ine}} = 0$. This is the basic problem with the dynamics presented in Ref. [42]. However, for $\Gamma^{\mathrm{ine}} \neq 0$ as used in this paper, the quantity $n_{T_+} - n_{T_-} + (N/2)P + (1/2)[n_\uparrow - n_\downarrow]$ is not conserved, which is evident from Eq.(58).

### B. Monte Carlo simulations

For $\Gamma^{\mathrm{ine}} \neq 0$ – even if it is very small – the rate equations (15-16) gives a reliable description of the DNP in the SB regime. In order to test this, we have performed Monte Carlo simulations leading to the same results as the rate equations, which we present here.

The idea of the Monte Carlo simulation is – in some sense – to carry out a numerical experiment. The simulation is begun by placing the system in some initial state, say $|T_\mathfrak{p}\rangle$, with some initial polarization $P(t = 0)$. Thereafter, the system is updated in discrete time steps. From each state $|i\rangle$, there is a certain probability $p_{f,i}$ to go to another state $|f\rangle$ of the system within a single time step. We use a computer-generated random number to decide, if the system goes to another state or simply remains in the same state in a time step. The probability for a certain transition in a time step is proportional to its rate. A HF induced transition changes the nuclear polarization for the next time step, and, in turn, also the transition probabilities. Thus, the polarization dynamically changes in time along with the probabilities during the simulation. At some point in time, the polarization is such that the system has found a stationary state on the average. Fig. 16 shows an example of dynamical polarization in a single Monte Carlo simulation. In order to get average properties, that can be compared to the results of the rate equation approach, we need to time average over the fluctuations of the simulation.

The main difference between the rate equation approach and the Monte Carlo simulation approach is that the rate equations solely deal with average quantities. Therefore, the rate equations allow in some sense many processes to take place on average side by side. In contrast, the system is in a specific state in each instant of time during a Monte Carlo simulation. Furthermore, both approaches neglect all quantum mechanical coher-

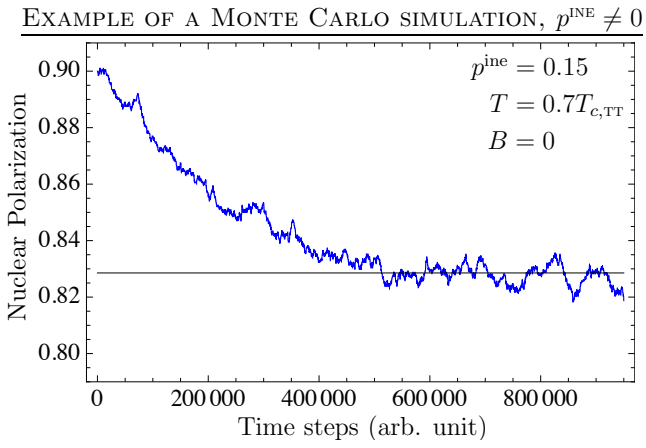


FIG. 16. (Color online) An example of a Monte Carlo simulation of the dynamical nuclear polarization (blue full line) versus time. The polarization is seen to level off to a stationary value of $P \simeq 0.829$ (black horizontal line) from an initial polarization of $P(t=0) = 0.9$. This is in perfect agreement with the rate equation result. As expected, the polarization is seen to fluctuate due to the randomness of the electron transport. The parameters are: $A_{\rm R} = 50\mu$eV, $A_{\rm L} = 30\mu$eV, $t = 310\mu$eV and $\gamma_{ph} = 5\mu$eV such that singlet and triplet levels are far apart for $B = 0$. The probability for tunneling into $T_\pm$ is set to $p_{\rm L} = p_{\rm R} = 0.45$ and the inelastic probability is chosen to be $p^{\rm ine} = 0.15$. Moreover, the change of the polarization due to a HF interaction is set to $dP = 0.0005$ and an overall prefactor of $\eta_{HF} = 0.1$ is used in the HF probabilities.

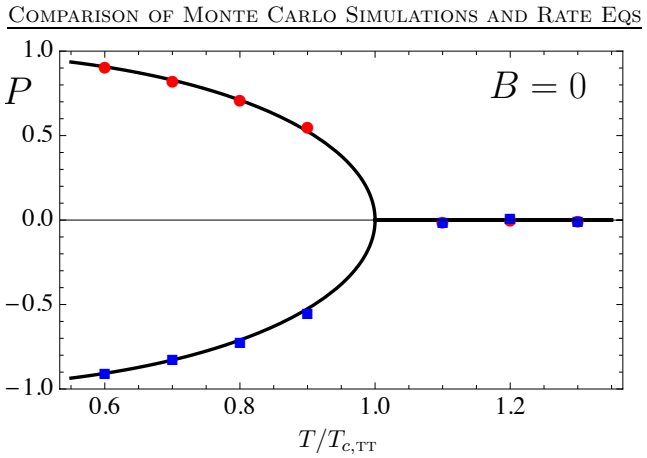


FIG. 17. (Color online) The stable nuclear polarization versus temperature $T/T_{c,\rm TT}$ close to the crossing of the triplets found using the rate equation approach (black full lines) and using the Monte Carlo simulations with positive (red circles) and negative (blue squares) initial polarization values. The two methods are seen to compare very well. The parameters are the same as in Fig. 16, except that we use $dP = 0.005$ and average over 25 simulations (see main text for details).

ences in the description.

In Fig. 17, we see that the rate equation description and the Monte Carlo simulations agree very well for the polarization versus temperature close to the crossing of the three triplet levels.[133] In the same way, we find excellent agreement between the two methods for finite magnetic fields close to the crossing of the triplet levels, and for magnetic fields corresponding to the singlet-triplet level crossing.

Furthermore, we have performed Monte Carlo simulations in the case of zero inelastic escape probability, $p^{\rm ine} = 0$, where the rate equation approach for the DNP breaks down. We find that if $p^{\rm ine} = 0$, then the time-averaged polarization is simply equal to the initial polarization of the simulation. See Fig. 18 for an example and it caption for a discussion. These simulations therefore confirm that no finite DNP is build up on average for HF interactions being the only mechanism lifting SB, as expected in Refs. 30 and 33.

*On the implementation of the Monte Carlo simulations*

We implement all the possible transitions between the states $\{\uparrow, \downarrow, T_+, T_-, T_{\mathfrak{p}}, S_+, S_-\}$ as shown graphically on Fig. 4. Therefore, we are not limited to simulate a specific level crossing. For the transition probabilities in a single time step, we use the same functional dependences as for the rate expressions (18,19,20,23,24), since rates and probabilities are proportional. In the formulas (18,19,20), we exchange the rates $\Gamma_{\rm R(L)}$ by $p_{\rm R(L)}$ and $\Gamma^{\rm ine}$ by $p^{\rm ine}$. For instance, $p_{T_{\mathfrak{p}},\uparrow} = p_{\rm L}/(2\mathcal{N}^2)$ is the probability for going to $T_{\mathfrak{p}}$ given that the system is in the one-electron state $\uparrow$. Likewise, we exchange the factor $1/(2N)$ in the HF rates (23,24) by the parameter $\eta_{HF}$ in the HF probabilities. Thereby we can tune the magnitude of the HF transition probabilities compared to the inelastic transition probabilities. Thus, we can easily study the same physical situation as in the rate equation approach. For instance, Figs. 6 and 17 both study large singlet-triplet energy separation and zero magnetic field.

To minimize the computational load, we choose the transition probabilities within a single time step as *high* as possible, such that the system does not remain in the same state over too many time steps. This can be understood as a long physical time duration for each time step. Nevertheless, we have to choose numbers such that the sum of all probabilities for leaving a specific state is always *smaller* than one in each time step, e.g. for $T_{\mathfrak{p}}$ this amounts to

$$2p^{\rm ine} + p_{\downarrow,T_{\mathfrak{p}}} + p_{\uparrow,T_{\mathfrak{p}}} + p^{HF}_{T_+,T_{\mathfrak{p}}}(t) + p^{HF}_{T_-,T_{\mathfrak{p}}}(t) < 1. \quad (59)$$

In this way, the possibility of staying in the same state (here $T_{\mathfrak{p}}$) within a time step remains in the simulation.

In the real experiment, the polarization change by $dP = \pm 2/N$ due to a *single* HF transition. In the simulation, however, $dP$ is increased substantially in order to obtain faster convergence to a stationary polarization. We emphasize that the choice of $dP$ does *not* affect the value of the stationary polarization, but it does indeed af-

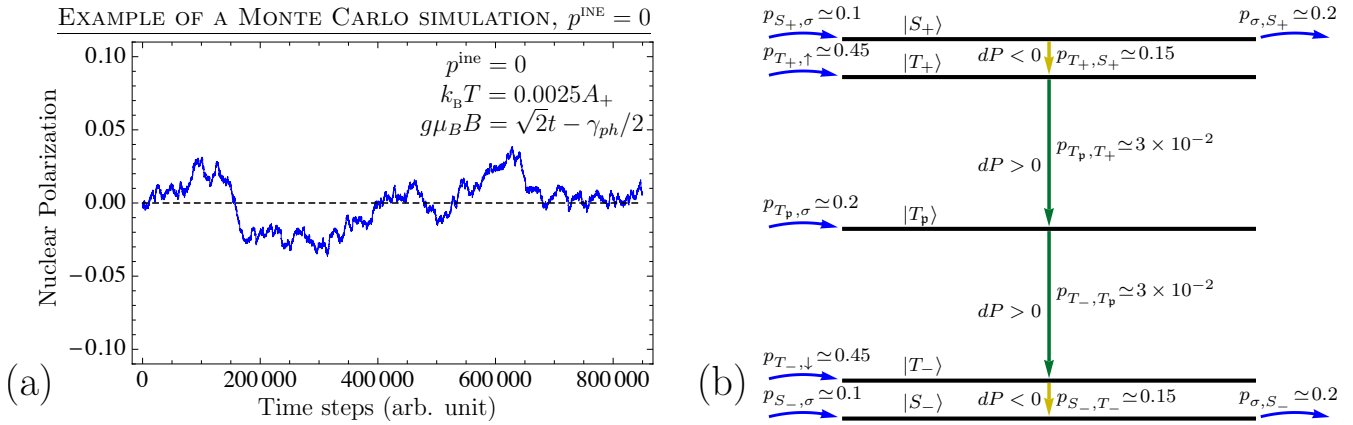


FIG. 18. (Color online) (a) An example of a Monte Carlo simulation showing that the nuclear polarization (blue full line) is not changed on the average due to the leakage current when *only* HF interactions lift the SB, i.e. $p^{\rm ine}=0$. The magnetic field is tuned close to the singlet-triplet crossing leading to a level ordering as seen in (b). Moreover, we choose a very low temperature such that finite DNP could appear for $p^{\rm ine}\neq 0$. The initial polarization, $P(t=0)=0$ (black dashed line), is found to be equal to the time-averaged polarization, $\overline{P}\simeq 0.002$, within the uncertainty. Similarly, the average occupations in the simulation are found to be $\overline{n}_{T_+}\simeq 0.26$, $\overline{n}_{T_-}\simeq 0.15$, $\overline{n}_{T_{\mathfrak{p}}}\simeq 0.48$, $\overline{n}_{S_+}\simeq 0.0063$, $\overline{n}_{S_-}\simeq 0.063$ and $\overline{n}_{\uparrow}\simeq\overline{n}_{\downarrow}\simeq 0.017$. Thus, in contrast to the $p^{\rm ine}\neq 0$ case, we find $\overline{n}_{T_+}\neq\overline{n}_{T_-}$. The parameters are: $A_{\rm R}=50\mu$eV, $A_{\rm L}=30\mu$eV, $t=50\mu$eV and $\gamma_{ph}=5\mu$eV such that the singlet and triplet energy levels are well separated, i.e. $t\gg\gamma_{ph}$. Moreover, we use $p_{\rm L}=p_{\rm R}=0.45$, $dP=0.0005$ and $\eta_{HF}=2$. (b) An illustration of why no nuclear polarization is expected to be induced, when HF interactions is the only mechanism lifting SB. In the figure, we include all transition probabilities $p$ larger than $10^{-4}$ for the numerical example shown in (a). The HF spin-flip processes either increase (green arrows) or decrease (yellow arrows) the polarization on the average. We begin by noting that escape from neither $S_-$ nor $S_+$ change the over all polarization. For instance, the escape path $S_+\to T_+\to T_{\mathfrak{p}}\to T_-\to S_-\to\sigma$ consist of an equal amount of positive and negative nuclear spin-flips: $-|dP|+|dP|+|dP|-|dP|=0$. Similarly, escape from $T_{\mathfrak{p}}$ also leave the polarization unchanged. In contrast, escape from $T_\pm$ polarize the nuclei by $\pm|dP|$, respectively. However, since $T_\pm$ also load with the same probability, $p_{T_+,\uparrow}=p_{T_-,\downarrow}$, no average DNP can be build up, even though escape from $T_+$ is less probable than from $T_-$ (as reflected in $\overline{n}_{T_+}>\overline{n}_{T_-}$) in the case considered here.

fect the typical fluctuations around this value. Thus, an artifact of choosing $dP$ larger than $2/N$ is the artificially increased fluctuations around the stationary polarization – as seen Figs. 16 and 18 – compared to the experimental situation. However, since we are only interested in average values, this is not a concern here. Choosing $dP$ is therefore a compromise between maximizing convergence time and minimizing fluctuations.

In order to find the stationary polarization in practices, we choose a $dP$, perform the Monte Carlo simulation a number of times for a given initial polarization and then average over the results. In practices, the averaging makes it easier to decide if convergence is reached in a computationally cheap way.[134] We stress that the stationary polarization can also be found from doing the single Monte Carlo simulation as seen in Fig. 16, but it requires a much smaller $dP$. Moreover, the fluctuations in DNP increase with temperature, since higher temperature increases the phonon-absorption HF transition probabilities, which in turn increases the number of likely transition processes.

## VI. SUMMARY, DISCUSSION AND OUTLOOK

In summary, we have analyzed the DNP and leakage current through a DQD in the SB regime due to a competition between HF interactions and another weaker inelastic escape mechanism from the triplets. We have demonstrated in detail how the DNP becomes bistable for temperatures $T$ below the transition temperature around both (i) the crossing of the three triplet levels and (ii) the crossing of the triplets $T_\pm$ with the singlets $S_\pm$. The bistable DNP leads naturally to hysteresis in the leakage current. We have found that the transition temperature for the crossing of the triplet levels, $T_{c,\rm TT}$, is generally different from the transition temperature for the singlet-triplet crossing, $T_{c,\rm ST}$. Moreover, $T_{c,\rm TT}<T_{c,\rm ST}$ for experimentally relevant parameters and the difference can be sizable, e.g. an order of magnitude. Yet, both transition temperatures are estimated to be within experimental reach. Therefore, if $T_{c,\rm TT}<T<T_{c,\rm ST}$, then current hysteresis appears around the singlet-triplet crossings at finite magnetic field, but is absent close to zero field. Furthermore, we found analytically $T_{c,\rm TT}=(A_{\rm L}+A_{\rm R})/(8k_{\rm B})$, where $A_{\rm L(R)}$ is the hyperfine constant of the left (right) dot. In contrast, $T_{c,\rm ST}$ depends on various parameters, e.g. the inhomogeneity of the Overhauser field. Furthermore, we have analyzed the details of the leakage current versus magnetic field and given various analytical limits in the case of the crossing of the triplet levels.

Importantly, we have identified that the asymmetry between phonon emission and absorption in the HF-induced spin-flip transitions is the crucial ingredient

for the existence of the transition temperatures at zero energy-detuning. This is in contrast to Refs. [33–35], where the emission and absorption of energy is equally likely, such that no DNP is found in these works for zero energy-detuning. Nevertheless, they find bistabilities and current hysteresis for finite energy-detuning.

Finally, we have observed that our results from the rate equation approach are consistent with those produced by Monte Carlo simulations, if the inelastic escape mechanism is included. Moreover, we discussed how the rate equation approach for the DNP becomes invalid without the inelastic escape rate.

Through out the paper, we have neglected depolarizing processes such as nuclear spin-diffusion, since these are typically much slower than the HF spin-flip processes. Nevertheless, such processes might affect our results slightly in the case of large DNP, where the depolarization is stronger. On the other hand, very large polarization have also been reported experimentally.[31]

Furthermore, we have modeled the polarization of the nuclear spins as a single valued quantity, $P$, as in e.g. Refs.[33–35, and 42]. In reality, the polarization will vary in space leading to a more complex behavior, which is more involved to model.[108] An extension of the model could be to use one polarization for each of the two dots.[36,37] In such an approach, it is an open question, if the two polarizations would become bistable at the same transition temperature or not. Moreover, as emphasized in the paper, the difference in the effective Overhauser magnetic field between the dots is important to produce an escape path from the triplet with zero angular moment projection. Here, we have included this effect by having slightly different hyperfine constants in the dots.

We have studied in detail the case of a single constant inelastic escape rate from the triplet levels, which compete with the HF-induced escape.[33–36] Neglecting the energy dependence of the inelastic rates is a valid approach as long as the inelastic rate is smaller than the dominant HF rate close to the level crossing, as we have analyzed in this paper. Nevertheless, the inelastic mechanisms can be increased experimentally, e.g. by choosing a material with stronger spin-orbit coupling[19] or by tuning the levels compared to the chemical potentials of the leads such that co-tunneling processes becomes more probable.[12] In such cases, it could be interesting to repeat our analysis including the energy dependences of the co-tunneling rates[15,16] and/or spin-orbit rates. Moreover, future work could also analyze the effects of including a more detailed description of the phonon part of the HF transitions. However, we believe that the essential physics is captured by including the asymmetry between emission and absorption of phonons in the HF transitions.

## VII. ACKNOWLEDGMENTS

We are especially thankful to János Asbóth and Andras Pályi for insightful discussions on the nature of non-zero nuclear polarization in the spin-blockade setup. Moreover, we thank Andrea Donarini, Sigmund Kohler, Rafael Sánchez, Gerold Kiesslich, Marta Prada, Jesús Iñarrea and Fernando Domínguez for useful discussions. AML acknowledges the Juan de la Cierva program (MICINN). AML, CLM and GP acknowledge Grant No. MAT2011-24331 and the ITN Grant 234970(EU). LLB and IV acknowledge Grant No. FIS2011-28838-C02-01. We acknowledge FIS2010-22438-E (Spanish National Network Physics of Out-of-Equilibrium Systems).

## Appendix A: Current expressions close to the crossing of the triplet levels for non-equal inelastic escape rates

Throughout the paper, we have considered the case of *equal* and constant inelastic escape rates $\Gamma^{\rm ine}_{\sigma,T}$ from the triplet states $T = T_\pm, T_{\rm p}$, see Eq.(18).[33–36] However, depending on the inelastic escape mechanism, the rates might be different. For completeness, we discuss this briefly in this appendix in a particularly simple case.

Here we consider the case, where the inelastic escape rates are invariant under the same exchange of indices as the tunneling rates Eq.(21), i.e.

$$\Gamma^{\rm ine}_{\uparrow,T_{\rm p}} = \Gamma^{\rm ine}_{\downarrow,T_{\rm p}}, \quad \Gamma^{\rm ine}_{\uparrow,T_+} = \Gamma^{\rm ine}_{\downarrow,T_-}, \quad \Gamma^{\rm ine}_{\downarrow,T_+} = \Gamma^{\rm ine}_{\uparrow,T_-}. \quad \text{(A1)}$$

Following the same steps leading to the polarization equation in Sec. III A, we find that $n_\uparrow = n_\downarrow$ and $n_{T_+} = n_{T_-}$ still hold true such that the implicit equation (32) for the polarization,

$$W_{T_{\rm p},T_+} = W_{T_+,T_{\rm p}} = W_{T_{\rm p},T_-} = W_{T_-,T_{\rm p}}, \quad \text{(A2)}$$

and the transition temperature, $k_{\rm B}T_{c,\rm TT} = A_+/4$ (35), remain unchanged compared to the main text. Furthermore, $n_{S_+} = n_{S_-}$ and Eqs.(38) and (39) also still hold true, whereas the explicit expressions for the occupations (40) and the current (41) are changed slightly. In the numerator of $n_{T_+}$ (40b), the rate $\Gamma^{\rm ine}$ is replaced by $\Gamma^{\rm ine}_{\uparrow,T_{\rm p}}$. Similarly, in the numerator of $n_{T_{\rm p}}$ (40a), one has to make the replacement $2\Gamma^{\rm ine} \to \Gamma^{\rm ine}_{\uparrow,T_+} + \Gamma^{\rm ine}_{\uparrow,T_-}$. The common denominator of the occupations (40) changes to $\tilde\Lambda = 2\Gamma_{T_+,\uparrow}\Gamma_{\uparrow,S_+}(\Gamma^{\rm ine}_{\uparrow,T_{\rm p}} + \Gamma_{\uparrow,T_{\rm p}}) + \big[3\Gamma_{T_+,\uparrow}\Gamma_{\uparrow,S_+} + (\Gamma^{\rm ine}_{\uparrow,T_{\rm p}} + \Gamma_{\uparrow,T_{\rm p}})\Upsilon + 3\Gamma_{\uparrow,S_+}\Gamma_{T_{\rm p},\uparrow}\big]W_{T_{\rm p},T_+} + (\Gamma^{\rm ine}_{\uparrow,T_-} + \Gamma^{\rm ine}_{\uparrow,T_+})\big[\Gamma^{\rm ine}_{\uparrow,T_{\rm p}}\Upsilon + (\Gamma_{S_+,\downarrow} + \Gamma_{S_+,\uparrow})(\Gamma_{\uparrow,T_{\rm p}} + W_{T_{\rm p},T_+}) + \Gamma_{\uparrow,S_+}(2\Gamma_{\uparrow,T_{\rm p}} + \Gamma_{T_{\rm p},\uparrow} + 2W_{T_{\rm p},T_+})\big]$. Therefore the current expression becomes

$$I = \frac{2\Gamma_{\uparrow,S_+}}{\tilde\zeta}(\Gamma_{T_+,\uparrow} + \Gamma_{S_+,\downarrow} + \Gamma_{S_+,\uparrow} + \Gamma_{T_{\rm p},\uparrow}) \quad \text{(A3)}$$
$$\times \Big[(\Gamma^{\rm ine}_{\uparrow,T_-} + \Gamma^{\rm ine}_{\uparrow,T_+})(\Gamma^{\rm ine}_{\uparrow,T_{\rm p}} + \Gamma_{\uparrow,T_{\rm p}}) + W_{T_+,T_{\rm p}}(\Gamma^{\rm ine}_{\uparrow,T_-} + \Gamma^{\rm ine}_{\uparrow,T_+} + \Gamma^{\rm ine}_{\uparrow,T_{\rm p}} + \Gamma_{\uparrow,T_{\rm p}})\Big]$$

where

$$\begin{aligned}\tilde{\zeta} \equiv&(\Gamma^{\rm ine}_{\uparrow,T_{\mathfrak{p}}}+\Gamma_{\uparrow,T_{\mathfrak{p}}})\big[2\Gamma_{T_+,\uparrow}\Gamma_{\uparrow,S_+}+(\Gamma^{\rm ine}_{\uparrow,T_+}+\Gamma^{\rm ine}_{\uparrow,T_-})\Upsilon\big]\\&+(\Gamma^{\rm ine}_{\uparrow,T_+}+\Gamma^{\rm ine}_{\uparrow,T_-})\Gamma_{\uparrow,S_+}\Gamma_{T_{\mathfrak{p}},\uparrow}\\&+W_{T_+,T_{\mathfrak{p}}}\Big[3\Gamma_{T_+,\uparrow}\Gamma_{\uparrow,S_+}+3\Gamma_{\uparrow,S_+}\Gamma_{T_{\mathfrak{p}},\uparrow}\\&\qquad+\Upsilon(\Gamma^{\rm ine}_{\uparrow,T_{\mathfrak{p}}}+\Gamma^{\rm ine}_{\uparrow,T_+}+\Gamma^{\rm ine}_{\uparrow,T_-}+\Gamma_{\uparrow,T_{\mathfrak{p}}})\Big].\end{aligned}$$

Note the similarity to the simpler case of equal inelastic rates in Eq.(41).

In passing, we note that even though the current expressions (A3) and (41) are similar, they have an interesting difference: *Without* singlet-triplet mixing $\mathfrak{p}=0$ the current (A3) still depends on the HF rate in contrast to the simpler case of the main text, see Eq.(43). In order to see this explicitly, we insert $\mathfrak{p}=0$ and the tunneling rates (19-20) into the current expression (A3), i.e.

$$\begin{aligned}I(\mathfrak{p}=0)=\frac{8\Gamma_{\rm L}}{\beth}\Big[&W_{T_+,T_{\mathfrak{p}}}(\Gamma^{\rm ine}_{\uparrow,T_-}+\Gamma^{\rm ine}_{\uparrow,T_+}+\Gamma^{\rm ine}_{\uparrow,T_{\mathfrak{p}}})\\&+\Gamma^{\rm ine}_{\uparrow,T_{\mathfrak{p}}}(\Gamma^{\rm ine}_{\uparrow,T_-}+\Gamma^{\rm ine}_{\uparrow,T_+})\Big]\end{aligned}\tag{A4a}$$

where $\Gamma_{\rm L}=\Gamma_{\rm R}$ was used for simplicity and

$$\begin{aligned}\beth\equiv&W_{T_+,T_{\mathfrak{p}}}\big[6\Gamma^{\rm ine}_{\uparrow,T_{\mathfrak{p}}}+6\Gamma^{\rm ine}_{\uparrow,T_-}+6\Gamma^{\rm ine}_{\uparrow,T_+}+9\Gamma_{\rm L}\big]\\&+(6\Gamma^{\rm ine}_{\uparrow,T_{\mathfrak{p}}}+\Gamma_{\rm L})(\Gamma^{\rm ine}_{\uparrow,T_-}+\Gamma^{\rm ine}_{\uparrow,T_+})+4\Gamma^{\rm ine}_{\uparrow,T_{\mathfrak{p}}}\Gamma_{\rm L}.\end{aligned}\tag{A4b}$$

Thus, the current for $\mathfrak{p}=0$ still depends on the HF rate $W_{T_+,T_{\mathfrak{p}}}$ in general.

In summary, when the inelastic rates have the same invariances under interchange of indices as the tunneling rates, then the polarization equation (32) does not change and the current expression changes only slightly. However, in other cases also the polarization condition (32) and the transition temperature can indeed change.


[1] K. Ono, D. G. Austing, Y. Tokura, and S. Tarucha, Science **297**, 1313 (2002)
[2] R. Hanson, L. P. Kouwenhoven, J. R. Petta, S. Tarucha, and L. M. K. Vandersypen, Rev. Mod. Phys. **79**, 1217 (2007)
[3] W. G. van der Wiel, S. De Franceschi, J. M. Elzerman, T. Fujisawa, S. Tarucha, and L. P. Kouwenhoven, Rev. Mod. Phys. **75**, 1 (Dec 2002)
[4] S. M. Reimann and M. Manninen, Rev. Mod. Phys. **74**, 1283 (Nov 2002)
[5] L. P. Kouwenhoven, D. G. Austing, and S. Tarucha, Reports on Progress in Physics **64**, 701 (2001)
[6] K. Ono and S. Tarucha, Phys. Rev. Lett. **92**, 256803 (2004)
[7] D. Weinmann, W. Häusler, and B. Kramer, Phys. Rev. Lett. **74**, 984 (1995)
[8] D. Weinmann, W. Häusler, and B. Kramer, Annalen der Physik **508**, 652 (1996), ISSN 1521-3889
[9] M. Ciorga, A. S. Sachrajda, P. Hawrylak, C. Gould, P. Zawadzki, S. Jullian, Y. Feng, and Z. Wasilewski, Phys. Rev. B **61**, R16315 (2000)
[10] F. H. L. Koppens, J. A. Folk, J. M. Elzerman, R. Hanson, L. H. W. van Beveren, I. T. Vink, H. P. Tranitz, W. Wegscheider, L. P. Kouwenhoven, and L. M. K. Vandersypen, Science **309**, 1346 (2005)
[11] A. C. Johnson, J. R. Petta, J. M. Taylor, A. Yacoby, M. D. Lukin, C. M. Marcus, M. P. Hanson, and A. C. Gossard, Nature **435**, 925 (2005)
[12] A. C. Johnson, J. R. Petta, C. M. Marcus, M. P. Hanson, and A. C. Gossard, Phys. Rev. B **72**, 165308 (Oct 2005)
[13] A. B. Vorontsov and M. G. Vavilov, Phys. Rev. Lett. **101**, 226805 (2008)
[14] K. Saito, S. Okubo, and M. Eto, Physica E **40**, 1149 (2008), ISSN 1386-9477, 17th International Conference on Electronic Properties of Two-Dimensional Systems
[15] F. Qassemi, W. A. Coish, and F. K. Wilhelm, Phys. Rev. Lett. **102**, 176806 (2009)
[16] W. A. Coish and F. Qassemi, Phys. Rev. B **84**, 245407 (2011)
[17] A. V. Khaetskii and Y. V. Nazarov, Phys. Rev. B **61**, 12639 (2000)
[18] V. N. Golovach, A. Khaetskii, and D. Loss, Phys. Rev. Lett. **93**, 016601 (2004)
[19] A. Pfund, I. Shorubalko, K. Ensslin, and R. Leturcq, Phys. Rev. Lett. **99**, 036801 (2007)
[20] J. Danon and Y. V. Nazarov, Phys. Rev. B **80**, 041301 (2009)
[21] S. Weiss, E. I. Rashba, F. Kuemmeth, H. O. H. Churchill, and K. Flensberg, Phys. Rev. B **82**, 165427 (2010)
[22] S. Nadj-Perge, S. M. Frolov, J. W. W. van Tilburg, J. Danon, Y. V. Nazarov, R. Algra, E. P. A. M. Bakkers, and L. P. Kouwenhoven, Phys. Rev. B **81**, 201305 (2010)
[23] D. Stepanenko, M. Rudner, B. I. Halperin, and D. Loss, Phys. Rev. B **85**, 075416 (2012)
[24] P. Stano and J. Fabian, Phys. Rev. Lett. **96**, 186602 (2006)
[25] C. F. Destefani and S. E. Ulloa, Phys. Rev. B **72**, 115326 (2005)
[26] W. A. Coish and J. Baugh, physica status solidi (b) **246**, 2203 (2009), ISSN 1521-3951, an excellent review on Hyperfine interaction.
[27] S. I. Erlingsson, Y. V. Nazarov, and V. I. Fal'ko, Phys. Rev. B **64**, 195306 (2001)
[28] M. Eto, T. Ashiwa, and M. Murata, J. Phys. Soc. Jpn. **73**, 307 (2004)
[29] S. Tarucha, Y. Kitamura, T. Kodera, and K. Ono, physica status solidi (b) **243**, 3673 (2006)
[30] O. N. Jouravlev and Y. V. Nazarov, Phys. Rev. Lett. **96**, 176804 (2006)
[31] J. Baugh, Y. Kitamura, K. Ono, and S. Tarucha, Phys. Rev. Lett. **99**, 096804 (2007)
[32] J. Baugh, Y. Kitamura, K. Ono, and S. Tarucha, physica status solidi (c) **5**, 302 (2008)
[33] M. S. Rudner and L. S. Levitov, Phys. Rev. Lett. **99**, 036602 (2007)
[34] M. S. Rudner and L. S. Levitov, Nanotechnology **21**,

274016 (2010)
[35] M. S. Rudner and E. I. Rashba, Phys. Rev. B **83**, 073406 (2011)
[36] M. S. Rudner, F. H. L. Koppens, J. A. Folk, L. M. K. Vandersypen, and L. S. Levitov, Phys. Rev. B **84**, 075339 (2011)
[37] J. Iñarrea, G. Platero, and A. H. MacDonald, Phys. Rev. B **76**, 085329 (2007)
[38] J. Iñarrea, C. Lopez-Monis, A. H. MacDonald, and G. Platero, Appl. Phys. Lett. **91**, 252112 (2007)
[39] J. Iñarrea, C. Lopez-Monis, and G. Platero, Appl. Phys. Lett. **94**, 252106 (2009)
[40] S. Tarucha and J. Baugh, J. Phys. Soc. Jpn. **77**, 031011 (2008)
[41] M. S. Rudner and L. S. Levitov, Phys. Rev. B **82**, 155418 (2010)
[42] C. López-Monís, J. Iñarrea, and G. Platero, New J. Phys. **13**, 053010 (2011)
[43] M. Gullans, J. J. Krich, J. M. Taylor, H. Bluhm, B. I. Halperin, C. M. Marcus, M. Stopa, A. Yacoby, and M. D. Lukin, Phys. Rev. Lett. **104**, 226807 (Jun 2010)
[44] R. Takahashi, K. Kono, S. Tarucha, and K. Ono, Phys. Rev. Lett. **107**, 026602 (2011)
[45] T. Kobayashi, K. Hitachi, S. Sasaki, and K. Muraki, Phys. Rev. Lett. **107**, 216802 (2011)
[46] R. Takahashi, K. Kono, S. Tarucha, and K. Ono, Applied Physics Express **5**, 025002 (2012)
[47] C. López-Monís, C. Emary, G. Kiesslich, G. Platero, and T. Brandes, Phys. Rev. B **85**, 045301 (Jan 2012)
[48] In Ref. [12], the gate-voltages are tuned to favor an electron virtually tunnels from the left dot into the left lead followed by an electron with opposite spin comes back into the left dot. This happens when the energy level comes closer to the chemical potential of the left lead such that the energy exchange in the virtual second order process becomes smaller.
[49] H. W. Liu, T. Fujisawa, T. Hayashi, and Y. Hirayama, Phys. Rev. B **72**, 161305 (Oct 2005)
[50] M. R. Buitelaar, J. Fransson, A. L. Cantone, C. G. Smith, D. Anderson, G. A. C. Jones, A. Ardavan, A. N. Khlobystov, A. A. R. Watt, K. Porfyrakis, and G. A. D. Briggs, Phys. Rev. B **77**, 245439 (Jun 2008)
[51] N. Shaji, C. B. Simmons, M. Thalakulam, L. J. Klein, H. Qin, H. Luo, D. E. Savage, M. G. Lagally, A. J. Rimberg, R. Joynt, M. Friesen, R. H. Blick, S. N. Coppersmith, and M. A. Eriksson, Nature Physics **4**, 540 (2008)
[52] H. O. H. Churchill, A. J. Bestwick, J. W. Harlow, F. Kuemmeth, D. Marcos, C. H. Stwertka, S. K. Watson, and C. M. Marcus, Nature Physics **5**, 321 (2009)
[53] N. S. Lai, W. H. Lim, C. H. Yang, F. A. Zwanenburg, W. A. Coish, F. Qassemi, A. Morello, and A. S. Dzurak, Scientific Reports **1**, 110 (2011)
[54] F. Kuemmeth, S. Ilani, D. C. Ralph, and P. L. McEuen, Nature **452**, 448 (2008)
[55] H. O. H. Churchill, F. Kuemmeth, J. W. Harlow, A. J. Bestwick, E. I. Rashba, K. Flensberg, C. H. Stwertka, T. Taychatanapat, S. K. Watson, and C. M. Marcus, Phys. Rev. Lett. **102**, 166802 (2009)
[56] T. S. Jespersen, K. Grove-Rasmussen, J. Paaske, K. Muraki, T. Fujisawa, J. Nygård, and K. Flensberg, Nature Physics **7**, 348 (2011)
[57] A. Pályi and G. Burkard, Phys. Rev. B **80**, 201404 (Nov 2009)
[58] A. Pályi and G. Burkard, Phys. Rev. B **82**, 155424 (2010)
[59] F. Pei, E. A. Laird, G. A. Steele, and L. P. Kouwenhoven, Nature Nanotechnology **7**, 630 (2012)
[60] H. W. Liu, T. Fujisawa, Y. Ono, H. Inokawa, A. Fujiwara, K. Takashina, and Y. Hirayama, Phys. Rev. B **77**, 073310 (Feb 2008)
[61] M. Prada, R. H. Blick, and R. Joynt, Phys. Rev. B **77**, 115438 (2008)
[62] C. B. Simmons, T. S. Koh, N. Shaji, M. Thalakulam, L. J. Klein, H. Qin, H. Luo, D. E. Savage, M. G. Lagally, A. J. Rimberg, R. Joynt, R. Blick, M. Friesen, S. N. Coppersmith, and M. A. Eriksson, Phys. Rev. B **82**, 245312 (Dec 2010)
[63] M. Raith, P. Stano, and J. Fabian, arXiv:1206.6906(2012)
[64] A. K. Hüttel, J. Weber, A. W. Holleitner, D. Weinmann, K. Eberl, and R. H. Blick, Phys. Rev. B **69**, 073302 (2004)
[65] A. W. Overhauser, Phys. Rev. **92**, 411 (1953)
[66] S. W. Brown, T. A. Kennedy, D. Gammon, and E. S. Snow, Phys. Rev. B **54**, R17339 (Dec 1996)
[67] D. Gammon, A. L. Efros, T. A. Kennedy, M. Rosen, D. S. Katzer, D. Park, S. W. Brown, V. L. Korenev, and I. A. Merkulov, Phys. Rev. Lett. **86**, 5176 (May 2001)
[68] A. S. Bracker, E. A. Stinaff, D. Gammon, M. E. Ware, J. G. Tischler, A. Shabaev, A. L. Efros, D. Park, D. Gershoni, V. L. Korenev, and I. A. Merkulov, Phys. Rev. Lett. **94**, 047402 (Feb 2005)
[69] C. W. Lai, P. Maletinsky, A. Badolato, and A. Imamoglu, Phys. Rev. Lett. **96**, 167403 (Apr 2006)
[70] P. Maletinsky, A. Badolato, and A. Imamoglu, Phys. Rev. Lett. **99**, 056804 (Aug 2007)
[71] M. S. Rudner and L. S. Levitov, Phys. Rev. Lett. **99**, 246602 (Dec 2007)
[72] A. I. Tartakovskii, T. Wright, A. Russell, V. I. Fal'ko, A. B. Van'kov, J. Skiba-Szymanska, I. Drouzas, R. S. Kolodka, M. S. Skolnick, P. W. Fry, A. Tahraoui, H.-Y. Liu, and M. Hopkinson, Phys. Rev. Lett. **98**, 026806 (Jan 2007)
[73] J. Danon and Y. V. Nazarov, Phys. Rev. Lett. **100**, 056603 (Feb 2008)
[74] X. Xu, W. Yao, B. Sun, D. G. Steel, A. S. Bracker, D. Gammon, and L. J. Sham, Nature **459**, 1105 (2009)
[75] J. Danon, I. T. Vink, F. H. L. Koppens, K. C. Nowack, L. M. K. Vandersypen, and Y. V. Nazarov, Phys. Rev. Lett. **103**, 046601 (Jul 2009)
[76] M. Dobers, K. v. Klitzing, J. Schneider, G. Weimann, and K. Ploog, Phys. Rev. Lett. **61**, 1650 (Oct 1988)
[77] K. R. Wald, L. P. Kouwenhoven, P. L. McEuen, N. C. van der Vaart, and C. T. Foxon, Phys. Rev. Lett. **73**, 1011 (Aug 1994)
[78] J. H. Kim, I. D. Vagner, and L. Xing, Phys. Rev. B **49**, 16777 (Jun 1994)
[79] D. C. Dixon, K. R. Wald, P. L. McEuen, and M. R. Melloch, Phys. Rev. B **56**, 4743 (Aug 1997)
[80] T. Machida, S. Ishizuka, T. Yamazaki, S. Komiyama, K. Muraki, and Y. Hirayama, Phys. Rev. B **65**, 233304 (May 2002)
[81] K. Hashimoto, K. Muraki, T. Saku, and Y. Hirayama, Phys. Rev. Lett. **88**, 176601 (Apr 2002)
[82] E. V. Deviatov, A. Würtz, A. Lorke, M. Yu. Melnikov, V. T. Dolgopolov, D. Reuter, and A. D. Wieck, Phys. Rev. B **69**, 115330 (Mar 2004)
[83] A. Würtz, T. Müller, A. Lorke, D. Reuter, and A. D. Wieck, Phys. Rev. Lett. **95**, 056802 (Jul 2005)
[84] A. Kou, D. T. McClure, C. M. Marcus, L. N. Pfeiffer, and K. W. West, Phys. Rev. Lett. **105**, 056804 (Jul 2010)

[85] T. Nakajima, Y. Kobayashi, and S. Komiyama, Phys. Rev. B **82**, 201302 (Nov 2010)

[86] T. Nakajima and S. Komiyama, Phys. Rev. B **85**, 115310 (Mar 2012)

[87] I. A. Merkulov, A. L. Efros, and M. Rosen, Phys. Rev. B **65**, 205309 (2002)

[88] S. I. Erlingsson and Y. V. Nazarov, Phys. Rev. B **66**, 155327 (Oct 2002)

[89] S. I. Erlingsson and Y. V. Nazarov, Phys. Rev. B **70**, 205327 (Nov 2004)

[90] W. A. Coish and D. Loss, Phys. Rev. B **72**, 125337 (Sep 2005)

[91] S. M. Frolov, J. Danon, S. Nadj-Perge, K. Zuo, J. W. W. van Tilburg, V. S. Pribiag, J. W. G. van den Berg, E. P. A. M. Bakkers, and L. P. Kouwenhoven, arXiv:1209.1510(2012)

[92] In passing, we remark that hysteretic behavior due to DNP is not limited to quantum dot systems, but have also been found experimentally for instance in quantum Hall systems[77,82].

[93] S. I. Erlingsson, O. N. Jouravlev, and Y. V. Nazarov, Phys. Rev. B **72**, 033301 (Jul 2005)

[94] B. Hu and X. R. Wang, arXiv:1209.1548(2012)

[95] M. S. Rudner and L. S. Levitov, arXiv:1209.2997(2012)

[96] J. R. Petta, J. M. Taylor, A. C. Johnson, A. Yacoby, M. D. Lukin, C. M. Marcus, M. P. Hanson, and A. C. Gossard, Phys. Rev. Lett. **100**, 067601 (2008)

[97] S. Foletti, H. Bluhm, D. Mahalu, V. Umansky, and A. Yacoby, Nature Phys. **5**, 903 (2009)

[98] This is because the nuclear magneton is about 2000 times smaller then the Bohr magneton, which stems from the fundamental mass ratio of the electron and the proton.

[99] T. A. Knuuttila, J. T. Tuoriniemi, K. Lefmann, K. I. Juntunen, F. B. Rasmussen, and K. K. Nummila, J. Low Temp. Phys. **123**, 65 (2001)

[100] T. Fujisawa, T. H. Oosterkamp, W. G. van der Wiel, B. W. Broer, R. Aguado, S. Tarucha, and L. P. Kouwenhoven, Science **282**, 932 (1998)

[101] T. Brandes and B. Kramer, Phys. Rev. Lett. **83**, 3021 (1999)

[102] Experimentally, phonon emission have been shown to play an important role even at low temperatures[100].

[103] The Fermi contact interaction is relevant for atomic orbitals with $S$ symmetry, but not for $P$-symmetry orbitals where other HF couplings become important[135–137].

[104] J. Schliemann, A. Khaetskii, and D. Loss, J. Phys.: Condens. Matter **15**, R1809 (2003)

[105] A. Khaetskii, D. Loss, and L. Glazman, Phys. Rev. B **67**, 195329 (May 2003)

[106] B. Erbe and J. Schliemann, Phys. Rev. B **81**, 235324 (Jun 2010)

[107] H. Bruus and K. Flensberg, *Many-body quantum theory in condensed matter physics*, 1st ed. (Oxford university press, 2004)

[108] F. Domínguez and G. Platero, Phys. Rev. B **80**, 201301 (Nov 2009)

[109] Note that this is formally equivalent to including the inter-dot tunneling and the Overhauser field in usual degenerate perturbation theory for the chosen states.

[110] The depolarization can be described e.g. by including a phenomenological term like $-W_{\rm rel}P$ in the polarization rate equation (16).

[111] U. Peskin, J. Phys. B: At Mol. Opt. **43**, 153001 (2010)

[112] In the wide-band approximation the tunneling couplings $t_{\alpha k}$ in $H_{\rm T}$ Eq.(6b) are assumed independent of $k$ over the relevant energy range, leading to the $k$-independent tunneling elements $\Gamma_{\rm L,R}$.

[113] A. M. Lunde and G. Platero, Phys. Rev. B **86**, 035112 (Jul 2012)

[114] V. A. Abalmassov and F. Marquardt, Phys. Rev. B **70**, 075313 (Aug 2004)

[115] T. Meunier, I. T. Vink, L. H. W. van Beveren, K.-J. Tielrooij, R. Hanson, F. H. L. Koppens, H. P. Tranitz, W. Wegscheider, L. P. Kouwenhoven, and L. M. K. Vandersypen, Phys. Rev. Lett. **98**, 126601 (2007)

[116] V. N. Golovach, A. Khaetskii, and D. Loss, Phys. Rev. B **77**, 045328 (Jan 2008)

[117] Here the energy difference between the nuclear energy levels is negligible compared to the electronic one[98].

[118] For very low temperatures compared to the triplet energy splitting, the phonon *absorption triplet-triplet* rates become heavily suppressed (see Sec. II C 3). Thus, they can become comparable to the *emission singlet-triplet* rates, which in turn can cause the approximation used here to fail. However, due to the difference between the overall prefactors ($W_{T,T} \propto A_+^2$ and $W_{T,S} \propto A_-^2$), the temperature $k_{\rm B}T$ indeed has to be very much lower than the triplet level splitting $|E_{T_\pm} - E_{\mathfrak{p}}|$ in order for the triplet-triplet absorption and singlet-triplet emission rates to be comparable. Here we do not consider such very low temperatures.

[119] Note for instance that if $E_{T_+} > E_{T_{\mathfrak{p}}}$ and we take $W_{T_{\mathfrak{p}},T_+} \propto n_B(E_{T_+} - E_{T_{\mathfrak{p}}}) + 1$ and $W_{T_+,T_{\mathfrak{p}}} \propto n_B(E_{T_+} - E_{T_{\mathfrak{p}}})$, then we get the same ratio on the right-hand side of Eq.(33) as if we use our model for the rates in Eq.(25). Thus, in this respect, the polarization becomes model independent. Here $n_B(E) = [e^{E/k_{\rm B}T} - 1]^{-1}$ is the Bose function.

[120] S. Strogatz, *Nonlinear dynamics and chaos : with applications to physics, biology, chemistry, and engineering*, 1st ed. (Perseus Books, 1994)

[121] This can for instance be done by using that Eq.(34) for $B = 0$ goes from having one to three solutions for $P$, when the derivative of $\tanh[A_+P/(4k_{\rm B}T)]$ at $P = 0$ is one.

[122] Remember that all the non-zero HF rates between the triplets become equal in steady state due to the implicit polarization equation (32), and therefore the final and initial state is not emphasized in the notation of $w$.

[123] Note that there is no need to choose the rate $\Gamma_{\rm L}$ explicitly in these plots. However, to specify the dimensionless hyperfine rate $w = W_{T_+,T_{\mathfrak{p}}}/\Gamma_{\rm L}$ Eq.(42b) one needs to give a number for $\hbar\Gamma_{\rm L}N$, where $N$ is the total number of nuclear spins in the DQD, around $10^4 - 10^7$ depending on the material etc. Choosing $\hbar\Gamma_{\rm L}N = 10^7\mu$eV corresponds to – for instance – having $\hbar\Gamma_{\rm L} \sim 100\mu$eV and $N \sim 10^5$.

[124] The lowest order term in the expansion in $\gamma_{\rm ine}$ gives the same for $\gamma_{\rm RL} \neq 1$.

[125] N. W. Ashcroft and N. D. Mermin, *Solid State Physics* (Thomson Learning, 1976)

[126] For $g\mu_B B < 0$ the energy levels that cross are reversed, i.e. $E_{T_+}$ cross $E_{S_-}$ and $E_{T_-}$ cross $E_{S_+}$. This means that one has to neglect other HF rates in order to construct a simpler model describing the level crossing for negative field. However, this is straight forward following the same principles as outlined in the text.

[127] This is indeed a very good approximation as long as $|\mathfrak{p}| \ll 1$

[128] We remark that this approach fails for the parameters considered here, e.g. $A_{\rm L} = 80\mu$eV, $A_{\rm R} = 70\mu$eV, $t = 100\mu$eV, $\gamma_{ph} = 1\mu$eV, $\Gamma_{\rm L} = \Gamma_{\rm R}$, $\hbar\Gamma_{\rm L}N = 10^6\mu$eV and $\gamma_{\rm ine} = 10^{-7}$. Nevertheless, the approximation becomes better (but far from perfect) very close to the singlet-triplet crossing by increasing the inter-dot coupling to $t = 10^4\mu$eV, since this decreases the influence of the triplet-triplet HF rates. However, we are not interested in such extreme cases of very large $t$.

[129] Technically, this amounts to having $\mathcal{F}_{ph}(E)$ even in Eqs.(23,24).

[130] To see that $G(P) > 0$ and $G(P) \neq 0$, we begin by noting that $G(P)$ is a sum of products of rates, which are all greater than or equal to zero. Thus, $G(P) \geq 0$. However, at least one of these terms is always strictly positive, namely $\Gamma_{T_+,\uparrow}\Gamma^{\rm ine} > 0$. Hence, $G(P) > 0$.

[131] We choose slightly different parameters in Fig. 12 compared to Fig. 8 for the crossing of the triplets. Using the parameters of Fig. 8, a very similar transition temperature is found, $T_{c,\rm ST} \simeq 2.81A_+/k_{\rm B}$, – even though the inelastic rate dominates for magnetic fields close to the singlet-triplet crossing.

[132] Remember that the triplet-singlet rates dominate over the triplet-triplet and inelastic rates by more than one order of magnitude close to the level crossing [compare Fig. 14 (a) and (b)].

[133] We remark that close to the critical temperature in Fig. 17, it is hard to obtain conclusive average polarization values of the Monte Carlo simulations due to fluctuations.

[134] To make sure that the found stationary polarization $\bar{P}$ is stable, we show that an initial polarization $P(t = 0) > \bar{P}$ decreases versus time and that an initial polarization with $P(t = 0) < \bar{P}$ increases versus time.

[135] J. Fischer, W. A. Coish, D. V. Bulaev, and D. Loss, Phys. Rev. B **78**, 155329 (Oct 2008)

[136] J. Fischer, B. Trauzettel, and D. Loss, Phys. Rev. B **80**, 155401 (Oct 2009)

[137] J. Fischer and D. Loss, Phys. Rev. Lett. **105**, 266603 (Dec 2010)